MECHANISMS OF *COXIELLA BURNETII* WHOLE CELL VACCINE REACTOGENIC RESPONSES

A Dissertation

by

ALYCIA PAULINE FRATZKE

Submitted to the Graduate and Professional School of
Texas A&M University
in partial fulfillment of the requirements for the degree of

DOCTOR OF PHILOSOPHY

Chair of Committee,	James E. Samuel
Committee Members,	Aline Rodrigues-Hoffman
	Jianxun (Jim) Song
	Albert Mulenga
Head of Department,	Ramesh Vemulapalli

May 2022

Major Subject: Biomedical Sciences

ABSTRACT

Q fever is a zoonotic disease caused by the obligate intracellular bacterium, *Coxiella burnetii*. *C. burnetii* is highly infectious, transmitted via aerosols, is resistant to many disinfectants, and persists in the environment for long periods. The currently available vaccine licensed for use in humans is Q-VAX, a whole cell, formalin-inactivated vaccine. Although highly protective, the use of this vaccine is heavily restricted due to the high rate of local and systemic reactions in persons with prior exposure to *C. burnetii.* Despite decades of work understanding the mechanisms of protective efficacy of *C. burnetii* vaccines, little is known about the pathogenesis of their reactogenicity.

We began our work by testing novel subunit vaccines against *C. burnetii* which lacked the phase I lipopolysaccharide, an antigen that was previously proposed as a potential cause for reactogenicity. Our work showed that while these subunits vaccines provided significant protection from pulmonary infection, many of the formulations still produces local reactogenic responses. These results indicated that the mechanisms of reactogenicity with *C. burnetii* vaccines is more complex and required further investigation.

To better understand the pathogenesis of reactogenicity to the current whole cell vaccine, we developed a sensitized mouse model of reactogenicity. Our work on this model showed that reactogenicity to the whole cell vaccine is mediated by memory CD4 T cells and enhanced by immune serum. Additionally, these reactions are partially mediated by the production of IFNγ, indicating that *C. burnetii* whole cell vaccine reactogenicity is a Th1-mediated hypersensitivity reaction. Lastly, we showed that the

whole cell vaccine causes local persistence of antigen at the injection site for at least six months which is likely contributing to the chronicity of local hypersensitivity reactions.

Overall, our work reveals some of the mechanisms of reactogenicity caused by the *C. burnetii* whole cell vaccine. Understanding the mechanisms behind vaccine reactogenicity provides information essential for the development safe and effective novel vaccines.

ACKNOWLEDGEMENTS

I would like to thank my committee chair, Dr. Samuel, and my committee members, Dr. Rodrigues-Hoffman, Dr. Song, and Dr. Mulenga, for their guidance and support throughout the course of this research and for pushing me to be a better scientist.

Thank you to my colleagues and the department faculty and staff for the endless willingness to teach, discuss, and assist with every aspect of this work. Collaboration is the backbone of all good science.

Thank you to my friends, who made sure my time in and out of the lab was unforgettable. I would not have made it through without you all.

Finally, thank you to my family. I would not be where I am today without your continued love and support.

CONTRIBUTORS AND FUNDING SOURCES

Contributors

This work was supervised by a dissertation committee consisting of Professors James Samuel, Aline Rodrigues-Hoffman, and Albert Mulenga of the Department of Veterinary Pathobiology and Professor Jianxun (Jim) Song of the Department of Microbial Pathogenesis and Immunology.

Whole cell vaccine (WCV) was prepared by Dr. Anthony Gregory. The vaccine materials for the subunit vaccines depicted in Chapter 2 were provided by Professor Phillip Felgner and the serum data in Chapter 2 was analyzed by Sharon Jan of the Department of Physiology and Biophysics at the University of California, Irvine. The transmission electron microscopy was performed by Dr. Joseph Szule.

All other work conducted for the dissertation was completed by the student independently.

Funding Sources

Graduate study was supported by a fellowship from Texas A&M University and the NIH T32 Ruth L. Kirschstein Institutional National Research Service Award.

This work was also made possible by the Wofford Cain Endowed Research Fund and the Defense Threat Reduction Agency. Its contents are solely the responsibility of the authors and do not necessarily represent the official views of the National Institutes of Health.

NOMENCLATURE

WCV	Whole cell vaccine
TLR	Toll-like receptor
Cb	*Coxiella burnetii*
LPS	Lipopolysaccharide
PAMP	Pathogen-associated molecular pattern
ABSL/BSL	Animal biosafety laboratory/Biosafety laboratory
NMI	Nine Mile I
TCA	Trichloroacetic acid
CME	Chloroform:methanol extract
CMR	Chloroform:methanol residue
BCA	Bicinchoninic acid
LAL	Limulus amebocyte lysate
MALDI-TOF	Matrix-assisted laser desorption/ionization-Time of flight
GE	Genomic equivalents
HE	Hematoxylin and Eosin
IHC	Immunohistochemistry
MPLA	Monophosphoryl-lipid A
TRIF	TIR-domain-containing adapter-inducing interferon-β
PBS	Phosphate buffered saline
SC	Subcutaneous

TMB	3,3′,5,5′-Tetramethylbenzidine
BSA	Bovine serum albumin
ELF	Ectopic lymphoid follicles
S1PR1	Sphingosine-1-phosphate receptor 1
TGFβ	Transforming growth factor β
TNFα	Tumor necrosis factor α
TEM	Transmission electron microscopy
SCV	Small cell variant

TABLE OF CONTENTS

Page

LIST OF FIGURES

Page

LIST OF TABLES

Page

1. INTRODUCTION TO *COXIELLA BURNETII* VACCINES AND HYPERSENSITIVITY RESPONSES

1.1. The Discovery of *Coxiella burnetii* and Q Fever

In the 1930's a new disease began affecting slaughterhouse workers in Australia[1]. Affected workers developed fever, anorexia, muscle ache, and intense headaches. This syndrome was colloquially named "abattoir fever" and later renamed query fever or Q fever[1,2]. In 1935, Edward Derrick, a pathologist in the Queensland Health Department, was tasked with determining the cause of this disease. Interestingly, this disease was occurring in workers at a large centralized abattoir while workers at older, smaller slaughterhouses remained unaffected. Derrick noted that unaffected slaughterhouses produced meat for export only, while the affected slaughterhouse produced meat for both export and local consumption[3]. In order to confirm Q fever in patients, Derrick developed a method of diagnosing the disease by injecting blood or urine from ill workers into guinea pigs and monitoring them for fever, a process requiring 2-4 weeks to complete.

Derrick attempted to isolate the causative agent by culturing it in various medias but was unsuccessful[2]. So, in 1936, Derreck sent infected guinea pig liver to F. MacFarlane Burnet, believing that the agent must be a virus. Burnet, with the help of Mavis Freeman, were unable to isolate an agent by culture in embryonated chicken eggs, but noted that this material was infective when injected in mice. They detected intracellular bacterial inclusions on smears of infected mouse spleens and staining the smears with a Castenada stain revealed intra- and extracellular coccobacilli[4].

Around the same time, Gordon Davis, a microbiologist at what would eventually become Rocky Mountain Laboratories in Montana, was studying Rocky Mountain Spotted fever. Attempting to isolate the agent for a vaccine, Davis tested ticks collected from a Civilian Conservation Corps camp near Nine Mile Creek and applied them to the abdomens of shaved guinea pigs. He noted that one guinea pig developed a fever 12 days later that was transmissible via blood[5]. Herald Cox, who joined Davis in studying this new Nine Mile fever, later developed a method of cultivating the agent in embryonated chicken yolk sacs. Cox, similar to Burnet, detected the agent on histopathology of infected tissues and described it as intracellular bacterial inclusions resembling *Rickettsia* spp.[6].

However, the Chief of Infectious Diseases at the National Institutes of Health, Rolla Dyer, was skeptical of Cox's reports on the Nine Mile agent and visited the facility to review Cox's work. After reading through some of Cox's data, Dyer relented and began working to investigate what the Nine Mile agent was. Shortly before this, Dyer had received Q fever-infected tissue from Burnet. Noting the similarities between Q fever and Nine Mile fever, Dyer performed an experiment to determine if these diseases were caused by the same agent. Dyer injected this material into guinea pigs which subsequently developed a fever as expected. However, when Dyer next injected the Nine Mile agent material into these same animals, they did not produce a fever, indicating that Q fever and Nine Mile Fever were caused by the same pathogen[7,8]. In 1939, Derrick published a paper suggesting the name *Rickettsia burneti*, honoring Burnet's isolation of the bacterium[9]. In 1948, the agent would be renamed *Coxiella burnetii* once new information revealed differences between Cb and *Rickettsia* spp[10].

During the course of their research, Dyer, Burnet, and Cox would all develop Q fever through laboratory exposures[8,11]. Indeed, until the mechanism of transmission was elucidated, laboratory outbreaks of Q fever would be disconcertingly common and often wide-spread[11–15]. Because Davis isolated Cb from ticks and Cox had described the *Rickettsia*-like morphology of the bacteria, scientists at the time believed the agent to be arthropod-borne and that laboratory workers must be infected by bites from an unknown insect vector[5]. However, during an outbreak of Q fever in a laboratory in Fort Bragg, North Carolina, investigators noted that technicians who wore masks were not affected, indicating that Q fever may be transmitted by aerosol[15].

A few years later, the host reservoir would finally be uncovered. In 1947, when Frank Young, a general practitioner in southeastern Los Angeles County, suspected a Q fever outbreak in several of his patients. He submitted blood samples to the National Institutes of Health (NIH) which showed positive antibody titers for Cb in 8 of 14 samples[16]. An investigation of this outbreak showed that all affected individuals had visited or lived near dairy farms[17]. Further studies found Cb in milk samples and in the placentas of infected dairy cattle[18]. The investigation concluded that Cb is transmitted by infected placentas and Cb's ability to survive heat and desiccation allow for persistent in the environment, such as animal bedding, ultimately leading to airborne transmission to humans[18].

This information would ultimately explain why, back in Australia, only the large centralized slaughterhouses were affected by Q fever outbreaks. At the time, Australia was exporting only high-quality beef to compete with the international market, while locally sold beef would come not only from beef cattle, but older dairy cattle[1]. Thus, only the

large slaughterhouses which produced beef for export and local consumption were handling dairy cattle harboring infected placental tissue. This subsequently contaminated facilities with infective Cb, leading to outbreaks among workers.

1.2. Development of Vaccines Against *Coxiella burnetii*

Q fever is asymptomatic in approximately 60% of infected individuals with the majority of the remaining acute cases developing fever, malaise, headache, and pneumonia[19–21]. However, Q fever can also manifest as severe forms of acute infection including placentitis and spontaneous abortion in pregnant individuals, acute hepatitis, and myocarditis leading to dilated cardiomyopathy[21–25]. Additionally, 1-5% of symptomatic individuals will progress to chronic forms such as Q fever fatigue syndrome and valvular endocarditis[26–28]. Q fever fatigue syndrome is a poorly understood manifestation of Q fever that presents as chronic fatigue, joint pain, and night sweats lasting several months to years after infection[28,29]. Valvular endocarditis occurs in individuals with pre-existing valvular disease or aneurysms and has a mortality rate of 6.1 to 19% in confirmed cases despite treatment[27,30]. Q fever is treatable using oral antibiotics, however, chronic infections require 18 to 24 months of antimicrobial therapy[22,31].

Epidemiologic studies since the discovery of *Coxiella burnetii* have shown Cb to be endemic worldwide except for New Zealand and Antarctica. Surveys in human populations in several countries revealed seropositivity in 23.4 to 27.8% tested, while studies in domestic sheep, goats, cattle, and camels showed seroprevalence ranging from 6.8 to 40.7%[32–34]. Cb is transmitted by aerosol, highly resistant to heat and disinfectants,

and persists for long periods in the environment[35]. Cb is maintained through persistent infection in sheep, goats, cattle, and camelids, making eradication of this pathogen extremely difficult[36]. Because of this, vaccination is considered the best strategy for preventing human infections. Although abattoir workers, farmers, and veterinary workers are considered to be at the greatest risk of infection due to close contact with reservoir species, development of vaccines against Q fever began after outbreaks among military personnel during World War II. A number of outbreaks of Q fever were recorded in Allied troops deployed to European countries and often occurred while troops occupied small farming communities[37]. Although mortality was low, in severe cases, it would take 2 to 3 weeks for soldiers to recover and return to duty; a potentially devastating consequence in a time of war[38]. These outbreaks would rapidly incentivize the United States and other countries to begin research in development of a vaccine to protect against Q fever.

A formalin-inactivated, whole cell vaccine (WCV) was the first Cb vaccine developed for human use and continues to be the only vaccine licensed for use in humans to this day. The development of this vaccine began by isolating bacteria from infected soldiers. Blood samples from actively symptomatic patients were inoculated into guinea pigs then cultured in embryonated yolk sacs. This work produced several strains of Cb, including the Henzerling strain; the strain currently used for the production of the whole cell, formalin-inactivated vaccine used in humans[39,40]. Early testing of this WCV in guinea pigs showed a reduction in mortality to less than 2% in vaccinated animals compared to 40-80% in the unvaccinated group during challenge[39]. Evaluation of this vaccine in humans showed similarly high levels of protection. A survey of abattoir workers in southern Australia

spanning 18 months reported no cases of Q fever among 924 workers vaccinated with a single dose of a formalin-inactivated, whole cell vaccine compared to 34 cases in 1349 unvaccinated control workers[41]. However, early studies in humans and animals reported a high frequency of local and systemic reactions to the vaccine[39]. These reactogenic responses to the whole cell, formalin-inactivated vaccine would become a major barrier to its widespread availability.

Two currently two licensed vaccines against Cb are Q-VAX® (Seqirus, Australia) for use in humans and Coxevac® (CEVA Sainté Animale, France) for use in livestock. Both of these are formalin-inactivated, whole cell vaccines. Q-VAX was developed from the phase I Henzerling strain of Cb in response to the high rate of infections among abattoir workers in Australia and is only licensed for use in that country. Clinical trials of a single dose regimen using Q-VAX and later retrospective studies showed long-lasting protection of greater than 90% of vaccinated persons in the 5 year period after vaccination[42,43]. Similarly, a vaccination program with Q-VAX in Australia in 2002 reduced Q fever cases between 2002 and 2006 by more than 50%[44]. Coxevac is produced from the phase I Nine Mile strain and licensed for use in livestock in Europe. Evaluation of infection rates in ruminants after vaccination with Coxevac showed no significant reduction, however this vaccine does lower the rate of Cb-induced abortion in infected herds and reduces exposure to humans by decreasing bacterial shedding from infected livestock[45,46].

Several alternative Cb vaccines have been tested since the creation of the WCV, including a phase II WCV, a modified live phase I vaccine, and subunit vaccines[47–50]. Phase variation of Cb is caused by serial passages through embryonated yolk sacs results

in attenuation of the bacterium. Phase variation was later determined to be due to alteration in the LPS expressed on the surface of Cb[51]. Phase I Cb, which is isolated from infected animals or humans, is highly virulent while the phase II form, isolated after multiple passages through embryonated yolk sacs, cell culture, or acellular media, shows marked reduction in virulence. While phase I Cb must be kept in a high-containment facility, the decreased virulence of phase II Cb allows it to be studied and cultured at biosafety level 2. This makes phase II Cb much safer to prepare for use in vaccines and drastically reduces manufacturing costs. Unfortunately, formalin-inactivated, whole cell vaccines derived from phase II Cb provide significantly less protection than phase I vaccines[52]. Further experiments on WCVs derived from phase I and phase II Cb showed that phase I LPS is essential for developing protective immunity with WCV[49].

An attempt was made to separate the protective and reactogenic components of WCV with a solubilized antigen vaccine was derived from phase I Cb using trichloroacetic acid (TCA) extraction[47]. This vaccine showed >90% protection against mortality in mice and guinea pigs infected intraperitoneally with phase I Cb[47]. In humans vaccinated with a prime-boost regimen, anti-Cb antibody titers were detected in 74.4% of vaccinees. The TCA vaccine also resulted in overall high rates of local reactions in humans, ranging from 27.9% to 63.9%, but these were described as local erythema, pain and swelling which resolved after several days with no evidence of injection site abscesses[47]. In the 1960's, M-44, a live attenuated vaccine, was developed in Russia by serial passage of the Grita strain of Cb forty-four times through embryonated chicken eggs. This attenuated strain showed significantly reduced when inoculated into guinea pigs and mice[53]. This vaccine

provided strong protection against Q fever in animal and human experiments and reduced local and systemic reactions were reported compared to WCV[48]. However, later testing of the vaccine in guinea pigs reported persistent infections in test animals with evidence of splenitis, hepatitis, and myocarditis[54]. These results precluded further use of the M-44 vaccine in humans due to concerns for safety.

A chloroform:methanol residue (CMR) vaccine was developed in the 1980's from the now named Rocky Mountain Laboratories in the United States. This vaccine was created by separating whole cell material into a soluble fraction which is mainly composed of lipids, called the chloroform:methanol extract (CME) and a precipitated or residual fraction composed of LPS, proteins, and peptidoglycans, which was developed as the CMR vaccine[50,55]. A prime-boost strategy with the CMR vaccine provided similar protection against mortality compared to WCV in guinea pigs challenged with phase I Cb intraperitoneally[50]. A phase I clinical trial of the CMR vaccine reported significant anti-Cb IgG titers and T cell priming. Though 75% and 65% of the 20 participants developed vaccine site reactions after the prime and boost vaccinations, respectively, these reactions appeared less persistent than those reported with WCV, resolving after about 7 days post-injection[56]. Unfortunately, further testing of this vaccine has not been pursued.

Between 2007 and 2010, an epidemic of over 4,000 cases of Q fever occurred in humans in the Netherlands linked to an outbreak of Cb in several dairy goat farms. An emergency vaccination program using Q-VAX was implemented to help control the outbreak, but 22% of high-risk individuals had to be excluded from the vaccination program due positive skin test or anti-Cb titers[57]. Epidemiologic studies of U.S. military

deployment to rural areas in developing countries in the early 2000's showed a high exposure risk in military personnel as evidenced by sporadic infections and seroconversion rates against Cb of 2.1-7.2% among deployed troops[58,59]. Cb is currently designated a category B select agent by the Centers of Disease Control and Prevention due to its low infectious dose, resistance to heat and chemical disinfectants, and its ability to infect humans via aerosols making it a high risk pathogen for use as a weapon of bioterrorism[60]. The risk of further epidemics and Cb's potential use as a bioweapon strongly support the need for effective, non-reactogenic vaccines against Cb.

Breakthroughs in vaccine research are allowing for the development of novel vaccine strategies. Potential novel vaccines include attenuated live and killed WCVs, conjugated and unconjugated subunit vaccines, and DNA- or mRNA-expressing recombinant vector vaccines[61,62]. These different technologies can modify the immune response by presenting antigen to immune cells in different ways. Similarly, adjuvants can be combined with vaccine antigens to enhance and modify the immune response such as skewing memory T cells towards Th1 or Th2 phenotypes[63]. Finally, the route of vaccination may guide induction of circulating and tissue resident memory cell populations towards sites of pathogen exposure[64–66]. These variables in vaccine strategies can greatly modify the resultant immune memory responses to immunization.

Novel vaccine adjuvants are allowing researchers to overcome the decreased protective efficacy of subunit vaccines and even alter the resulting immune memory responses resulting in some new vaccine candidates against Cb[67–69]. A pair of studies on a Cb subunit vaccine using different combinations of toll-like receptor (TLR) agonist

adjuvants reported that this strategy was effective in protecting mice and guinea pigs against aerosol challenge. While some adjuvant combinations still incited vaccine site granulomas, one adjuvant combination demonstrated a significant reduction in local reactive lesions[70,71]. Another group of researchers developed a solubilized protein vaccine derived from phase II Cb combined with the TLR9 agonist adjuvant, CpG, which produces strong T cell memory. This vaccine showed significant protection against aerosol challenge with Cb in mice, guinea pigs, and nonhuman primates and marked reduction in vaccine site reactions in sensitized guinea pigs[72].

A mutant strain of phase I Cb lacking the type IV secretion system, Cb *dot/icm*, markedly reducing its virulence, was recently tested as an alternative WCV[73]. Similar to phase II Cb, the *dot/icm* mutant's inability to produce significant infections allows it to be cultured outside of high containment. This mutant whole cell vaccine provided similar protection to the wild-type, formalin-inactivated, WCV in a guinea pig challenge experiment. However, evaluation in sensitized guinea pigs did not reveal a significant reduction in the severity of reactogenic lesions at the vaccination site based on histopathologic evaluation[73].

1.3. Reactogenicity and *Coxiella burnetii* Vaccines

Throughout the use of the Cb WCV, local reactions, such as induration, erythema, and granulomas, and systemic symptoms, such as fever, malaise, and anorexia, were frequently reported in vaccinated humans[39]. Injection site granulomas from the WCV may last for weeks to months and occasionally require surgical excision to resolve[47,74]. In one

early case report, a researcher from Rocky Mountain Laboratories was vaccinated with a Cb WCV which led to severe local swelling and inflammation. Over the course of more than four years, the vaccine site would become irritated and swollen, presumably related to re-exposure within the lab, until the affected tissue was ultimately surgically excised[74]. Similar local reactions to Cb WCVs have been reported in sensitized ruminants, rabbits, and guinea pigs[75].

To reduce the rate of severe reactions to the WCV, humans receiving Q-VAX must undergo pre-vaccination screening which includes measuring anti-Cb antibody titers in serum and intradermal sensitivity testing. This intradermal test uses a low dose of whole cell material which is injected into the dermis. Local induration and erythema are measured 48-72 hours later, similar to the tuberculin skin test[76]. However, unlike the tuberculin test, which uses a solubilized protein extract from *Mycobacterium*, the Cb intradermal skin test uses the same formalin-inactivated, whole cell material as the vaccine, but with about 1/10th the amount of antigen[77]. Despite this pre-vaccination screening strategy, a survey from the 2007-2011 outbreak of Cb in the Netherlands reported local reactions in 80% and systemic reactions in 43% of seronegative or skin test negative vaccinees[78]. Similarly, a 2018 survey of seronegative and skin test negative veterinary students reported local and systemic reactions in 98% and 60%, respectively[79]. This suggests two possibilities: the current pre-vaccination screening tests are not sensitive enough to detect all sensitized persons or the intradermal skin test is sensitizing individuals prior to vaccination[77].

Despite being the main barrier to the availability of the vaccine, the pathogenesis and underlying causes of Cb WCV reactogenicity have been severely understudied. Some early research speculated that phase I lipopolysaccharide (LPS) may be the cause for local reactogenic responses, but more recent studies have disproven this hypothesis[47,71,73]. One research group reported similar reactogenic responses in sensitized guinea pigs vaccinated with a formalin-inactivated, WCV derived from phase II Cb and our own work evaluating subunit vaccines against Cb, which did not contain any Cb LPS, produced severe local granulomas[71,73]. Notably, in the latter publication, local vaccine site reactions lacked abscess formation recorded with Cb WCVs, but still showed marked granulomatous and lymphoplasmacytic inflammation[71].

Review of clinical and histopathologic data on Cb WCV reactions can provide some insights into the mechanisms of these vaccine reactions. Reactions to the Cb WCV have a delayed onset, with local induration being most severe at about 12-15 days post-vaccination in sensitized guinea pigs[80]. Adverse reactions to the Cb WCV are also more frequent and severe in individuals with antibody titers against Cb from prior exposure, indicating that these reactions are a type of hypersensitivity response caused by re-exposure through vaccination[47]. Lastly, histopathologic evaluation of vaccine site reactions shows granuloma formation characterized by infiltration of activated macrophages, neutrophils, and lymphocytes with central abscesses[47,74,80]. Together this data suggests that Cb WCV reactions are a granulomatous, delayed-type hypersensitivity response.

Delayed-type hypersensitivities, also known as type IV hypersensitivities, may be divided into contact, tuberculin, and granulomatous types[81]. Contact hypersensitivity is caused by percutaneous exposure to haptens. Haptens are low molecular weight, electrophilic molecules, which can bind to nucleophilic residues of cutaneous proteins to form novel allergens[81,82]. Their lipophilic nature and small size allow haptens to rapidly penetrate the skin and mucous membranes. These allergens are picked up by epidermal-resident antigen-presenting cells such as Langerhans dendritic cells which migrate to the draining lymph node and activate hapten-specific T cells[82]. Tuberculin and granulomatous hypersensitivity occur when antigens penetrate tissue and are picked up by interstitial dendritic cells then presented to T cells to form adaptive immune responses. While contact and tuberculin hypersensitivities occur at approximately 24 to 72 hours post-exposure, granulomatous hypersensitivities have a significantly more delayed onset, on average 21 to 28 days post-exposure. This delayed reaction time is believed to be caused by antigens which are difficult to degrade and remove from the inoculation site[81].

Vaccine-associated hypersensitivity responses are not uncommon, but most are non-life-threatening and are infrequent enough that they do not prohibit approval by regulatory bodies. Most vaccine hypersensitivities are either type I, mediated by IgE, or type IV, mediated by T cells[83]. Type I hypersensitivities occur within minutes to a few hours of administration and range from mild symptoms, such as hives, to severe acute syndromes, such as anaphylactic shock. In contrast, type IV hypersensitivities to vaccines have a delayed onset of 2 to 21 days post-vaccination and generally produce maculopapular rashes or chronic injection site induration and are usually self-limiting[83].

Hypersensitivity reactions may result from either vaccine antigens or other additives such as egg proteins and gelatin. Similarly, vaccine adjuvants have been implicated in prolonged inflammation and reactogenicity in vaccines, but do not necessary indicate a hypersensitivity response[83].

Mild forms of reactogenic responses to vaccines are often considered an important sign that a vaccine is producing significant immune memory. The purpose of adjuvants is to induce local inflammation, stimulate antigen-presenting cells to take up the vaccine antigen, and prolong inflammatory responses to incite development of memory T and B cells[83,84]. Because of this, immunogenicity and reactogenicity are often considered two sides of the same coin. Type IV hypersensitivity may be induced by CD4 or CD8 T cells or require a combination of both depending on the antigen. Additionally, hypersensitivities induced by different antigens may produce either Th1 or Th2 type hypersensitivity responses which differ in their severity and immune cell infiltrate. Similarly, the Cb WCV provides protection through induction of CD4 memory T cells[49]. However, challenge experiments in mice have shown that allow both CD4 and CD8 T cells can provide protective immunity to Cb, CD8 T cells are required for bacterial clearance from organs and CD4 T cell responses may actually increase pathologic lesions during infection[49,85,86]. However, since T cells also mediate type IV hypersensitivity responses, novel vaccine strategies against Cb must produce a balanced immune response to maintain protective immunity while reducing adverse responses.

1.4. Overcoming *C. burnetii* Vaccine-Induced Reactogenic Responses

In this work, our lab began by testing novel subunit vaccines composed of six antigens derived from *C. burnetii* based on serologic data indicating strong immunogenicity[70]. These vaccine candidates would presumably be less reactogenic due to their limited antigen composition. Although we showed significant improvement in reactogenicity with some vaccine antigen-adjuvant formulations, local reactive lesions were still evident in all candidate vaccines when evaluated in a sensitized guinea pig model[71].

Indeed, many labs, including ours, have attempted to or are currently developing novel vaccines against *C. burnetii* that provide protection without producing reactogenic responses. However, the methods used focus on predicting immunogenicity while reactogenicity is tested empirically later in development[70,87,88]. Failure of these novel vaccines to abrogate reactogenic responses wastes both time and funding. By understanding the pathogenesis of pathologic versus protective responses to vaccination, we can guide development of novel vaccines and determine predictive markers of vaccine reactogenicity.

One barrier to the investigation of *C. burnetii* vaccine reactogenic responses is the use of a guinea pig model which is the current standard model to evaluate *C. burnetii* vaccine reactogenicity[80,89]. Although guinea pigs are highly susceptible to *C. burnetii* infection and sensitized animals readily produce local reactions to vaccination, commercial antibodies to target and evaluate markers for guinea pig cells are not widely available which limits their use for immunologic experiments[20]. In contrast, mice are more commonly used for evaluation of immune responses because of the wide variety of target-

specific antibodies for immune cell and cytokine analyses and accessibility of inbred and knockout strains[20]. Use of a mouse model also provides advantages by decreased overall costs and reduced housing requirements. Although mice are frequently used for protection studies for novel *C. burnetii* vaccines, there is no published mouse model for *C. burnetii* vaccine reactions[19,20,90]. To address this problem, our lab has developed a mouse model of *C. burnetii* vaccine-induced reactions. We then utilize our mouse model to evaluate local and systemic immune responses during elicitation of *C. burnetii* vaccine-induced reactogenic responses and characterize the immunopathogenesis of these reactions.

2. SUBUNIT VACCINES USING TLR TRIAGONIST COMBINATION ADJUVANTS PROVIDE PROTECTION AGAINST *COXIELLA BURNETII* WHILE MINIMIZING REACTOGENIC RESPONSES*

2.1. Introduction

Q fever is a zoonotic disease caused by the obligate intracellular bacterium, *Coxiella burnetii* (Cb). Although overall mortality due to Q fever is low in humans, severe infections may cause atypical pneumonia, myocarditis, hepatitis, and spontaneous abortion[19,22,24,31]. Symptomatic cases can also lead to chronic debilitating syndromes such as valvular endocarditis and Q fever fatigue syndrome in 1-2% of cases[19,21,91]. Cb is highly contagious by aerosol transmission, has a low infectious dose, and remains viable in the environment for long periods, making this agent a concern for bioterrorism[21]. Q-VAX, a whole-cell, formalin-inactivated vaccine that provides long-term protection against Cb, has not been approved for use in humans outside of Australia due to the high rate of local and systemic reactions in previously sensitized individuals. These reactions necessitate costly pre-vaccination serologic screening and intradermal skin testing which delays vaccination[42,47,79]. Surveys for anti-Cb antibodies in at-risk populations, particularly those who work in animal husbandry and veterinary fields, reported seroprevalence rates of

* Reprinted with permission from: Fratzke AP, Jan S, Felgner J, Li L, Nakajima R, Jasinskas A, Manna S, Nihesh FN, Maiti S, Albin T, Esser-Kahn AP, Davies DH, Samuel JE, Felgner P, Gregory AE. 2021 Subunit Vaccines using TLR Triagonist Adjuvants Produce Protective *Coxiella burnetii* Vaccines while Minimizing Reactogenic Responses *Frontiers in Immunology*. Mar;12:1-13. doi: 10.3389/fimmu.2021.653092

18.3-45.13%[34,92,93]. The high seroprevalence rates show that these groups that would most benefit from vaccination also bear the greatest risk of hyper-reactive responses. Thus, there is a significant need to develop novel vaccine strategies against Cb that provide long-term protection without inducing adverse reactions.

Subunit vaccines can provide a safer alternative to whole-cell vaccines with a lower risk of adverse reactions, but must overcome their lower immunogenicity with the use of adjuvants[67,69,94]. The need for adjuvants to produce immunologic memory provides the opportunity to tailor immune responses to target antigens by altering adjuvant formulations. One class of adjuvant is toll-like receptor (TLR) agonists which activate innate immune receptors and induce proinflammatory cytokines through NF-κB transcription. Use of TLR agonists can mimic whole-cell vaccines which similarly activate TLRs through endogenous pathogen-associated molecular patterns (PAMPs) such as lipopolysaccharide (LPS), lipopeptides, and nucleic acids[67,69,95]. By applying different combinations of TLR agonists to subunit vaccines, immune responses may be directed to enhance immunogenicity while minimizing adverse responses. Although individual TLR agonists have been associated with systemic toxicity secondary to diffusion from the vaccination site, conjugation of TLR agonists with polymers prevents rapid dispersal and markedly reduces this risk[68,96,97]. Linking TLR agonists in diagonist and triagonist combinations has also been shown to alter and enhance immune responses by mimicking the spatial orientation of endogenous TLR agonists present on pathogens during infection[68,96,98].

In this study, we evaluated the protective efficacy and reactogenicity of five Cb subunit vaccine formulations containing different linked (triagonist) or unlinked TLR agonist adjuvants in a guinea pig model of aerosol infection. Antigen and adjuvant combinations were selected based on the results of a previous publication (Table 1)[70]. Our publication showed vaccines containing the triagonists TLR1/2_4_9a and TLR4_7_9a produced a greater Th1-biased immune response when compared to other triagonist adjuvants in both in vivo and in vitro experiments[70,96]. This Th1-biased response has been previously shown to be essential in vaccine-induced protection against Cb[49]. AddaVax™, an MF59-like squalene oil-in-water emulsion adjuvant, was added to vaccine candidates because of its ability to enhance Th1-skewing[70]. Similarly, a dendronized polymer (DP), was used as an adjuvant in one candidate vaccine because of its ability to enhance T cell responses to antigens[99].

In this report, we show that several vaccine candidates produce significant protection in a guinea pig model of aerosol infection with Cb Nine Mile I (NMI). In addition, we identify a Cb subunit vaccine using a TLR4_7_9 triagonist adjuvant that results in significantly less local reaction in pre-sensitized guinea pigs compared to a whole-cell vaccine (WCV) while providing similar protection from infection. Our results show how TLR triagonists may be utilized to modify immune responses to vaccination in favor of protective memory while limiting adverse hyper-reactive lesions.

Vaccine	Antigen	Adjuvant
A	CBU1910, CBU0307, CBU0545, CBU0612, CBU0891, CBU1398	None
B	CBU1910, CBU0307, CBU0545, CBU0612, CBU0891, CBU1398	AddaVax™, DP, MPLA
C	CBU1910, CBU0307, CBU0545, CBU0612, CBU0891, CBU1398	AddaVax™, MPLA, CpG1018, 2Bxy
D	CBU1910, CBU0307, CBU0545, CBU0612, CBU0891, CBU1398	AddaVax™, Triagonist TLR4_7_9
E	CBU1910, CBU0307, CBU0545, CBU0612, CBU0891, CBU1398	AddaVax™, Triagonist TLR1/2_4_9
F	CBU1910, CBU0307, CBU0545, CBU0612, CBU0891, CBU1398	AddaVax™, pyrimido-indole, CpG1018, 2Bxy
Sham	PBS	None
WCV	Whole-cell Vaccine	None

Table 2.2.1: Formulations of vaccine candidates.
Candidate vaccines contained 0.25 nmol of each antigen per vaccine dose. For adjuvants, AddaVax™ was dosed at 50% v/v, DP at 80 µg, and all TLR agonists at 2 nmol each. WCV was dosed at 25 µg of antigen per vaccine dose. Conjugated TLR triagonists were composed of Pam_3CSK_4 (TLR1/2), pyrimido-indole (TLR4), 2Bxy (TLR7), and CpG1018 (TLR9) as indicated.

2.2. Materials and Methods

2.2.1. Cb antigens

Six Cb antigens, CBU1910, CBU0307, CBU0545, CBU0612, CBU0891, and CBU1398, were expressed in Escherichia coli BL21 cells, and purified by multiple column chromatography and endotoxin removal procedure at Genescript (Piscataway, NJ). Two antigens, CBU0612 and CBU1910 contained a His-tag. Purified proteins were evaluated by SDS-PAGE gel, Bicinchoninic acid (BCA) protein assay, and endotoxin removal confirmed using a Limulus Amebocyte Lysate (LAL) assay (MPL Laboratories, Sparta, NJ) (data not shown).

2.2.2. TLR triagonists and adjuvants

The TLR triagonists were designed and generated as previously described[96]. In brief, TLR triagonists were formed by bioconjugation reactions (amide bond formation, maleimide-thiol Michael addition, and azide-alkyne click chemistry) of individual TLR agonists to a central triazine core. The agonists used in this study include monophosphoryl lipid A (MPLA, TLR4), pyrimido-indole (TLR4), CpG ODN 1018 (TLR9), 2Bxy, an imidazoquinoline derivative (TLR7), and Pam3CSK4 (TLR1/2). Pyrimido-indole, CpG, 2Bxy, and Pam3CSK4 were used to form the linked triagonist adjuvants indicated in Table 1. TLR triagonist adjuvants, pyrimido-indole, 2Bxy, Pam3CSK4, and the imidazoquinoline derivative were purified by either high performance liquid chromatography or gel extraction and their masses were confirmed by MALDI-TOF or electrospray ionization-mass spectrometry (data not shown). CpG ODN 1018 (IDT, Coralville, IA) and MPLA (Avanti Polar Lipids, Alabaster, AL) were commercially purchased. Additional adjuvants used in our candidate vaccines include the squalene oil-in-water emulsion, AddaVax (Invivogen, San Diego, CA), and DP, a dendronized polymer analog[100,101]. Endotoxin in pyrimido-indole was quantitated using limulus amebocyte lysate (LAL) assay. All other lab-prepared adjuvants were analyzed for endotoxin contamination with Endotoxin Assay Kits (Genscript, Piscataway, NJ) or HEK TLR4 reporter cell assay (Invivogen, San Diego, CA). Antigen-adjuvant combinations were chosen based on previously published immunogenicity and challenge experiments[70].

2.2.3. *Coxiella burnetii* strains and growth

For intratracheal infection, Cb Nine Mile phase I (NMI) clone 7 (RSA493) was grown in embryonated yolk sacs and purified using gradient centrifugation as previously

described[90]. Experiments involving Cb NMI were performed in biosafety level 3 (BSL3) facilities at Texas A&M Health Science Center. For formalin-inactivated whole-cell vaccine (WCV), live NMI cultures grown in ACCM-2 media as previously described were inactivated with 2% formalin for 48 hours[102].

2.2.4. Guinea Pigs

Hartley guinea pigs, weighing 350-450 g, were purchased from Charles River Laboratories (Wilmington, MA). Guinea pigs were individually housed in microisolator cages under pathogen-free conditions and provided with free access to water, pelleted feed, and hay. Animals were housed in approved animal biosafety level 3 (ABSL-3) facilities and all experiments were performed under an animal use protocol approved by the Institutional Animal Care and Use Committee at Texas A&M University. Prior to infection, an IPTT-300 thermal transponder (Bio Medic Data Systems) was placed within the subcutis between the shoulder blades and temperatures were measured for 1-3 days to obtain individual baselines.

2.2.5. Challenge Experiments

For challenge experiments, guinea pigs were administered candidate vaccines, WCV, or PBS (Sham) in 100 µL sterile PBS by intramuscular injection in the semitendinosus and semimembranosus muscles (Table 1). A boost vaccine was given in the opposite hindlimb two weeks later. Blood was collected from the lateral saphenous vein on days -3, 7, and 21, and 45 post-prime vaccination. Seven weeks after prime vaccination, guinea pigs were intratracheally infected with 105 genomic equivalents (GE) of live Cb as previously described[90]. Briefly, animals were anesthetized with an

intraperitoneal injection of 100 mg/kg ketamine and 10 mg/kg xylazine in PBS. A small animal laryngoscope (model LS-2; Penn-Century, Wyndmoor, PA, USA) was used to visualize the larynx then a MicroSprayer aerosolizer model IA-1B device was inserted to administer the bacteria in 50 µL of PBS. Guinea pigs were monitored daily for clinical signs including weight and temperature measurements. Five guinea pigs were utilized for each experimental group.

2.2.6. Hypersensitivity Experiments

For hypersensitivity experiments, guinea pigs were infected with 10^6 GEs of Cb and monitored for two weeks post-infection as above then rested for an additional four weeks. To elicit hypersensitivity responses, two or four approximately 2-3 cm areas were shaved using electric clippers and depilatory cream on the right and left flanks. A vaccine candidate or WCV was then injected into the subcutis at each of the shaved sites (3 candidates and WCV per guinea pig). Temperature, weight, and reaction sites were monitored daily for two weeks. Each vaccine candidate was evaluated in four or five guinea pigs. Four uninfected guinea pigs were used as controls for unsensitized WCV and PBS responses.

2.2.7. Cb array composition

Purified His-tagged Cb proteins were purchased (GenScript, Piscataway, NJ, USA) and purified lipopolysaccharide (LPS) from NMI was produced using the hot phenol method previously described[103]. Purity of the LPS was confirmed using a SDS-PAGE gel that was subsequently silver stained (data not shown).

Cb protein microarrays were produced as previously published with modifications[104]. Briefly, purified proteins were mixed with array printing buffer and then printed onto nitrocellulose coated glass slides with an Omni Grid 100 microarray printer (Genomic Solutions). Serum samples were diluted to 1:100 and mixed with E. coli lysate (GenScript, Piscataway, NJ) and a His-tag-containing peptide (HHHHHHHHHHGGGG) (Biomatik, Wilmington, DE) to a concentration of 0.1 mg/ml, and pre-incubated at room temperature for 30 min to block any anti-His antibodies generated by the immunizations. Meanwhile, arrays were rehydrated for 30 min in blocking buffer. Arrays were probed with pre-incubated serum or PBS with 0.05% Tween (negative control) overnight at 4°C. Arrays were washed with TBS plus 0.05% Tween 20 then probed with anti-mouse IgG with streptavidin-conjugated Qdot®800 (Cat #Q10171MP, Thermofisher) at 1:200 dilution. Array images acquired using an ArrayCAM® Imaging System (Grace Bio-Labs, Bend, OR, USA) to measure relative signal intensity corrected for negative control arrays.

2.2.8. Quantification of Cb bacterial loads

At two weeks post-infection, guinea pigs were euthanized and spleens and lungs were collected in for quantification of Cb genomic DNA (gDNA) using qPCR[90]. Tissues were homogenized and DNA extracted using the High Pure PCR template preparation kit (Roche, Basel, Switzerland) according to the manufacturer's recommendations. Samples were analyzed on a StepOne Plus real time PCR System (Applied Biosystems) using com1-specific primers and probe (com1_L1 [CGCGTTGTCTTCAAAGAACT], com1_R1 [GCGTCGTGGAAAGCATAATA], and 5=-6-carboxyfluorescein-[FAM]-CGGCCAATCGCAATACGCTG-3'-6-carboxytetramethylrhodamine [TAMRA]).

2.2.9. Histopathology

Lungs and skin sites from guinea pigs were fixed in 10% neutral buffered formalin for 72 hours at room temperature. For lungs from challenge experiments, four transverse sections were cut from the right lung (two from the caudal, one from the middle, and one from the cranial lobes). For vaccination sites, two to three sections were cut containing the epidermis to the underlying abdominal or intercostal muscle. Trimmed tissues were submitted to AML Laboratories (Jacksonville, FL, USA) for processing, embedding, and sectioning at 5 µm before staining with hematoxylin and eosin (HE). Histopathology slides were de-identified and evaluated by an ACVP boarded pathologist. Histopathologic scoring was performed on a 0-6 scale (Figs. 2.4A and 2.6A).

2.2.10. Statistical Analysis

Statistical analyses were performed with GraphPad Prism v7.0 (GraphPad Software, La Jolla, CA, USA). Results were compared using one-way or two-way ANOVA with Dunnett's correction for multiple comparisons. Differences were considered significant if p-value ≤ 0.05 (*), ≤ 0.01 (**), ≤ 0.001 (***), or ≤ 0.0001 (****).

2.3. Results

2.3.1. Serum IgG responses to vaccine candidates

Specific IgG production to Cb antigens has been shown to be an important mediator of vaccine-induced protection[105]. The antigen combination in our candidate vaccines was chosen based on previous results evaluating serum from acutely and chronically infected humans which revealed seroreactive antigens as well as antigen-specific IgG responses to Q-VAX vaccination in mice[70,106,107]. We measured antigen-

specific IgG production in vaccinated guinea pigs to assess humoral responses to our vaccine candidates. Groups of five animals were given a prime vaccination on day 0 with a boost on day 14 and serum was collected from guinea pigs on days 7, 21, and 45 post-prime immunization. Samples were assessed by protein microarray for the six Cb antigens in the vaccine formulations as well as purified phase I LPS (Fig. 2.1A). Subsequently, day 45 serum samples were assessed for anti-specific IgG isotyping (Fig. 2.1B).

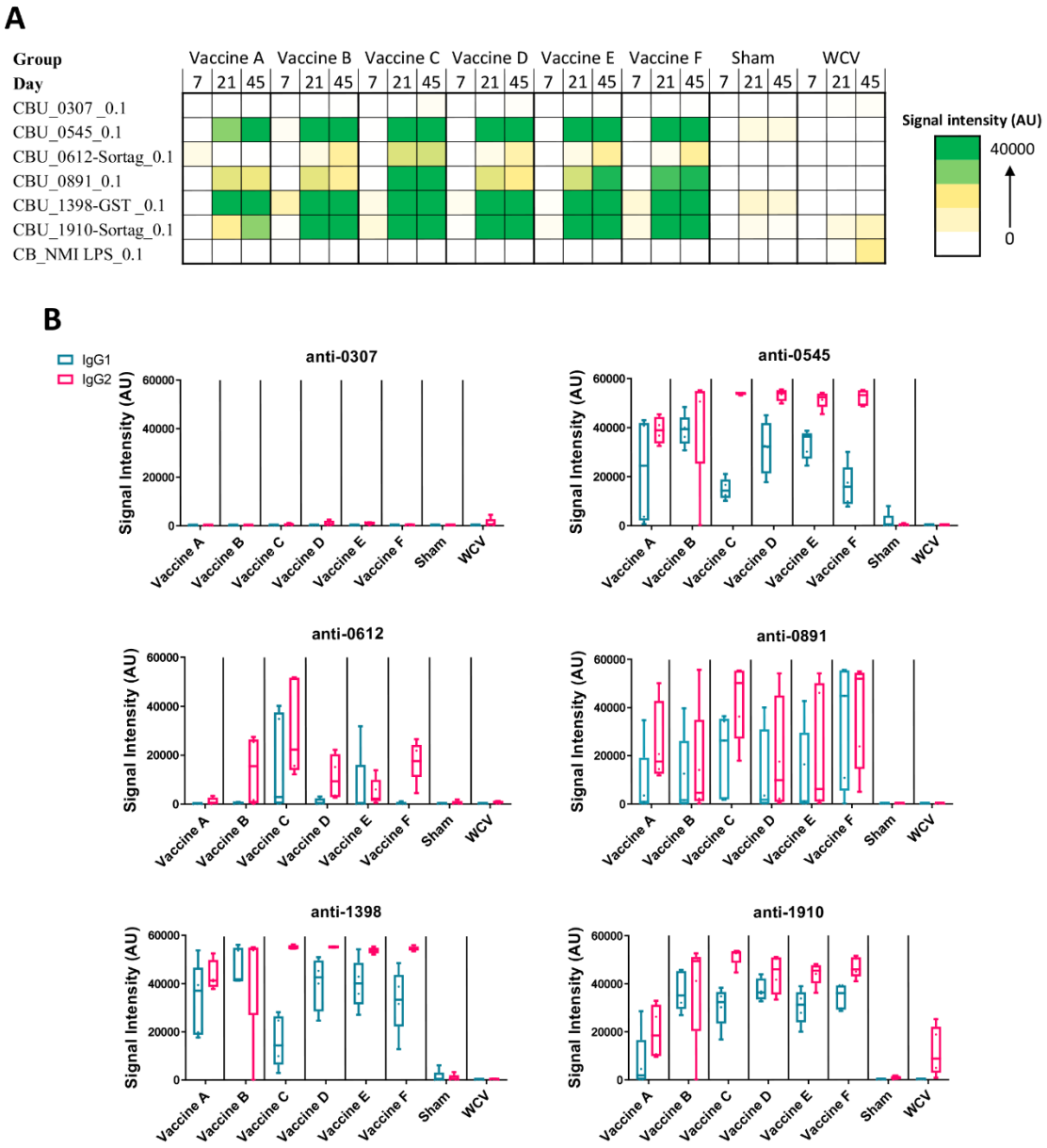

Figure 2.1 Antigen-specific serum IgG responses to vaccination.
C. burnetti protein microarrays containing the six antigens from the vaccine candidates and NMI LPS. (A) Guinea pig sera collected from days 7, 21, and 45 post-prime vaccination were probed for total IgG. Values displayed as colorized scale are the means of the intensity from each group (n=4-5 per group). AU=arbitrary units. (B) Day 45 samples were probed on the protein microarray for antigen-specific IgG1 (blue bar) and IgG2 (pink bar) subtype responses.

All candidate vaccines, including the unadjuvanted vaccine A, induced robust IgG responses against CBU_0545, CBU_1398, and CBU_1910 by day 45. IgG production against CBU_0891 was more variable across vaccines, but all candidates induced significantly elevated serum IgG compared to Sham. Vaccine C produced the strongest response to CBU_0612, with milder responses in vaccines B, E, and F. None of the candidate vaccines resulted in significant IgG responses to CBU_0307, which is similar to our previously published data using mice[70]. IgG isotyping for vaccines A to F were mostly IgG2-biased or IgG1/IgG2 balanced responses. The WCV vaccine group only induced significant IgG response to phase I LPS, with a mild response to CBU_1910 (mean signal intensity: 10937 ±3042). WCV vaccination induced anti-CBU1910 IgG2-polarized response. As expected, none of the vaccine candidates produced anti-phase I LPS IgG.

2.3.2. Subunit vaccines provide protection against intratracheal Cb infection

We assessed the protective efficacy of our candidate vaccines using a guinea pig model of aerosol infection[90]. Guinea pigs were chosen for this study since they develop similar pulmonary disease compared to humans in response to aerosol infection and are more susceptible to acute infection than most immune-competent mouse strains[108–110]. To evaluate protection, guinea pigs were vaccinated using the prime-boost schedule described above and rested for seven weeks post-prime prior to intratracheal infection with Cb NMI (Figure 2.2A). Five guinea pigs were assessed per experimental group. Guinea pigs were monitored daily for changes in weight and body temperature for 14 days post-challenge.

WCV and sham vaccinated guinea pigs were used as positive and negative controls, respectively.

Sham-vaccinated guinea pigs had markedly elevated body temperature from days 4 to 10 after infection. All vaccine formulations provided significant protection against fever response compared to sham. Vaccines C, D, and F, which each contained TLR4, TLR7, and TLR9 agonists as a triagonist or unconjugated adjuvants, were able to mitigate any significant elevation in temperature compared to WCV (Fig. 2.2B). All experimental groups showed some weight loss one to two days after challenge, which was presumed secondary to anesthesia required for intratracheal infection. Sham-vaccinated guinea pigs showed marked weight loss following infection which partially resolved by the end of the 14-day observation period. Similarly, guinea pigs vaccinated with vaccine C showed some transient but significantly greater weight loss compared to the WCV group at day 6 post-infection. Vaccine groups A, B, D, E, and F showed no significant decrease in weight compared to WCV-vaccinated guinea pigs. All vaccinated groups increased in weight by the end of the study period, except for vaccine C group which sustained a mild reduction in body weight (Fig. 2.2C).

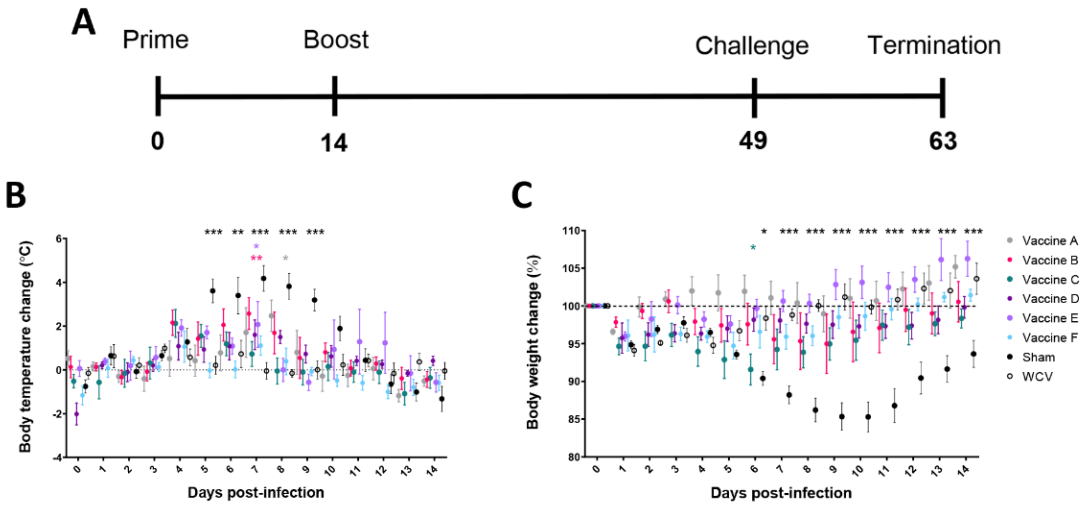

Figure 2.2 TLR agonist vaccines protect against weight loss and fever during aerosol infection.
(A) Timeline of challenge experiment in days post-prime vaccination. Guinea pigs were challenged 7 weeks after prime vaccination. (B) Temperatures are presented as change from average individual temperature recorded prior to infection. (C) Change in starting body weight for 14 days post-infection. Body temperature and weight were monitored daily for 14 days post-infection. Graphs show the means for each group (n=5 per group) with error bars indicating the standard error of the mean. Data were analyzed using two-way ANOVA with Dunnett's correction for multiple comparisons. Asterisks indicate significant differences between candidate- and WCV-vaccinated group (*: $p<0.05$, **: $p<0.01$).

Animals were euthanized fourteen days after challenge, at which point spleens and lungs were weighed and collected for quantification of Cb genome equivalents (GEs) and for histopathologic evaluation. All adjuvanted vaccine candidates and WCV provided significant protection against splenomegaly compared to sham-vaccinated guinea pigs (Fig. 2.3A). Lungs were weighed as an indirect measure of pulmonary consolidation. Interestingly, all vaccine candidates had significantly lower lung weights compared to sham (Fig. 2.3B). Bacterial burden in the lungs of all vaccinated groups was significantly less than sham, and comparable to WCV (Fig. 2.3C). Pulmonary lesions were evaluated

by histopathology using semi-quantitative scoring on a scale of 0-6 (Fig. 2.4A). Sham-vaccinated guinea pigs produced severe granulomatous and lymphocytic inflammation frequently causing consolidation of >50% of lung sections. Vaccine groups C, D, E, F, and WCV showed significantly less pulmonary inflammation compared to sham-vaccinated controls (Fig. 2.4B). Lung lesions in these groups consisted of mild to moderate interstitial infiltrates of macrophages, lymphocytes, and few heterophils with rare foci of consolidation. Guinea pigs immunized with vaccine B presented with severe consolidation of the lungs (>50% of lung section) often affecting multiple lung lobes, similar to sham-vaccinated controls. Guinea pigs in vaccine A group showed moderate multifocal consolidation with macrophages, lymphocytes, and heterophils (Fig. 2.4C).

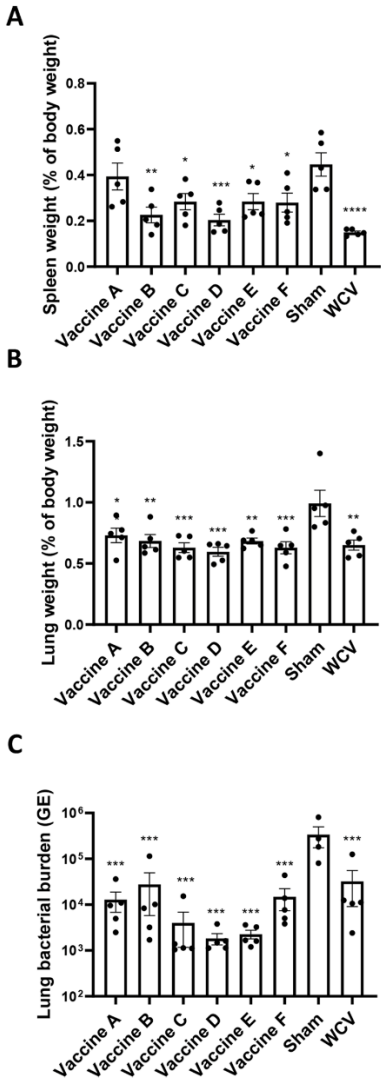

Figure 2.3 TLR agonist vaccination protects against splenomegaly and reduces pulmonary bacterial burden.

(A) Mean spleen weight presented as a percentage of body weight. Vaccines B-F and WCV show significantly less splenomegaly compared to unvaccinated. (B) Mean lung weight presented as a percentage of body weight as an indicator of consolidation. Unvaccinated guinea pigs have significantly heavier lungs than vaccinated groups. (C) Mean genomic equivalents recovered from infected lungs show reduced bacterial burden in all vaccine groups compared to unvaccinated controls. Graphs show the means of each group (n=4-5 per group) with error bars that represent the standard error of the mean. Data were analyzed using one-way ANOVA with Dunnett's correction for multiple comparisons. Asterisks indicate significant differences compared to sham-vaccinated group (*: $p<0.05$, **: $p<0.01$, ***: $p<0.001$, ****: $p<0.0001$).

A

Lung Histopathologic Scoring Criteria

Score	Histopathologic Features
0	No lesions
1	Mild, multifocal interstitial inflammation
2	Mild, coalescing interstitial inflammation
3	Moderate interstitial inflammation, small areas of consolidation
4	Moderate interstitial inflammation, consolidation of <50% of lung sections
5	Marked inflammation with consolidation of >50% of one lung section
6	Marked inflammation with consolidation of >50% of multiple lung sections

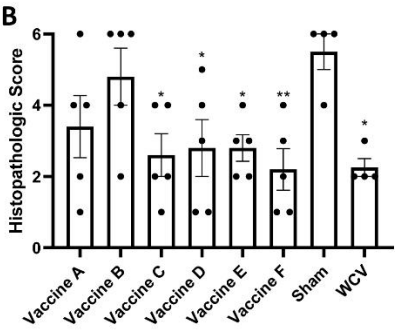

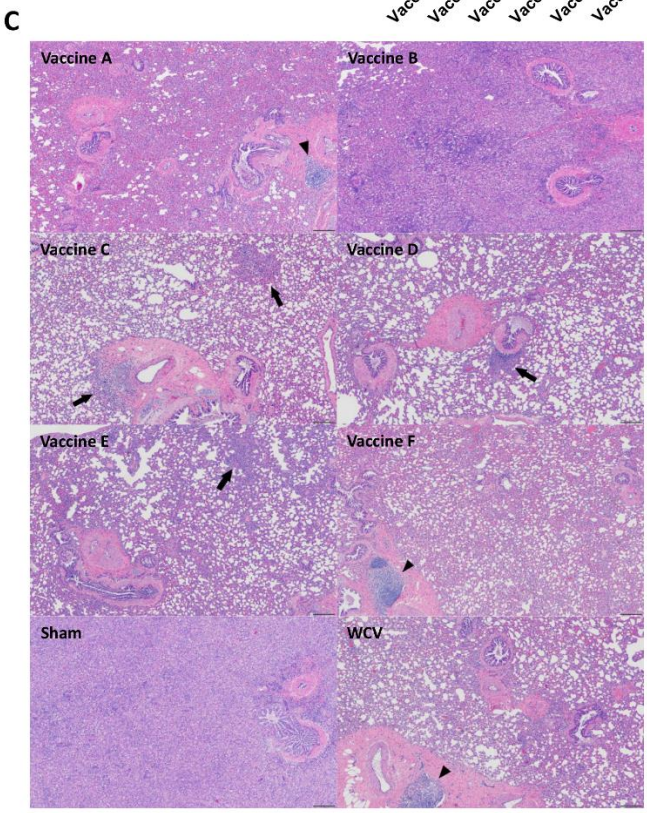

Figure 2.4 TLR agonist vaccines protect against pathologic lesions in the lungs. Histopathologic evaluation of the lungs 14 days after challenge. (A) Histopathologic scoring criteria for lung lesions. (B) Four representative sections of lung were examined and scored for severity of lesions. (C) Representative images of lungs from each experimental group showing foci of consolidation (black arrows) and BALT hyperplasia (arrowheads). Vaccine B and Sham lungs show consolidation of >80% of lung section. 4x magnification, HE stain, scale bar=200 µm. Graphs show the means of each group (n=4-5 per group) with error bars that represent the standard error of the mean. Data were analyzed using one-way ANOVA with Dunnett's correction for multiple comparisons. Asterisks indicate significant differences compared to sham-vaccinated group (*: $p<0.05$, **: $p<0.01$).

2.3.3. TLR triagonist adjuvants modulate the reactogenicity of Cb vaccines

Next, we evaluated reactogenic responses in guinea pigs with prior exposure to Cb to subcutaneous vaccination with our candidate vaccines. Guinea pigs were intratracheally infected with 1x106 GEs of Cb NMI and then rested for six weeks before vaccination to mimic the most likely exposure route for pre-sensitization in humans (Fig. 2.5A). Nine sensitized guinea pigs divided into two groups (Groups 2 and 3) were vaccinated with vaccines A-C and D-F, respectively, plus WCV (WCV+). Unsensitized guinea pigs (Group 1) were vaccinated with WCV (WCV-) and PBS (Sham) as controls (Fig. 2.5B).

Body temperature and weight changes were monitored for two weeks post-infection and post-vaccination. Although all groups showed transient weight loss one to two days post-challenge due to anesthesia, infected guinea pigs displayed prolonged weight loss that resolved at 12-14 days post-infection. Infected guinea pigs also produced markedly elevated temperatures, up to 40.7 °C, from days 4 to 10 post-infection indicating successful infection (Fig. 2.5C). Uninfected control guinea pigs did not have any significant changes in body temperature during the 14-day observation period. None of the guinea pigs showed significant changes in body temperature post-vaccination. Similar to infection, guinea pigs lost weight during days 1 to 3 post-vaccination secondary to anesthesia, but maintained weight over the remainder of the observation period (Fig. 2.5D).

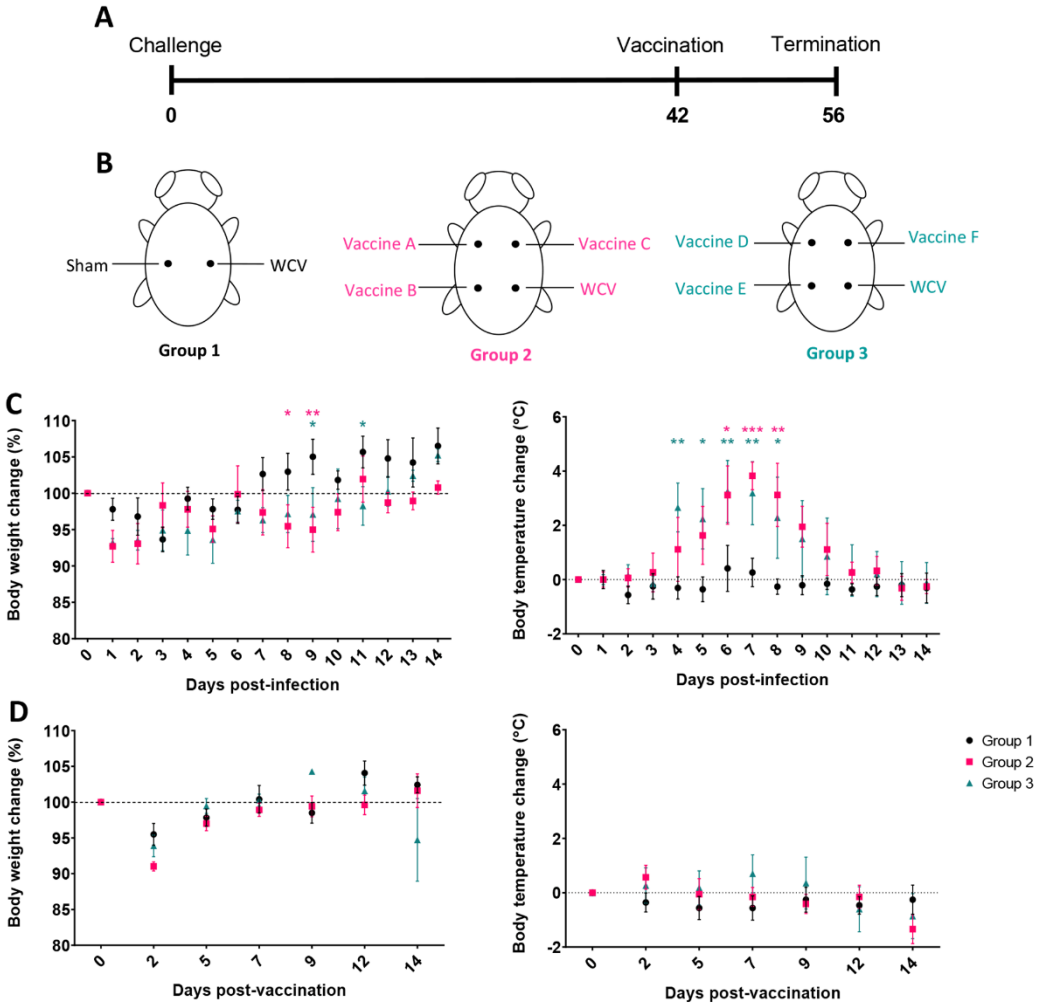

Figure 2.5 Guinea pigs were sensitized by aerosol infection prior to evaluation of the reactogenicity of TLR agonist vaccines.

(A) Timeline of hypersensitivity experiment. Guinea pigs (Groups 2 and 3) were challenged by aerosol infection then rested for 6 weeks before SC injection with vaccine candidates. Uninfected guinea pigs (Group 1) were used to provide sham and unsensitized WCV skin sites as controls. (B) Location of injections for each experimental group. (C) Post-infection changes in body temperature and weight. Infected groups (2 and 3) show transient fever and weight loss compared to uninfected group (1). (D) Post-vaccination changes in weight and temperature. Graphs show the means of each group (n=4-5 per group) with error bars showing the standard error of the mean. Data were analyzed using two-way ANOVA with Dunnett's correction for multiple comparisons. Asterisks indicate significant differences compared to uninfected group (Group 1) (*: $p<0.05$, **: $p<0.01$, ***: $p<0.001$).

To assess the presence of local reactogenic responses to vaccine candidates, histopathology of the vaccine sites was performed 14 days post-vaccination. Two to three sections of each vaccination site were assessed by semi-quantitative scoring on a scale of 0-6 (Fig. 2.6A). Although all adjuvanted vaccines induced local inflammatory lesions, vaccine D produced significantly less local inflammation compared to WCV+ (Fig. 2.6B). Sensitized guinea pigs vaccinated with WCV showed severe granulomatous inflammation with multifocal areas of necrotic heterophils (micro-abscesses) and degeneration of adjacent collagen and myofibers similar to previously published reports[80,89]. Vaccine D caused mild to moderate histiocytic and lymphocytic inflammation with rare Langhans-type giant cells which occasionally extended to the subjacent muscle. Vaccines B, C, E, and F induced moderate to severe inflammation composed of macrophages, lymphocytes, and Langhans-type giant cells contain up to 30 nuclei with areas of degenerate collagen and hemorrhage. These lesions extended into the overlying deep dermis and underlying abdominal musculature. Unsensitized guinea pigs induced mild lymphohistiocytic inflammation within the subcutaneous tissue in response to WCV. Vaccine A produced only rare perivascular lymphocytic infiltrates (Fig. 2.6C). Interestingly, although small numbers of heterophils were present in vaccine lesions in all of the candidate groups, none of the candidate vaccines produced abscesses seen in WCV lesions, even in the most severe reactions.

A

Vaccine Site Histopathologic Scoring Criteria	
Score	**Histopathologic Features**
0	No lesions
1	Minimal to mild multifocal inflammation
2	Mild inflammation, minimal collagen degeneration
3	Moderate inflammation, mild collagen degeneration
4	Moderate inflammation, degenerate collagen, occasional giant cells
5	Marked inflammation, degenerate collagen, hemorrhages, giant cells
6	Marked inflammation, degenerate collagen, hemorrhages, giant cells, micro-abscesses

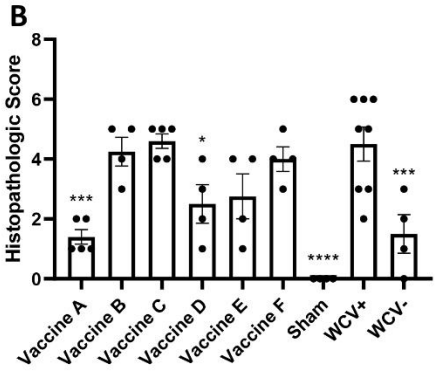

C

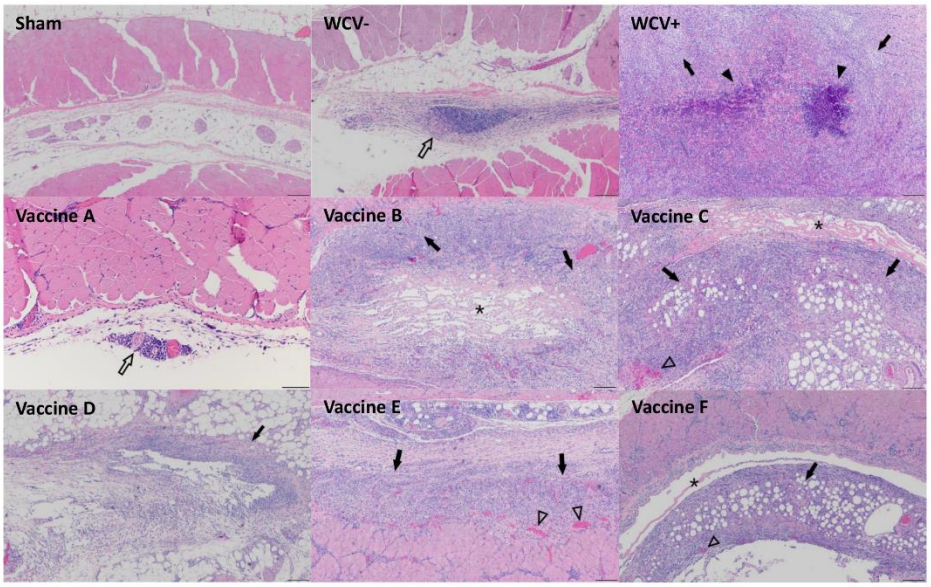

Figure 2.6 TLR agonist vaccines modulate local reactogenic responses to vaccination in pre-sensitized guinea pigs.

(A) Histopathologic scoring criteria for vaccination site lesions. (B) Mean histopathologic scores for each experimental group. (C) Representative images of vaccine site lesions from each experimental group. WCV+ produces severe granulomatous inflammation (arrows) with multifocal micro-abscesses (arrowheads). Vaccines B, C, E, and F produce moderate to severe granulomatous inflammation (arrows) with areas of degenerate collagen (asterisks) and occasional foci of hemorrhage (open arrowheads). Vaccine D shows mild lymphohistiocytic inflammation (open arrow). Vaccine A shows minimal perivascular lymphohistiocytic inflammation (open arrow) 4x magnification, HE stain, scale bar=200 µm. WCV+: WCV vaccination in sensitized guinea pigs. WCV-: WCV vaccination in unsensitized guinea pigs. Graphs show the means of each group (n=8 for WCV+, n=4-5 for all other groups) with error bars that represent the standard error of the mean. Data were analyzed using one-way ANOVA with Dunnett's correction for multiple comparisons. Asterisks indicate significant differences compared to WCV+ vaccinated site in the same group (*: $p<0.05$, **: $p<0.01$, ***: $p<0.001$, ****: $p<0.0001$).

2.4. Discussion

Cb is a zoonotic, facultative intracellular bacterium that can induce a wide-range of acute and chronic syndromes in humans and animals. Although a whole-cell, formalin-inactivated vaccine against Cb, Q-VAX, provides long-term protection, adverse systemic and local reactions in previously sensitized individuals prevent wide-spread licensure and use[21,79]. In this report, we tested the protective efficacy and reactogenicity of subunit vaccines utilizing TLR agonist combination adjuvants as a safer alternative to WCV. We previously evaluated the protective efficacy of several antigens and TLR triagonist combinations in a mouse model of aerosol infection showing that vaccines containing the TLR triagonists TLR1/2_4_9 and TLR4_7_9 produced Th1-skewed immune responses and provided protection against aerosol challenge[70]. To further this, we used a guinea pig model of aerosol infection to assess both protection and reactogenicity of five vaccine candidates using TLR agonist and triagonist combinations.

Our data showed that all of our vaccine candidates provided measurable levels of protection against aerosol challenge. Surprisingly, even the antigen-only control appeared to provide some degree of protection against pulmonary infection based on pulmonary bacterial burden but did not prevent systemic responses, as evidenced by splenomegaly. Considering all measured indicators of protective efficacy, vaccine formulations D and F showed the greatest efficacy by preventing fever, weight loss, and splenomegaly, reducing lung bacterial burden, and minimizing pulmonary inflammation. These vaccines are very similar, containing agonists against TLR4, TLR7, and TLR9, but use a triagonist adjuvant and individual agonists, respectively. TLR4, TLR7, and TLR9

are all inducers of Th1-skewed immune response, which has previously been shown to be critical for immunity to Cb infection[49,67,69]. For example, T cell-deficient and IFNγ-deficient mice have increased susceptibility to Cb infection, and humoral and cellular evaluation of Q-VAX vaccinated mice revealed a Th1-skewed immune response[49,111]. Thus, vaccines D and F likely induced robust Th1 memory resulting in greater protection during challenge. This is supported by the IgG isotyping showing mostly IgG2-baised responses to specific Cb antigens in serum samples from vaccinated guinea pigs.

Although vaccine C provided similar protection across multiple parameters, this candidate failed to prevent significant weight loss during challenge compared to WCV. This was interesting considering that vaccines C and F only differ in their TLR4 agonist, containing MPLA and pyrimido-indole, respectively. Pyrimido-indoles are considered less potent stimulators of TLR4 compared to MPLA but are structurally better suited for conjugation with triagonist cores[96,112]. Additionally, pyrimido-indoles induce TLR4 signaling via MyD88 whereas MPLA mainly induces signaling via the TIR-domain-containing adaptor protein inducing interferon-β (TRIF) pathway[113,114]. Activation of MyD88 leads to the production of pro-inflammatory cytokines, while TRIF activation causes formation of type I interferons[115]. The roles of MyD88- and TRIF-signaling in induction of immune memory are complex, but several studies indicate that MyD88 signaling is important for formation of memory T cells. In a MyD88 KO mouse model, dendritic cell maturation and trafficking to local lymph nodes occurs, but the production of pro-inflammatory cytokines from MyD88 activation has been shown to be necessary for the subsequent formation of memory T cells[116]. Similarly, MPLA induces clonal

expansion of T cells similar to LPS; however, MPLA also promotes contraction and terminal differentiation leading to fewer memory T cells[113,117]. MyD88-independent signaling also leads to a higher frequency of Th2, rather than Th1, cells in the absence of IFNγ secretion[116,118]. This differential signaling between MPLA and pyrimido-indole may explain why vaccine F provided greater protection from challenge than vaccine C.

In contrast, vaccine B produced the least protection against challenge based on lung pathology and lung bacterial burden. Notably, this vaccine candidate was the only one to lack a TLR9 agonist, suggesting that TLR9 agonism is important for vaccine-induced protection against Cb. TLR9 is an intracellular toll-like receptor which detects bacterial and viral DNA by the presence of unmethylated CpG motifs. Whole-cell vaccines, such as Q-VAX, retain nucleic acids which may act as endogenous TLR9 ligands[67]. Signaling via TLR9 is a potent stimulator of cellular immunity, including memory CD8 T cells which are important in bacterial clearance during infection[67,85]. We, and others, have previously shown that adjuvanting Cb vaccine candidates with a TLR9 agonist significantly improves their efficacy (Gregory et al. unpublished data)[96]. TLR9 signaling is important in generating resistance to other intracellular bacteria including Mycobacterium tuberculosis, Brucella abortus, and Salmonella enterica and may be an essential mediator of vaccine-induced protection against Cb[119–121].

We next evaluated the reactogenicity of our candidate vaccines using a sensitized guinea pig model. Vaccine D induced significantly less local inflammation compared to WCV. Despite containing the same TLR agonists, this TLR triagonist in vaccine D showed decreased local inflammation compared to individual TLR agonist vaccine

counterparts, vaccines C and F. Triagonist conjugations modulate the activity of individual agonists by reducing individual potency, decreasing diffusion from the vaccination site, enhancing cellular co-activation, and mimicking the distribution of endogenous agonists on pathogens[68,97,98]. Although experiments show TLR triagonists reduce systemic inflammation by decreasing diffusion from the vaccination site, their effect on local reactions is not as well studied[97,98]. Conceptually, TLR agonist conjugations increase local inflammation by retention of immunostimulatory adjuvants, but the effects of conjugated TLR agonists on immune responses can vary depending on the TLR agonist combinations used[96]. A comparison of linked versus unlinked TLR4, TLR7, and TL9 agonists showed the linked TLR triagonist induced less IL12p70 systemically compared to unlinked TLR agonists in mice, but significantly greater TNFα, IL6, and IFN-β in in vitro stimulation of bone marrow-derived macrophages which suggested the triagonist would induce greater local inflammation[96]. However, this does not correlate with the histopathology results in our experiments as the linked triagonist vaccine produced less reactogenicity than the unlinked counterpart. Further investigation is necessary to understand how TLR agonist combinations and conjugations alter the risk of local reactogenic responses.

Surprisingly, many of our candidate vaccines produced local lesions with similar severity to WCV despite containing only six Cb antigens. It has been suggested that phase I lipopolysaccharide (LPS) is responsible for reactogenicity, but our candidate vaccines do not contain LPS yet some formulations still produced reactive lesions[47,89]. The lack of local inflammation in response to the unadjuvanted vaccine indicates that Cb antigens alone do not induce local reactogenicity. Local inflammation may be the result of innate

responses to adjuvants within the candidate vaccine. However, similar adjuvants and TLR agonists have been evaluated in vaccine trials against influenza, human immunodeficiency virus, and tuberculosis and did not result in the prolonged local inflammation shown in our experiments[122–124]. It should be noted that these publications evaluated reactogenicity using unsensitized mice or in human trials where prior exposure to the target antigen is unlikely. Thus, their effects in pre-sensitized individuals are not well understood. It is likely that the combination of one or multiple Cb antigens combined with certain TLR agonist adjuvants is producing local reactive lesions in pre-sensitized animals.

An interesting observation from the reactogenicity results was that local reaction sites from all candidate vaccines lacked micro-abscesses present in WCV-vaccinated guinea pigs. Although heterophils were present in smaller numbers in the lesions, there were no foci of necrotic heterophils. Mammalian heterophils differ from neutrophils in their cytochemical staining of cytoplasmic granules but are functionally analogous[125]. Neutrophils participate in both innate and adaptive responses, however, since abscessation is not present in the vaccination sites of unsensitized guinea pigs, this is more likely a modification of the adaptive response[126]. Neutrophil recruitment and activation is associated with Th17 cell cytokines in adaptive immunity and stimulation of Th17 has been associated with TLR2 stimulation[127]. Only vaccine E contained an agonist that activates TLR1/2 which similarly did not show histologic evidence of abscessation. However, as discussed above TLR agonists show reduced activity upon conjugation with a triazine core and so decreased TLR2 agonism may explain the altered local inflammation in reactogenic responses caused by our candidate vaccines[96].

In these experiments, we evaluated the protective efficacy and reactogenicity of five subunit vaccine formulations using TLR agonist and triagonist combinations against Cb. We showed that all of our vaccine candidates provided a measurable degree of protection, while those using a combination of TLR4, TLR7, and TLR9 appeared to produce the most significant protection against aerosol challenge. Evaluation of the reactogenic potential showed that all of subunit vaccines produced a measurable degree of reactogenicity in previously sensitized guinea pigs. However, candidate vaccine D, containing a TLR4_7_9 triagonist adjuvant, produced significantly less local inflammation compared to WCV. This result shows our Cb subunit vaccine containing the TLR4_7_9 triagonist adjuvant can induce protection while mitigating local reactogenicity. Further experiments are needed to evaluate protection and reactogenicity of our subunit vaccines in non-human primates prior to progression of this vaccine towards human clinical trials. Overall, the TLR triagonist platform produces a favorable alternate vaccine strategy compared to Q-VAX for providing protection against Cb.

3. COXIELLA BURNETII WCV PRODUCES A TH1 DELAYED-TYPE HYPERSENSITIVITY RESPONSE IN A SENSITIZED MOUSE MODEL[*]

3.1. Introduction

Coxiella burnetii is a facultative intracellular, Gram-negative bacterium and the cause of the zoonotic disease Q fever. Acute Q fever is usually self-limiting causing fever, headache and myalgia, however, severe infections may cause atypical pneumonia, hepatitis, myocarditis, and spontaneous abortion[19,22,24,27]. Approximately 1-2% of clinical cases will develop chronic syndromes include Q fever fatigue syndrome and valvular endocarditis[19,21,91]. Infection in humans is usually due to exposure to reservoir species including sheep, goats, cattle, and camels, or from contaminated animal products[19,32,58]. Q-VAX® (Seqirus), a formalin-inactivated, WCV (WCV) for Cb is only licensed for use in humans in Australia[42,79]. Although this vaccine provides long-term protection against Q fever, local and systemic reactions to Q-VAX in previously sensitized individuals prevent the licensure of this vaccine outside of Australia[80,128]. To reduce the risk of vaccine reactions, individuals must undergo costly and time-consuming pre-vaccination screening including anti-Cb titers and intradermal skin testing[79].

Understanding the differences between protective and pathologic responses to vaccination is essential to develop safe, novel vaccines against Cb and other infectious

[*] Reprinted with permission from: Fratzke AP, Gregory AE, Van Schaik EJ, Samuel JE. 2021 *Coxiella burnetii* Whole Cell Vaccine Produces a Th1 Delayed-type Hypersensitivity Response in a Mouse Model. *Frontiers in Immunology*. Sep;12:1-15. doi: 10.3389/fimmu.2021.754712

agents. Clinical and histopathologic evaluation of local Cb WCV reactions in humans and animals report a delayed onset of signs, an influx of macrophages, lymphocytes, and neutrophils at the vaccine site, and more severe lesions in those with prior exposure to Cb[42,75,79,80]. These results strongly suggest that Cb WCV reactogenic responses are a granulomatous type IV hypersensitivity reaction. Type IV hypersensitivities, also referred to as delayed-type hypersensitivities, are a T cell-mediated response and are subdivided into contact, tuberculin, and granulomatous types. Granulomatous type IV hypersensitivity differs from contact and tuberculin type IV hypersensitivities by a prolonged clinical course to respond, average of 21-28 days, and an influx of activated macrophages[81]. Although CD4+ Th1 cells are most commonly implicated in type IV hypersensitivities, several studies in contact hypersensitivity show some reactions are mediated by CD4+ Th2 cells and CD8+ T cells[82,129,130]. Based on the previously published clinical and histopathologic descriptions of WCV lesions and our own observations, we suspected that Cb WCV reactions are a Th1-mediated type IV hypersensitivity response[47,74,80,89].

Despite decades of research on novel vaccine strategies against Cb, the pathogenesis and cause of these vaccine reactions are poorly understood. It was just recently, in 2021, that some publications reported that the phase I lipopolysaccharide of Cb is not necessary for WCV reactogenicity as earlier research postulated[47,71,73,89]. Currently, the standard model of WCV reactogenicity is a sensitized guinea pig model[20,89]. Guinea pigs are highly susceptible to Cb infection, produce pulmonary lesions after intratracheal infection similar to those described in humans, and readily produce vaccine

reactions with WCV. However, the lack of immune markers for this species inhibits in-depth investigation of local and systemic immune responses[80,89,90]. Here we developed a mouse model of the Cb WCV reactogenic response for use in immunologic studies of adverse vaccine reactions. We then went on to determine the elicitation dose that maximizes lesions in sensitized compared to unsensitized animals to target adaptive responses. Finally, we show that WCV reactions stimulate IFNγ- and IL17a-producing CD4 T cells, indicating that Cb WCV reactions are a Th1-mediated type IV hypersensitivity.

3.2. Materials and methods

3.2.1. Bacterial strains and vaccine materials

For intratracheal infections, Cb Nine Mile phase I (NMI) clone 7 (RSA493) was grown in embryonated yolk sacs, then purified using gradient centrifugation as described previously[90]. To produce WCV, cultures of Cb NMI RSA493 were grown in ACCM-2 media as described in prior publications, then inactivated in 2% formalin for 48 hours[102]. WCV was administered as 2 µg, 10 µg, 30 µg, or 50 µg doses by dry weight (1 mg WCV = $3.7x10^{10}$ cells)[131]. Experiments involving live Cb NMI RSA493 were performed in biosafety level 3 (BSL3) facilities at Texas A&M Health Science Center.

3.2.2. Experimental animals

Female C57Bl/6NHsd (C57) and BALB/c mice (BAL), 6-8 weeks old, were purchased from Envigo (Huntingdon, UK) and female SKH1-Elite (SK) mice, 6-8 weeks old, were purchased from Charles River Laboratories (Wilmington, MA). Mice were housed in microisolator cages under pathogen-free conditions and given free access to food and

water. Animals were housed in approved animal biosafety level 3 or level 2 facilities and all experiments were performed under an animal use protocol approved by the Institutional Animal Care and Use Committee at Texas A&M University.

3.2.3. Sensitization and elicitation of responses

For infection-sensitization (NMI), mice were intratracheally inoculated with 10^5 or 10^6 genomic equivalents (GE) of live Cb as previously described with some modifications[90]. Briefly, mice were anesthetized by intraperitoneal injection of 100 mg/kg ketamine and 10 mg/kg xylazine. Mice were then placed on a Mouse Intubation Platform (Penn-Century; Wyndmoor, USA) at a 45° angle and a 20-gauge catheter, needle removed, was inserted into the trachea. Live bacteria were administered through the catheter in 30 µL of sterile PBS. Infection-sensitized mice were monitored for clinical signs and weighed three times per week for two weeks post-inoculation. For vaccine-sensitization (WCV), mice were anesthetized as above and 50 µg of WCV in 50 µL of sterile PBS was administered subcutaneously (SC) in the middle of the back. Unsensitized control mice (PBS) were given a subcutaneous vaccination with 50 µL PBS alone. Mice were rested for 5-6 weeks post-sensitization prior to elicitation.

For elicitation of vaccine reactions mice were anesthetized as above. In haired mice, vaccination sites were first shaved using electric clippers followed by the application of a depilatory cream for 30 seconds. Mice were vaccinated SC with 2 µg, 10 µg, or 30 µg of WCV in 50 µL of sterile PBS or with 50 µL sterile PBS alone into the right and left flanks. Vaccine sites were visually monitored daily for two weeks, then mice were euthanized and tissues were collected for histopathology or flow cytometry.

3.2.4. Serum antibody responses

Serum samples were collected from either the submandibular vein or by intra-cardiac stick at pre-sensitization, post-sensitization, and post-elicitation time points for measurement of anti-Cb IgG titers. Briefly, flat-bottomed 96-well plates were coated in 5 µg/mL Cb antigen overnight then blocked in 3% powdered milk for 2 hours. Serum was pooled from 5 mice per group, diluted in PBS with 1% powdered milk, and serial dilutions were applied to the plate and incubated for 2 hours at 37°C. After washing three times with PBS with 0.05% tween 20, plates were then incubated with HRP-conjugated goat anti-mouse IgG antibody (1:10,000) for 2 hours at 37°C. 3,3′,5,5′-Tetramethylbenzidine (TMB) was used as substrate and OD was measured at 490 nm by a Biotek 800 TS Absorbance Reader

3.2.5. Histopathology and immunohistochemistry

Vaccination sites, lungs, and spleens were collected into 10% neutral buffered formalin and fixed for a minimum of 48 hours. Tissues were serially trimmed (2-4 sections per tissue) and placed in cassettes before submission to AML Laboratories (Jacksonville, FL, USA) for processing, embedding, and sectioning at 5 µm. Slides were stained with hematoxylin and eosin (HE). Histopathology of vaccine sites was assessed on de-identified, HE-stained slides using semi-quantitative scoring by a board-certified veterinary pathologist. Vaccine sites were scored from 0-5 based on lesion size, immune cell infiltrate, and areas of suppurative necrosis. Briefly, 0: no lesions, 1: minimal immune cell infiltrate, 2: mild, focal immune cell infiltrate, 3: moderate multifocal immune cell infiltrate, 4: moderate to severe, diffuse immune cell infiltrate, 5: severe, diffuse immune cell infiltrate with areas of suppurative necrosis.

For immunohistochemistry (IHC), unstained slides were deparaffinized and rehydrated by incubating in three washes of xylene, three washes of 100% ethanol, and one wash in 95% ethanol, 70% ethanol, 50% ethanol, and deionized water for 3 minutes each. Slides were then incubated in 3% hydrogen peroxide at room temperature for 10 minutes. Antigen retrieval was performed by incubated slides in Tris-EDTA buffer (10mM Tris Base, 1 mM EDTA, 0.05% Tween 20, pH 9.0) at 100°C for 20 min followed by washing in tap water for 10 min. Slides were blocked in TBS with 1% powdered milk for 2 hours. Primary antibodies were diluted in TBS with 0.5% bovine serum albumin (BSA) and applied to slides for 2 hours at room temp or overnight at 4°C. Slides were washed in TBS with 0.025% Triton-X 100 then incubated with HRP-conjugated goat anti-rabbit IgG diluted in TBS with 0.5% BSA for 2 hours at room temp or overnight. For fluorescence, Tyramide Reagents (Thermofisher) were applied to the slide per manufacturer directions for 10 min at room temp, then antigen retrieval was repeated for 2 min to strip antibodies before repeating the antibodies for the next antigen. Finally, TrueVIEW Autofluorescence Quenching Kit with DAPI (Vector, cat. SP-8500) was used to decrease autofluorescence, stain nuclei with DAPI and coverslip the slides. Slides were allowed to cure overnight at room temp.

HE-stained and IHC slides were scanned at 20X magnification using an Olympus VS120 Slide Scanner (Integrated Microscopy and Imaging Laboratory, Texas A&M University). For HE slides, brightfield images were collected. For fluorescent slides, DAPI, FITC, and TxRed channels were used to acquire images. Lesion measurements and cell counts on slide images were performed using QuPath v0.2.0-m8[132]. Neutrophils,

macrophages, and lymphocytes were evaluated by morphology and quantified by counting cells within ten representative 100 μm^2 fields on H&E. For CD3+ T cells and CD19+ B cells, all cells within the lesions area were quantified using positive cell analysis on IHC slides.

Primary antibodies were purchased from Cell Signaling Technology: anti-CD3ε (D7A6E) and anti-CD19 (D4V4B). HRP-conjugated Goat anti-rabbit IgG (Novus Biologicals) diluted 1:1000 was used as the secondary antibody. Fluorescent Tyramide Regents (Thermofisher) used were AlexaFluor 488 and AlexaFluor 555 or AlexaFluor 594.

3.2.6. Flow Cytometry

For spleens, single cell suspensions were produced by pressing spleens through a 70 µm cell strainer in cold 3 mL FACs buffer (PBS with 2% fetal bovine serum, 0.1% NaN3, pH 7.2) then washing with FACs buffer. Splenocytes were centrifuged then resuspended in ACK Lysing Buffer (Thermofisher) for 1 min to remove red blood cells. Cells were resuspended in 1 mL RPMI complete and an aliquot was mixed with 10 µL trypan blue to quantify cells using a Countess II (Thermofisher). Splenocytes were then diluted to 10^7 cells/mL.

For vaccination sites, a 10 mm punch biopsy was used to collect the skin and subcutis at the elicitation site. Using a razor blade the subcutis and dermis were scraped from the overlying epidermis and placed in a gentleMACS C-tube for processing using the gentleMACS mouse adipose tissue dissociation kit (Miltenyi Biotec). Vaccine sites were dissociated using the Miltenyi Biotec gentleMACS Octo Dissociator with heaters.

Cell suspensions were centrifuged and resuspended in 1 mL RPMI complete and cells were quantified as above then diluted to 10^7 cells/mL.

Cells were centrifuged and resuspended in 1:1000 anti-mouse CD16/CD32 in FACs buffer and incubated on ice for 10 min. Next cells were stained with 1 µL/mL Zombie Violet or Zombie Aqua live/dead dye (Biolegend) and incubated on ice for 5 min. Cells were then incubated in fluorochrome-conjugated cell surface antibodies on ice for 30 min. For intracellular staining, cells were fixed and permeabilized using FoxP3/Transcription Factor Staining Buffer Set (eBioscience) followed by incubation with intracellular antibodies for 30 min on ice. Cells were then resuspended in FACs buffer and kept at 4°C until analysis. For intracellular cytokine and FoxP3 expression, cell suspensions from spleens and vaccine sites were aliquoted into a round-bottomed 96-well plate with or without 20 µg/mL WCV and cultured for 18 hours at 37°C with 5% CO_2 followed by the addition of GolgiPlug (BD Biosciences) for 6 hours prior to antibody staining.

Flow cytometric antibodies include CD3ε-PE/Cy7, CD8-FITC, CD4-APC/Cy7, IL17a-BV711, IFNγ-APC, IL4-PE, FoxP3-BV421, CD69-BV711, CD44-PE, and CD62L-APC (BioLegend). Cells were counted using the BD LSRFortessa X-20 Flow Cytometer and analyzed using FlowJo v10.6.2 (FlowJo LLC.).

3.2.7. Statistics

Statistical analyses were calculated using Prism v7.0 (GraphPad Software Inc.). Results were compared using one-way ANOVA with Dunnett's correction for multiple

comparisons. Differences were considered significant if p-value ≤ 0.05 (*), ≤ 0.01 (**), ≤ 0.001 (***), or ≤ 0.0001 (****).

3.3. Results

3.3.1. Sensitized mice produce local reactogenic responses to Cb WCV

Guinea pigs are the current animal model of choice for evaluation of hyper-reactive lesions to Cb vaccines, however, antibodies targeting guinea pig cell markers are limited which inhibits immunologic investigation of these responses. To develop our mouse model, we tested the ability to reproduce Cb reactogenic responses in SKH1(SK), C57Bl/6 (C57), and BALBc (BAL) mice. SK mice are outbred, immune-competent, and hairless due to a mutation in the *Hr* gene[133]. C57 and BAL mice were chosen as Th1- and Th2-biased strains, respectively, to compare responses by immunophenotype[134]. C57, BAL, and SK mice (n=4-5/group) were sensitized to Cb by intratracheal inoculation with 10^5 or 10^6 GE Cb RSA493 (NMI), by SC vaccination with 50 µg WCV in 50 µL sterile PBS (WCV), or by SC vaccination with 50 µL sterile PBS (PBS). Mice were monitored for 14 days post-sensitization by measuring weight change. Infection-sensitized SK and C57 mice showed transient weight loss followed by recovery by day 14 while infection-sensitized BAL, all vaccination-sensitized, and all control groups showed no overt weight loss over the observation period (Fig. 3.1A). For elicitation, mice were given a SC vaccination of 10 µg WCV in 50 µL sterile PBS and PBS alone into the right and left flanks, respectively, and vaccination sites were monitored for swelling and erythema daily for 14 days until euthanasia. Day 14 post-elicitation was chosen as the endpoint based on previous reports and our own work in guinea pigs showing induration is most severe at approximately 11-

15 days post-vaccination[80]. Mice in all experimental groups showed no evidence of weight loss during elicitation (Suppl. Fig. 1).

Blood samples were collected prior to sensitization (pre-sensitization), one day before elicitation (post-sensitization), and at necropsy (post-elicitation) to evaluate antigen-specific antibody formation in serum as a measure of sensitization. Anti-Cb IgG titers showed seroconversion at post-sensitization and post-elicitation time points in both infection- and vaccine-sensitized groups in all mouse strains. SK and BAL mice as well as infection-sensitized C57 mice produced IgG titers of ≥1:1600. Vaccine-sensitized C57 mice produced modest IgG titers of 1:200. No anti-Cb IgG titers were detected in unsensitized controls at any time point (Fig. 3.1B).

A

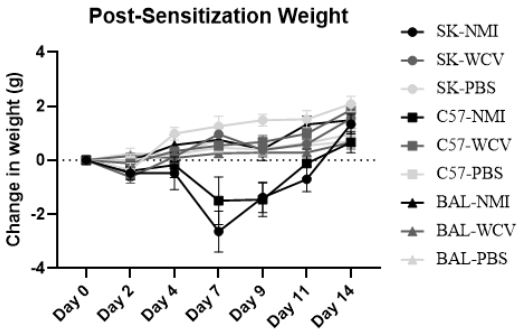

B

Anti-*C. burnetii* IgG Titers

Vaccine Groups	Pre-Sensitization	Post-Sensitization	Post-Elication
SK-NMI	0	3200	3200
SK-WCV	0	1600	1600
SK-PBS	0	0	0
C57-NMI	0	1600	1600
C57-WCV	0	200	50
C57-PBS	0	0	0
BAL-NMI	0	1600	3200
BAL-WCV	0	3200	3200
BAL-PBS	0	0	0

Figure 3.1 Weight and antigen-specific IgG responses to sensitization methods. A) Weight changes during 14 days post-sensitization. Infection-sensitized SK and C57 show transient weight loss. The graph shows the means of each group with error bars that represent the standard error of the mean, n=5 mice per group. B) Anti-Cb IgG responses to infection-, vaccine-, and sham-sensitized mice. Infection- and vaccine-sensitization produced similar IgG titers in SK and BAL mice. Vaccine-sensitized C57 mice produced reduced IgG response compared to infection-sensitized. Serum IgG results from pooled sera (n=5) represent values one standard deviation above the mean of negative control sera.

Focal swellings at the WCV site were observed beginning at day 8 in infection-sensitized and day 10 in vaccine-sensitized SK mice (Fig. 3.2A, Suppl. Fig. 1). Swellings were not observed grossly in the control SK mice or any of the C57 and BAL mouse groups, however, hair regrowth in both strains and skin pigmentation in C57 mice were common during the elicitation period and likely inhibited observation of gross lesions.

Vaccination sites were collected in formalin at 14 days post-elicitation for histopathology. HE-stained slides of vaccination sites showed more severe lesions in infection- and vaccine-sensitized C57 and SK mice compared to unsensitized controls, but vaccine lesions in BAL mouse groups did not significantly differ (Fig. 3.2B). Local reactive lesions consisted of infiltrates of macrophages, neutrophils, and lymphocytes with multifocal areas of suppurative necrosis and degeneration (Fig. 3.2C). Infection- and vaccine-sensitized lesions in C57 and SK mice did not significantly differ by the type of cellular infiltrate or overall severity of lesions.

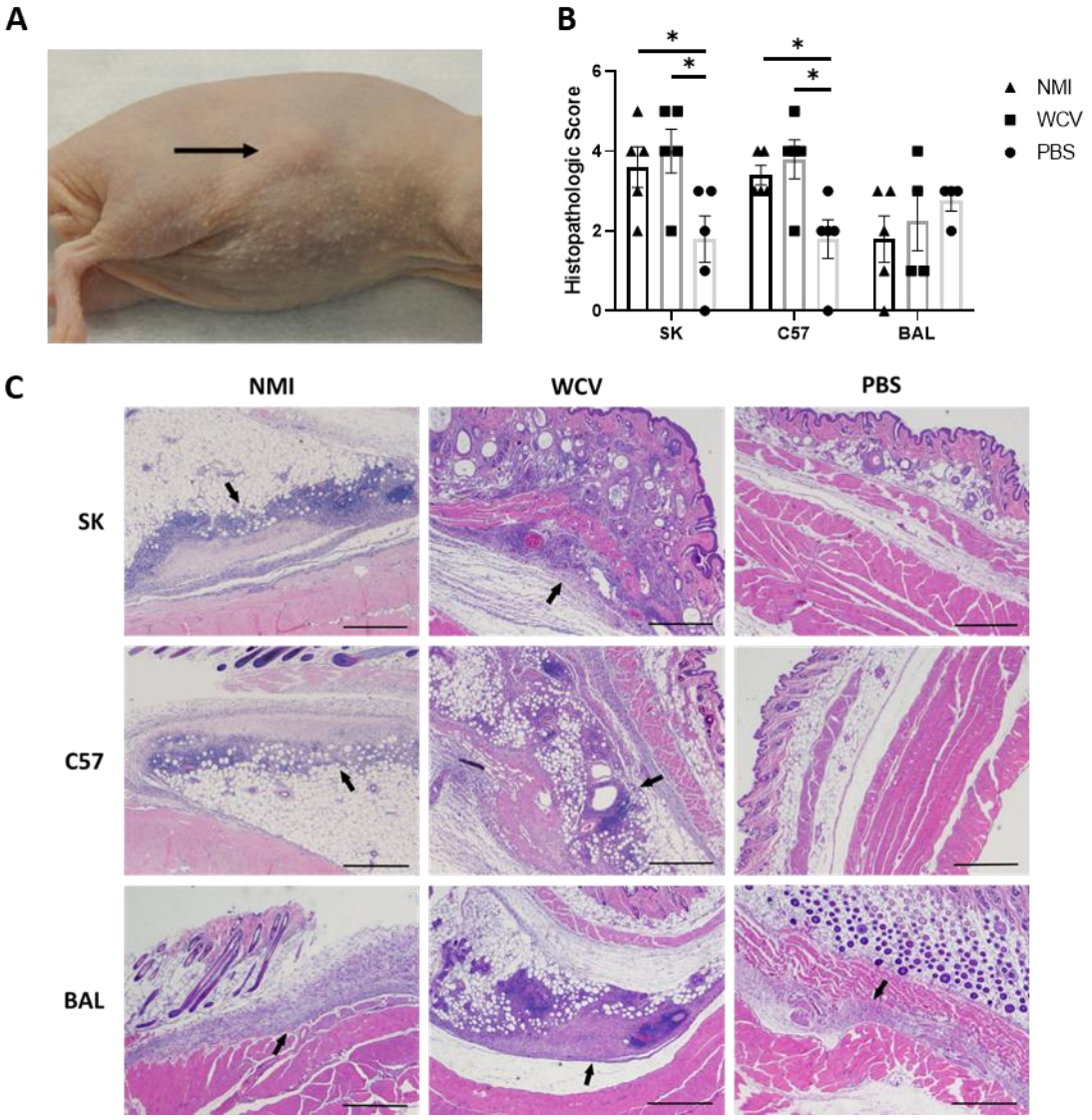

Figure 3.2 Responses to WCV in sensitized and unsensitized mice.
A) Example of the local induration observed in SK mice, day 14 post-elicitation (arrow). B) Histopathologic scores of local vaccination sites. Lesions are more severe in infection- and vaccine-sensitized C57 and SK mice. C) Representative histopathology of local vaccination sites. Marked local inflammation (arrow) is evident in infection- and vaccine-sensitized SK and C57 mice. BAL mice show variable inflammation with either sensitization method. 2x, HE stain. Graphs show the means of each group with error bars that represent the standard error of the mean, n=4-5 mice per group. Data were analyzed using one-way ANOVA with Dunnett's correction for multiple comparisons. Asterisks indicate significant differences between groups (*: $p<0.05$).

3.3.2. Severity of local WCV reactions is dose-dependent

Although Cb WCV reactogenicity is mainly associated with previous sensitization, higher doses of WCV can produce significant local inflammation through innate responses that may obscure the hypersensitivity response[89]. To target the hypersensitivity response, we continued by assessing multiple elicitation doses to determine which dose maximized the cellular influx produced by adaptive immunity without obscuring the lesions with excessive innate responses. C57 mice were sensitized with WCV or PBS as described above then administered a SC elicitation dose of 2 µg, 10 µg, 30 µg, and sterile PBS in a volume of 50 µL into either the right or left flank. At 14 days post-elicitation, vaccine sites were collected in formalin for histopathology and immunohistochemistry. Both sensitized and unsensitized groups showed dose-dependent responses to vaccination, however sensitized mice consistently showed significantly more severe responses than unsensitized mice at the same dose based on semi-quantitative scoring of HE-stained slides(Fig. 3.3A-B). However, the mean size of the lesions only significantly differed between sensitization groups at the 30 µg dose (Fig. 3.3C). Interestingly, suppurative necrosis was only evident in sensitized mice at the 10 µg and 30 µg doses (Figure 3.3C). Individual cell counts of neutrophils, lymphocytes, and macrophages showed variable differences within dose groups. Neutrophils were increased in sensitized mice compared to unsensitized mice at all doses, while macrophages were only increased at the 2 µg dose and lymphocytes were only increased at the 10 µg dose when comparing sensitization (Fig. 3.4A).

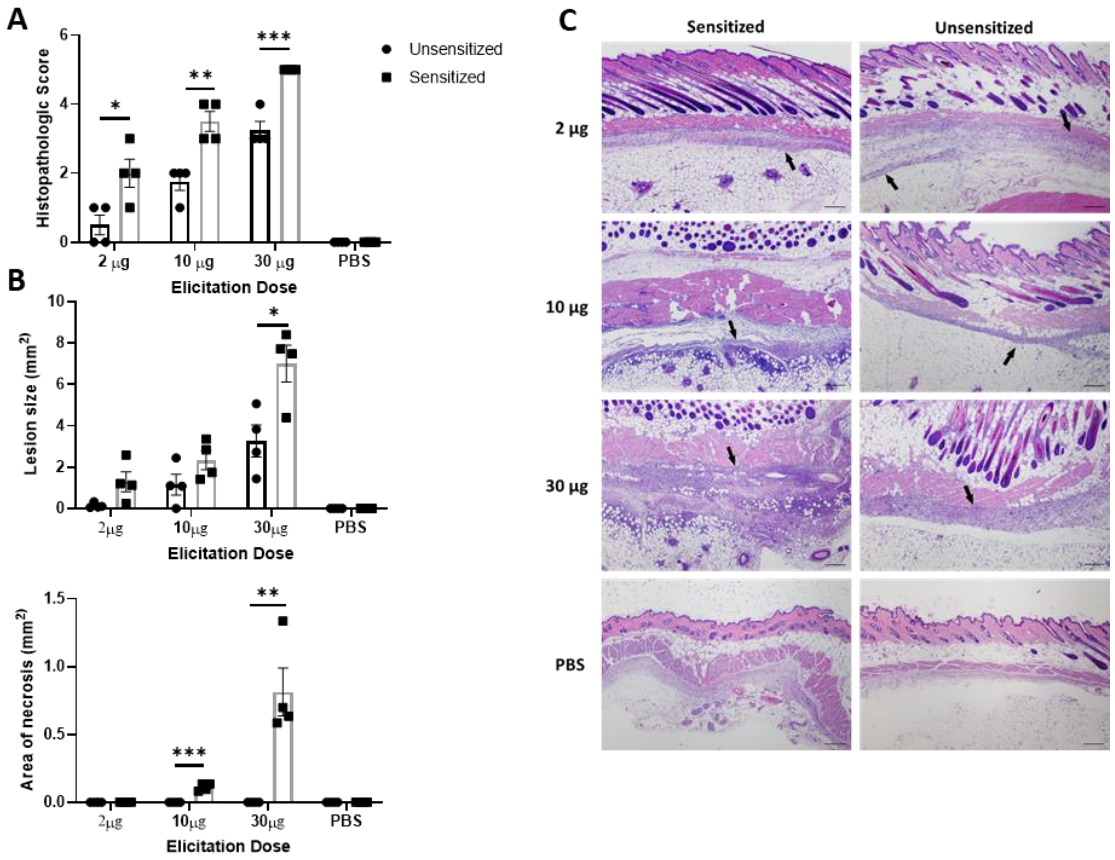

Figure 3.3 Severity of vaccine site reactions to Cb WCV are dose-dependent.
A) Histopathologic scores of local vaccination sites. Reactions are significantly more severe in sensitized mice with at all doses evaluated. Local reactions are dose-dependent in both sensitized and unsensitized mice. B) Lesion size and area of necrosis in local reaction sites. Only 30 µg dose showed significantly greater lesion size when comparing sensitized to unsensitized mice. Necrosis was only evident in sensitized mice at 10 µg and 30 µg doses. C) Representative histopathology sections from each dose group showing dose-dependent amounts of inflammatory infiltrate (arrows). 2x, HE stain. Graphs show the means of each group with error bars that represent the standard error of the mean, n=4 mice per group. Data were analyzed using one-way ANOVA with Dunnett's correction for multiple comparisons. Asterisks indicate significant differences between groups (*: $p<0.05$, **: $p<0.01$, ***: $p<0.001$).

Immunohistochemistry was used to further differentiate lymphocytes into CD3+ T cells and CD19+ B cells. At the 10 µg dose, both B and T cells were significantly

increased in sensitized mice compared to unsensitized, but there was no difference in these populations at the 30 µg dose (Fig. 3.4B). In all sections, T cells were distributed evenly throughout the lesion except in deep, often perivascular, clusters of lymphocytes forming ectopic lymphoid follicles (ELF) where they formed dense aggregates with CD19+ B cells. There were significantly more ELFs in sensitized mice at the 10 µg dose but not the 30 µg dose (Fig. 3.4C) compared to unsensitized mice. In contrast, B cells were only present within ELFs (Fig. 3.4D).

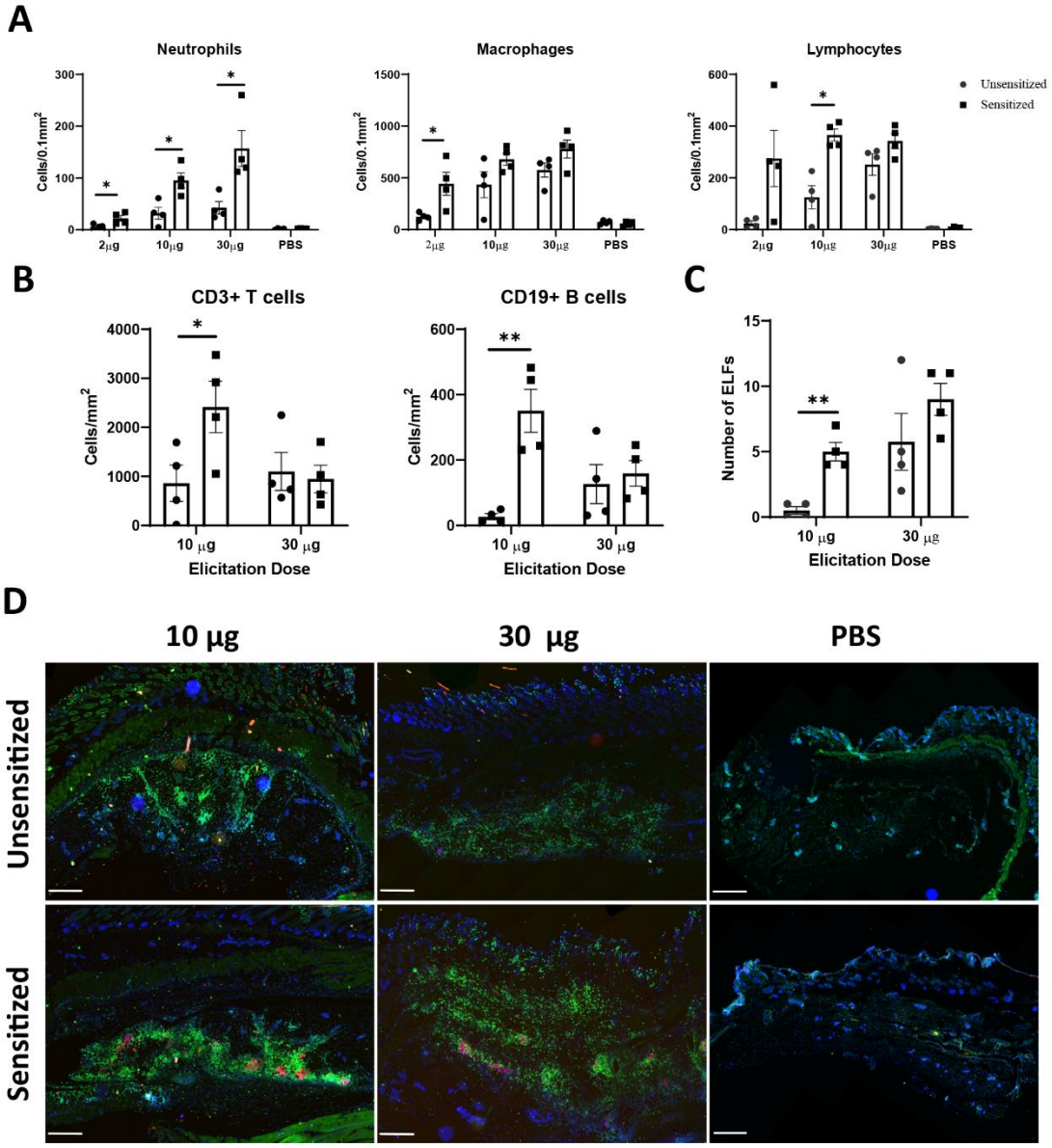

Figure 3.4 Immune cell infiltrate and ELF formation depend on both sensitization status and elicitation dose.

(A) Numbers of cells within a 0.1 mm^2 area of each vaccine site. Neutrophils were increased at all doses, however only the 10 μg dose showed significantly different lymphocyte numbers. Cells were defined by morphology and counted manually within ten representative 100 μm^2 fields on HE stained slides. (B) Both T and B cell numbers are significantly greater in sensitized mice at the 10 μg dose, but not the 30 μg dose. Cells were counted using QuPath based on fluorescence immunohistochemistry results. (C) Total numbers of ELFs within vaccine reaction sites. Sensitized mice develop more ELFs at the 10 μg dose. (D) Representative IHC from vaccine sites of unsensitized and

sensitized mice from 10 µg, 30 µg, and PBS injection sites. CD3+ T cells are diffusely distributed throughout the lesion while CD19+ B cells are confined to clusters within ectopic lymphoid follicles. 2x, anti-CD3 (green), anti-CD19 (red), nuclei (blue), bar=500 µm. Graphs show the means of each group with error bars that represent the standard error of the mean, n=4 mice per group. Data were analyzed using one-way ANOVA with Dunnett's correction for multiple comparisons. Asterisks indicate significant differences between groups (*: $p<0.05$, p<**:0.01).

3.3.3. WCV reactions induce local influx of IFNγ+ and IL17a+ CD4 T cells

Because delayed-type hypersensitivities are mediated by T cells and experiments showed a marked influx of CD3+ T cells on immunohistochemistry of vaccine site lesions, we used flow cytometry to further characterize the types of T cells that are increased during WCV reactogenic responses both locally and systemically. To do so, we extracted cells from the vaccine sites and spleens of mice at 14 days post-elicitation. Vaccine-sensitized and unsensitized mice as described above were vaccinated SC at four separate sites in the right and left flank, then spleens and vaccine sites were collected at 14 days post-elicitation. The four vaccine sites from each mouse were pooled prior to cell separation for flow cytometric evaluation. The 10 µg elicitation dose was chosen for these experiments since this dose produced maximal differences in lymphocyte responses between sensitization groups. Extracted cells were stimulated with WCV and stained for surface markers and expression of IFNγ, IL4, IL17a, and FoxP3 as markers for Th1, Th2, Th17, and Treg cells, respectively. Unsensitized mice elicited with injections of PBS only were used to compare responses to normal cell populations in the skin and spleen (Sham).

Local vaccine sites showed marked influx of total cells and T cells compared to unsensitized and sham mice (Figure 3.5A-B). CD4 and CD8 T cells in sensitized mice were similarly increased at vaccine sites compared to unsensitized and sham groups

(Figure 3.5A-B). Evaluation of cytokine production by CD4 T cells in sensitized mice showed a significant increase in IFNγ production compared to the sham group but not unsensitized mice. Although the mean of IFNγ+ CD4 T cells in unsensitized mice was increased compared to sham mice, this result was not significant (p=0.0818) (Fig. 3.6A-B). Similarly, CD4+ IL17a-secreting cells were elevated in sensitized mice compared to unsensitized and sham mice (Fig. 3.6A-B). However, unsensitized mice did not have an increase in IL17a-secretion by CD4+ T cells compared to sham mice. In contrast, IL4+ CD4 T cells were significantly decreased in sensitized mice compared to sham (Fig. 3.6A-B). FoxP3+ CD4 T cells and production of IFNγ, IL4, and IL17a by CD8+ T cells did not significantly differ between experimental groups (Fig. 3.6A-B, Suppl. Fig. 2).

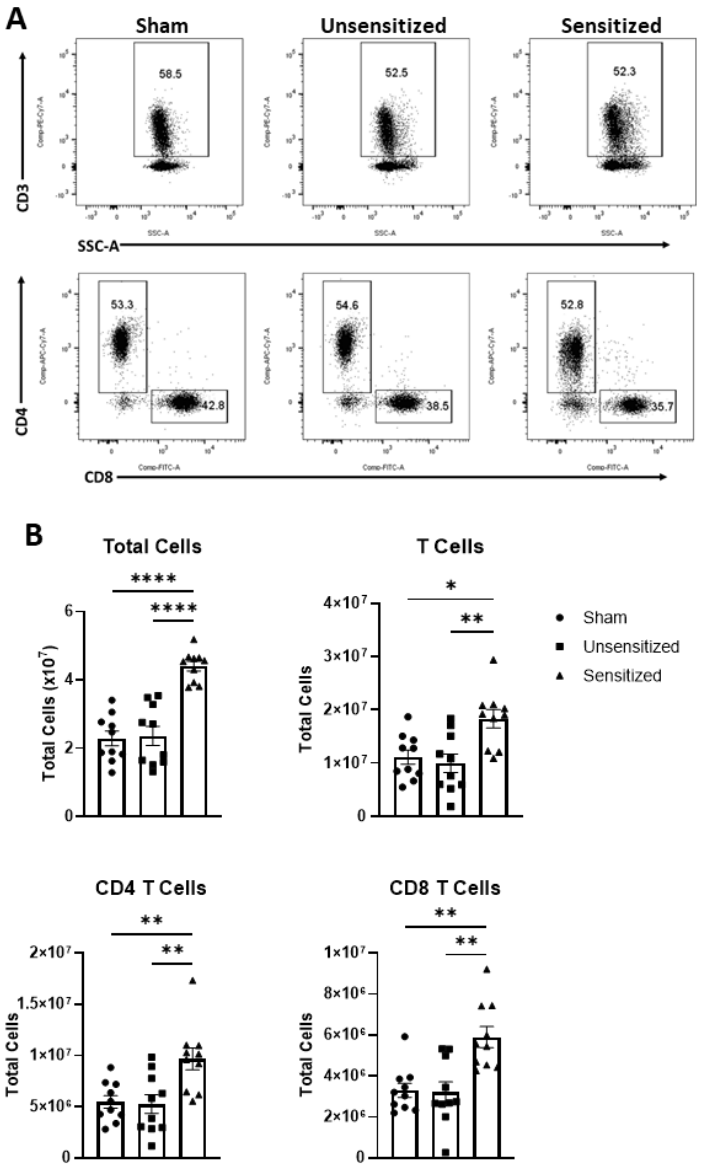

Figure 3.5 Vaccine site reactions in sensitized mice have an influx of CD4 and CD8 T cells.

A) Gating Strategy for evaluation of T cells and subpopulations in vaccination sites. B) Total cell numbers for all cells, CD3+ T cells, CD3+CD4+ T cells, and CD3+CD8+ T cells. Sensitized mice show a marked increase in all cell groups. Graphs show the means of each group with error bars that represent the standard error of the mean. Cell counts are the sum of four vaccination sites from each mouse. Data are the result of two experiments, n=10 mice per group. Data were analyzed using one-way ANOVA with Dunnett's correction for multiple comparisons. Asterisks indicate significant differences between groups (*: $p<0.05$, **: $p<0.01$, ****: $p<0.0001$).

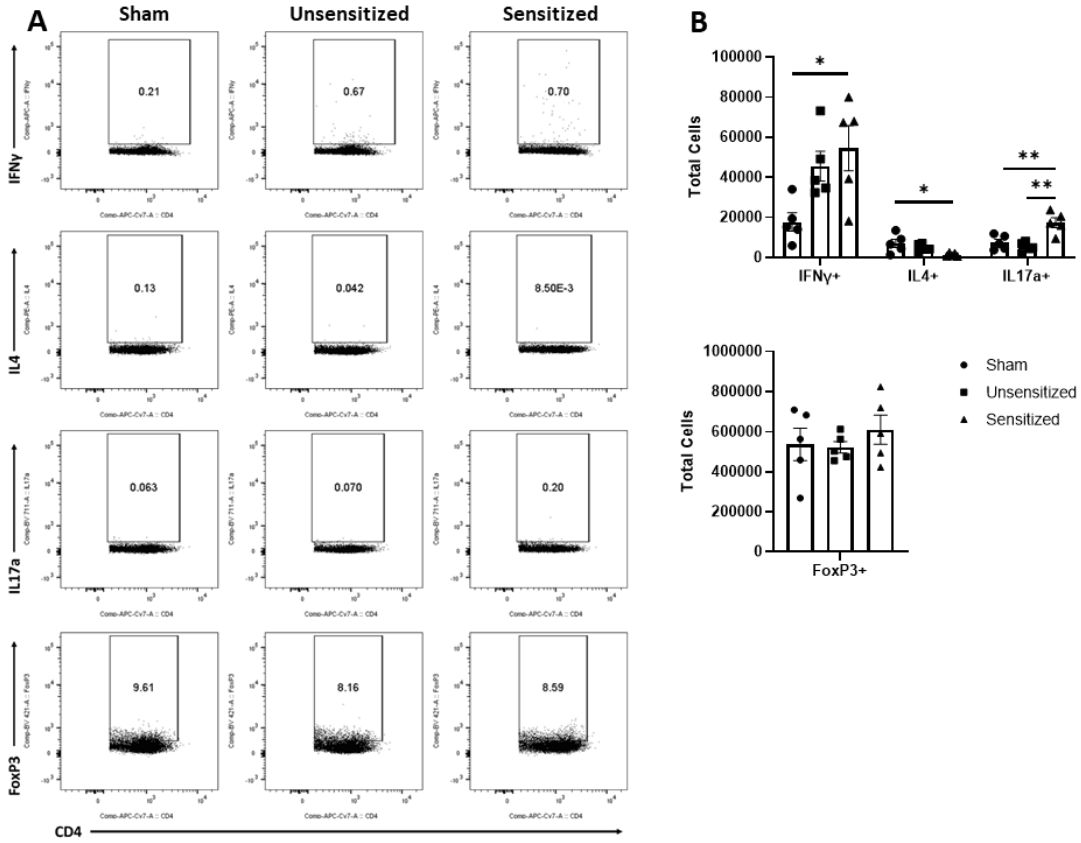

Figure 3.6 CD4 T cells within vaccine reactions in sensitized mice are IFNγ+ and IL17a+.
A) Representative gates for cytokine production and FoxP3 expression by CD4+ T cells. B) Total CD4+ T cells expressing IFNγ, IL4, IL17a, and FoxP3 (Treg). IFNγ and IL17a expression from sensitized mice are significantly increased compared to sham while IL4 expression is significantly decreased. No differences in numbers of FoxP3+ CD4 T cells are observed between experimental groups. Graphs show the means of each group with error bars that represent the standard error of the mean. Cell counts are the sum of four vaccination sites from each mouse, n=5 mice per group. Data were analyzed using one-way ANOVA with Dunnett's correction for multiple comparisons. Asterisks indicate significant differences between groups (*: $p<0.05$, **: $p<0.01$).

We next evaluated the local effector, central, and resident memory T cells populations within vaccine sites using the surface markers CD44, CD62L, and CD69. CD44 is upregulated in activated T cells and is important for recruitment to sites of

inflammation while CD62L is a lymph node homing receptor[135]. CD44+CD62L+ central memory T cells (T_{CM}) normally circulate within the blood and lymphoid tissues and rapidly expand in response to antigen re-stimulation while CD44+CD62L- effector memory T cells (T_{EM}) home to peripheral tissues in response to chemoattractants and produce cytokines in response to re-stimulation[136,137]. Similar to T_{EM}, resident memory T cells (T_{RM}) downregulate CD62L but also upregulate CD69 which sequesters sphingosine 1-phosphate receptor 1 (S1PR1) preventing tissue egress. This causes T_{RM} to remain within the peripheral tissues after sensitization to provide tissue-specific immune memory[136,138]. Evaluation of memory T cell populations from vaccine sites showed significant increases in CD4 and CD8 T_{EM} and T_{CM} populations in sensitized mice compared to unsensitized and sham controls (Fig. 3.7A-B). CD4+ T_{RM} from sensitized mice were also significantly increased compared to unsensitized and sham controls, while CD8+ T_{RM} from sensitized mice were significantly increased compared to sham mice but not unsensitized mice. There were no significant differences in memory T cell populations between unsensitized and sham mice.

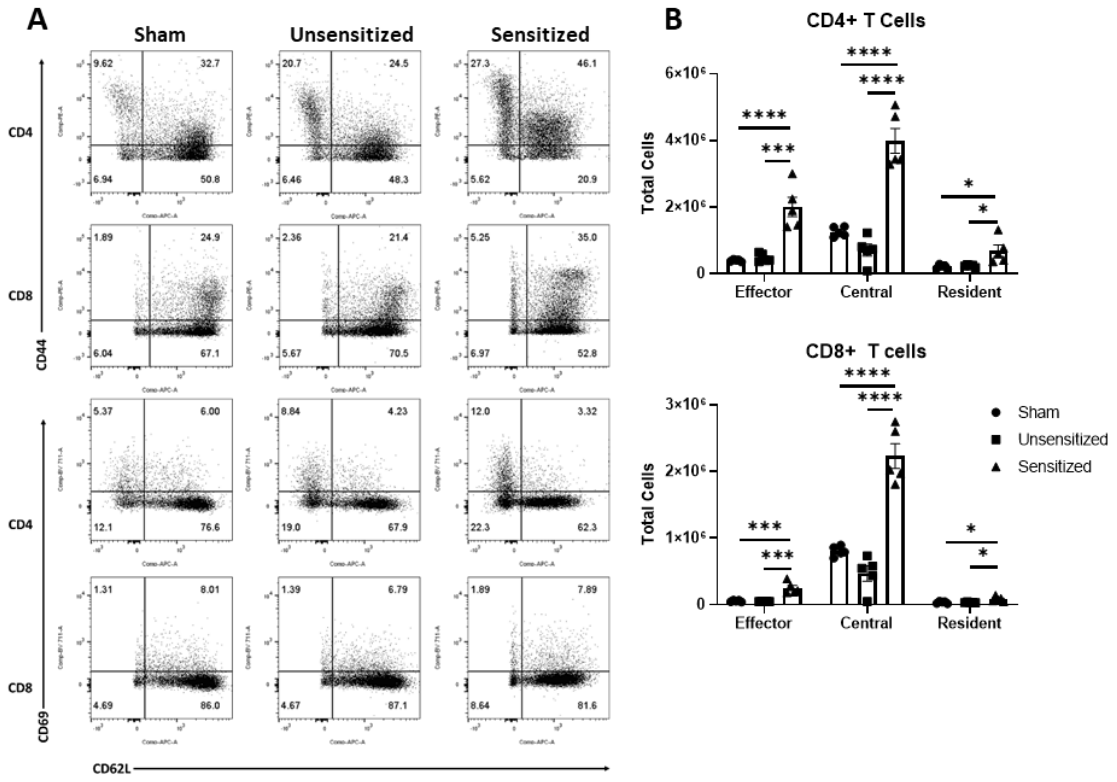

Figure 3.7 Vaccine site reactions in sensitized mice have increased of both CD4 and CD8 memory T cells.

A) Representative flow cytometry gates for evaluation of CD4+ and CD8+ T_{EM}, T_{CM}, and T_{RM} cells from vaccine sites. B) Total cell counts of memory T cells from vaccination sites. Locally, there is expansion of effector, central, and resident memory CD4 and CD8 T cells in sensitized mice compared to unsensitized and sham groups. Graphs show the means of each group with error bars that represent the standard error of the mean. Cell counts are the sum of four vaccination sites from each mouse, n=5 mice per group. Data were analyzed using one-way ANOVA with Dunnett's correction for multiple comparisons. Asterisks indicate significant differences between groups (*: $p<0.05$, ***: $p<0.001$, ****: $p<0.0001$).

3.3.4. WCV reactions produce systemic expansion of IFNγ- and IL17a-producing CD4+ T cells

WCV reactogenic responses reported in humans are not confined to the vaccine site and may manifest as fever, fatigue, malaise, and joint pain[47,79]. To determine if these systemic

responses are reflected in systemic T cell expansion and activation, we also evaluated T cell subpopulations extracted from spleens of sensitized, unsensitized, and sham mice at 14 days post-elicitation. The total numbers of cells extracted from the spleens of mice did not significantly differ between experimental groups (Fig. 3.8B). Evaluation of splenocytes showed a decrease in the proportion of CD4 T cells in sensitized compared to unsensitized and sham controls in response to elicitation (Fig. 3.8A-B). Both CD4 and CD8 T cells showed significant increases in the proportions of T_{CM} compared to unsensitized and sham groups (Fig. 3.8A-B). CD8+ T_{EM} from sensitized mice were decreased compared to sham but not unsensitized mice, while CD4+ T_{EM} did not differ among groups (Fig. 3.8A-B).

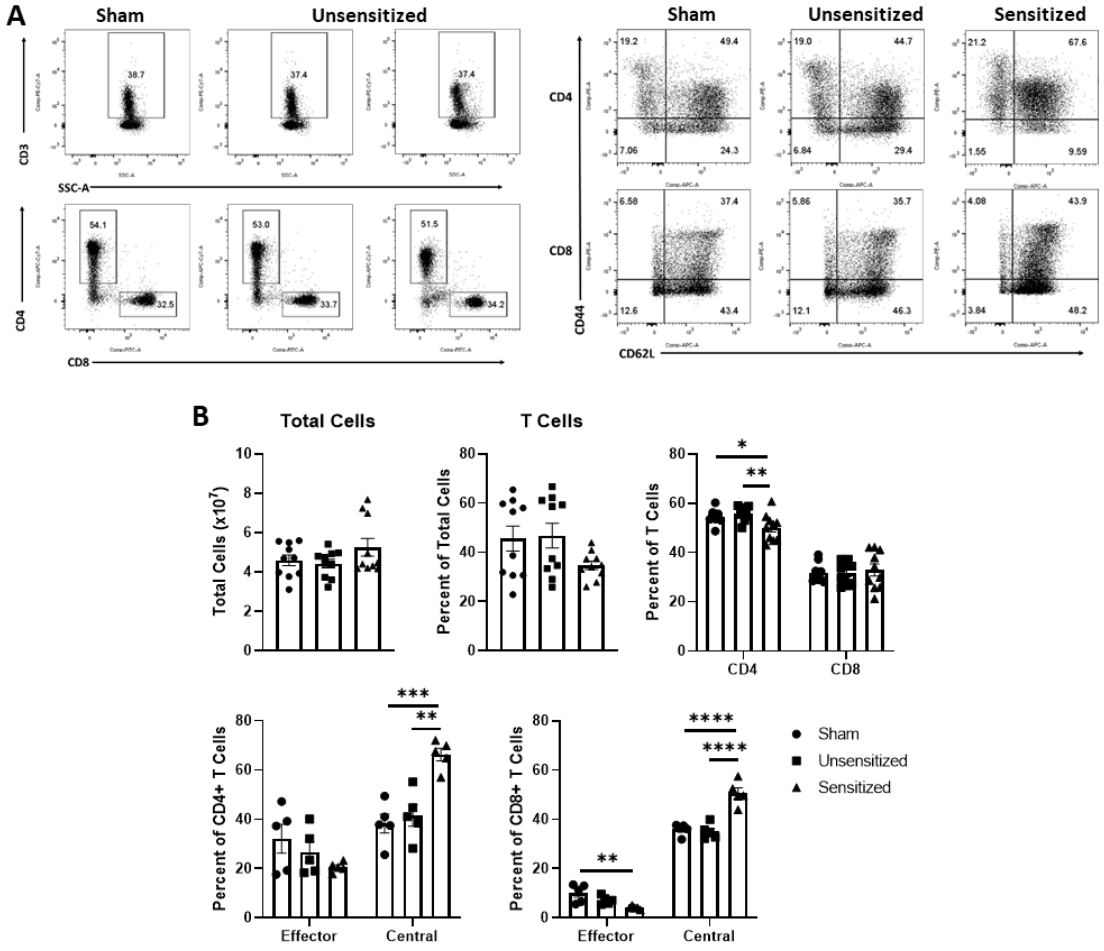

Figure 3.8 Systemic central memory T cells are expanded in sensitized mice.
A) Representative flow cytometry gates for CD3+ T cells, CD4+ and CD8+ T cells, and CD44+CD62L- T_{EM} and CD44+CD62+ T_{CM} of cells extracted from spleens. B) Summary graphs showing the total cells extracted from spleens and the numbers of T cell populations expressed as a percentage of the parent group. Total cells extracted from spleens show no significant differences, however both sensitized mice show a mild decrease in the proportion of CD4 T cells in the spleen compared to controls. Both CD4 and CD8 T cells from sensitized mice show significant increases in T_{CM} compared to unsensitized and sham groups. CD8 T_{EM} from sensitized mice are significantly decreased compared to sham mice. Graphs show the means of each group with error bars that represent the standard error of the mean, n=5 mice per group. Data were analyzed using one-way ANOVA with Dunnett's correction for multiple comparisons. Asterisks indicate significant differences between groups (*: $p<0.05$, **: $p<0.01$, ***: $p<0.001$, ****: $p<0.0001$).

Similar to local vaccine sites, splenic CD4 T cells from sensitized mice produced significantly more IFNγ+ and IL17a+ cells compared to unsensitized and sham controls. CD4 T cells from sensitized mice also showed significantly less IL4+ cells than sham mice (Fig. 3.9A-B). FoxP3+ CD4 T cells did not differ across experimental groups (Fig. 3.9A-B). Among CD8 T cells in the spleen, IFNγ+ cells were significantly increased in unsensitized mice compared to sensitized mice, but not sham mice. There were no significant differences in IL4+ and IL17a+ CD8 T cells among experimental groups (Suppl. Fig. 3).

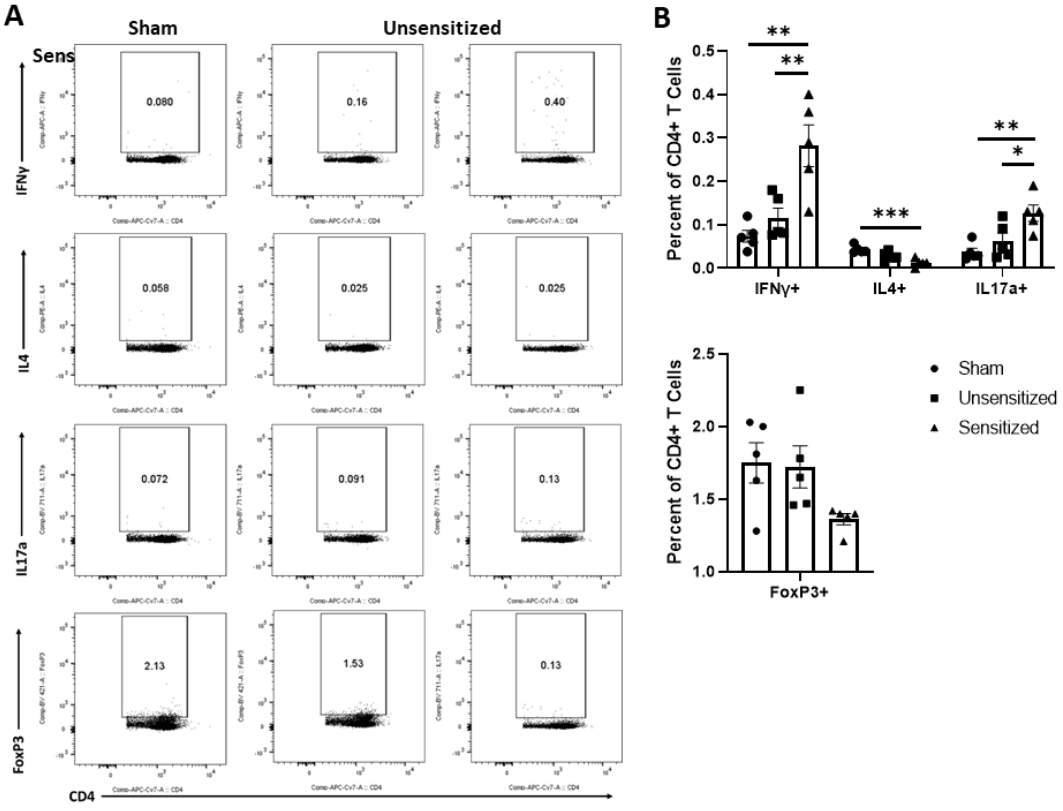

Figure 3.9 Sensitized mice show systemic increases in IFNγ+ and IL17a+ CD4 T cells. A) Representative flow cytometry gates for IFNγ, IL4, IL17a, and FoxP3 expression by CD4+ T cells from spleens. B) Summary graphs of IFNγ, IL4, IL17a, and FoxP3 expression. CD4+ T cells show an increase in IFNγ+ and IL17a+ cells in sensitized mice compared to unsensitized and sham groups. Sensitized mice also display reduction in IL4-expressing CD4+ T cells compared to sham mice. FoxP3+ Tregs do not significantly differ across experimental groups. Graphs show the means of each group with error bars that represent the standard error of the mean, n=5 mice per group. Data were analyzed using one-way ANOVA with Dunnett's correction for multiple comparisons. Asterisks indicate significant differences between groups (*: $p<0.05$, **: $p<0.01$, ***: $p<0.001$).

3.4. Discussion

Cb WCV reactogenic responses have long stood as a barrier to the widespread availability of protective vaccines against Cb infection[80,128]. Despite the importance of preventing

adverse responses to vaccination in developing novel vaccines, little is understood about the pathogenesis of these reactions. Although guinea pigs are the current animal model of choice to evaluate reactogenicity of novel vaccine candidates, the lack of guinea pig-specific markers limits investigation of vaccine reactions in this species[80,89,128]. To facilitate immunologic evaluation of local and systemic Cb reactogenic responses, we tested the ability of three strains of mice: SKH1, C57Bl/6, and BALB/c, to produce reactions to WCV, with and without prior sensitization, similar to those described in humans.

SK and C57 mice produced significant local reactions after infection- and vaccine-sensitization. Local responses were only observable grossly in SK mice, despite hair removal in C57 and BAL strains, making SK strain mice a potential alternative model for gross and histologic evaluation of reactogenicity in novel Cb vaccine candidates. In contrast, sensitized BAL mice did not produce more severe local reactions compared to unsensitized controls despite developing high anti-Cb IgG titers after sensitization. Since BAL mice have a Th2-skewed immunophenotype where C57 and SK mice are Th1-skewed, this gave an early indication that Cb WCV reactions are likely Th1-mediated[133,134]. Histologically, local lesions did not differ in severity or quality of the granulomatous inflammation based on sensitization method. While all tested elicitation doses produced significantly more severe reactions in sensitized mice, the 10 µg dose provided the most dramatic differences in lymphocyte infiltration between sensitization groups, indicating that this would be the best dose for later evaluation of adaptive T cell responses within vaccine reaction sites. Although both SK and C57 mice readily produced

significant hyper-reactive lesions to vaccination with WCV, C57 mice were chosen for subsequent experiments because of their inbred background and the wide variety of available congenic strains that will allow for future investigation of the immunologic mechanisms of Cb WCV reactogenicity.

To investigate the pathogenesis of local and systemic Cb reactogenic responses, T cell subpopulations isolated from the vaccine sites and spleens were evaluated by flow cytometry. Within vaccine sites, a significant increase in IFNγ+ CD4 T cells was observed in sensitized mice, indicating a Th1 type response. Canonically, Th1 cells enhance M1 macrophage polarization which increases ROS production, phagocytic activity, and induces production of cytokines that recruit neutrophils and stimulate Th1 and Th17 cells[139]. On histopathology, WCV reactive lesions show infiltrations of activated macrophages, neutrophils, and lymphocytes with central areas of suppurative necrosis. Thus, the results of our evaluation of local T cell subpopulations concur with the morphology of the local lesions and infiltrating immune cells described in our earlier experiments. Traditionally, CD4 T cells were thought to mediate cutaneous hyper-reactive responses, however, studies in contact hypersensitivity have shown that either CD4 or CD8 cells may facilitate these responses[130,140,141]. The results of this work suggest that WCV reactogenicity is mediated by CD4 T cells, however, effector CD8 T cells may cause lesions by production of molecules other than the ones assessed here, such as granzyme B and perforin[142,143]. Further work is necessary to determine whether CD8 T cells play a significant role in Cb WCV reactogenic responses.

Locally, we also observed increased numbers of CD4+IL17a+ Th17 cells in sensitized mice but not unsensitized or sham mice. Th17 cells have been associated with severe lesions in hyper-reactive responses as well as auto-immune diseases[144,145]. These cells produce IL17a and other cytokines that enhance neutrophil activation and recruitment[136,146,147]. In our experiments, although neutrophils were present in vaccine sites of both sensitized and unsensitized mice, areas of suppuration and necrosis were only evident in sensitized mice. This suggests that Th17 cell activation is necessary for suppuration of neutrophils and abscess formation in Cb WCV reactions. Additionally, Th17 cells have been associated with the formation of ELFs through their production of IL17 and IL22. ELFs are areas of inducible lymphoid tissue that form in response to chronic antigenic stimulation and correlate with severity of inflammation in some diseases[146]. In our experiments, ELFs were present in both sensitized and unsensitized mice, but at the 10 µg elicitation dose, ELFs were more numerous in sensitized mice. Thus, although Th17 cells do not seem necessary to form ELFs in WCV reactogenic responses, they may enhance ELF formation at lower elicitation doses.

The effect of Treg cells on cutaneous hypersensitivity responses has been investigated in several studies on contact hypersensitivity[148–150]. Treg cells abrogate inflammation during elicitation of hypersensitivities by the production of IL10 and adenosine. This Treg response is considered essential for the resolution of inflammation in mouse models of contact hypersensitivity[148,149]. Our experiments showed no significant influx of CD4+FoxP3+ Treg cells in vaccine reactions and spleens of sensitized mice at 14 days post-elicitation compared to controls. This lack of Treg response during elicitation

despite the late time point is likely contributing to the prolonged inflammation. This is may be at least partially due to the Th17 response evident in sensitized mice. Treg cells form when naïve CD4 T cells are activated in the presence of transforming growth factor β1 (TGFβ). However, naïve CD4 T cells activated with a combination of low levels of TGFβ and high levels pro-inflammatory cytokines, such as IL1 and IL6, will form of Th17 cells instead[151]. Thus, Th17 cell activation prevents the formation of Treg cells at sites of severe inflammation. This process may explain the lack of Treg response in Cb WCV hypersensitivity reactions.

Our experiments showed local influx of central, effector, and resident memory CD4 and CD8 T cells during WCV reactogenic responses. Memory-inducing immune responses in peripheral tissues produce not only T_{CM} and T_{EM} but tissue-specific T_{RM} as well[64,129,152]. These memory T cell subpopulations likely develop from a common naïve T cell precursor[152]. In sites of inflammation, central memory and effector memory T cells may home to ELFs that form in peripheral tissues[153]. ELF formation was more frequent in sensitized mice at the 10 µg elicitation dose on histopathology and immunohistochemistry and can partially explain the local expansion of these T cell subpopulations. The increase in T_{EM} and T_{RM} suggests a role for both circulating and tissue specific memory T cell responses during elicitation of WCV reactogenic responses[129,152]. Since T_{RM} normally home to the originally affected tissue, it is reasonable to suspect that local reactions may be altered depending on the route of sensitization[64,137]. However, in our initial experiments, no differences were observed in the severity or the types of infiltrating immune cells in local reactions when comparing infection- and vaccine-sensitized mice.

In experiments on contact hypersensitivity, inhibition of T_{RM} causes a delayed hyper-reactive response during elicitation compared to controls indicating that although T_{RM} produce a more rapid response to re-stimulation, T_{RM} are not necessary to induce reactive lesions in the skin[152]. Interestingly, in our experiments, infection-sensitized SK mice began developing local induration two days earlier than vaccine-sensitized mice when elicited with WCV. However, infection-sensitized SK mice had higher anti-Cb IgG titers than vaccine-sensitized mice and this may simply reflect variability in the degree of sensitization. Understanding the roles of circulating and resident memory cells in mediating Cb WCV reactions warrants further studies.

To investigate systemic responses to WCV, we also evaluated changes in T cell populations within the spleen during elicitation. In humans, systemic reactions to Cb vaccination are frequent and include headache, lethargy, fever, and joint pain[47,79]. In our experiments, systemic responses during the elicitation phase were milder than local reactions, however the increase in IFNγ- and IL17a-producing CD4 T cells and expansion of central memory T cells in the spleens of sensitized mice indicate that Cb WCV reactogenic responses in mice are not confined to the local vaccine site. Elevations in several circulating cytokines have been implicated in systemic reactions to vaccination including IL1β, IL6, and tumor necrosis factor α (TNFα), as well as C-reactive protein[84]. Elevated IFNγ levels in serum have been correlated with systemic symptoms of reactogenicity at 7 days after vaccination with a modified live smallpox vaccine and after booster doses of a liposome adjuvanted hepatitis vaccine[154,155]. While IL1β, IL6, and TNFα are early innate mediators of inflammation, IFNγ is mainly secreted by activated T

cells, which may explain the delayed onset of reactions and reactions in boost, but not prime, doses of vaccines[84,142]. Although IL17a has not been implicated in systemic reactions to vaccines, elevations in systemic IL17a have been associated with disease severity in systemic auto-immune diseases in humans such as rheumatoid arthritis, systemic lupus erythematosus, and psoriasis and may be contributing to systemic adverse reactions to Cb WCV as well[145,147].

Here we presented a sensitized mouse model of Cb WCV reactogenic responses similar to vaccine reactions reported in humans. This mouse model may act as an alternate to the guinea pig model for evaluation of novel Cb vaccine candidates and be utilized for in-depth immunologic investigation of Cb WCV reactogenic responses. We went on to show that local Cb WCV-induced reactions in sensitized mice are characterized by an increase in IFNγ- and IL17a-producing CD4 T cells indicating a Th1-type hypersensitivity response. The similar increases in IFNγ+ and IL17a+ CD4 T cells in the spleens of sensitized mice suggest a potential pathogenesis for systemic reactogenic responses to Cb WCV reported in humans. Our work provides insights into the pathogenesis of Cb WCV reactogenic responses which will help guide the development of novel vaccines against Cb that are protective without causing adverse reactions.

4. MECHANISMS OF COXIELLA BURNETII WHOLE CELL VACCINE REACTOGENICITY

4.1. Introduction

Coxiella burnetii (Cb), an obligate intracellular bacterium, is the causative agent of the zoonotic disease Q fever[19]. Exposure to this pathogen most often results in mild or asymptomatic infections, however Q fever can present as several severe manifestations including myocarditis, placentitis, valvular endocarditis, and Q fever fatigue syndrome[22,24,27,28]. Endemic worldwide, except New Zealand and Antarctica, this pathogen is maintained in environments through persistent infections in domestic ruminants and camelids. Additionally, Cb is an exceptionally infectious pathogen, with an infectious dose of 1-10 bacteria in humans, transmission via aerosols, and exceptional resistance to heat and chemical disinfection[36,156,157]. This has resulted in Cb being designated a biosafety level 3 select agent by the Centers for Disease Control and Prevention due to concerns for its potential as a weapon of bioterrorism[91]. As such, an effective vaccination program is considered the best strategy to prevent infections and outbreaks of Q fever and crucial for ensuring the protection of military personnel.

Q-VAX® is a whole cell, formalin-inactivated vaccine against Q fever which is licensed for use in humans in Australia. A recent retrospective study on the efficacy of Q-VAX reported that this vaccine provides a protective efficacy of 94.37% compared to unvaccinated[43]. However, it is associated with a high rate of local and systemic adverse responses which prevents its approval in other countries. These adverse reactions to Q-

VAX are reported to be most severe and frequent in those with prior exposure to Cb. So, in order to reduce the risk of these reactions, individuals must undergo pre-vaccination screening including detection of anti-Cb titers and intradermal skin testing[157]. Despite the fact that these reactions have been reported in humans and animal models for several decades, the mechanisms and causes of these vaccine-associated hypersensitivity reactions are poorly understood.

Histopathologic assessment of the vaccine site reactions to the Cb WCV in humans and animal models shows pyogranulomatous and lymphocytic inflammation which is characteristic of a granulomatous, delayed-type hypersensitivity[74,89,158]. Delayed-type hypersensitivities are mediated by T cells, while the granulomatous component suggests that the inciting antigen is difficult to degrade or remove from the injection site[81]. Some investigators developing novel vaccines against Cb have begun to elucidate components of Cb whole cell vaccine (WCV) reactivity. Long et al. showed that vaccine reactions occur with both phase I and phase II-derived WCVs in a sensitized guinea pig model[73]. Phase II Cb is an attenuated strain characterized by a truncated lipopolysaccharide (LPS), while the virulent phase I Cb has a full-length LPS. Phase I LPS has been shown to be an important contributor to vaccine-mediated immunity with Cb WCV, but apparently does not significantly contribute to local reactogenicity[49,73]. Additionally, Fratzke et al. showed that an unadjuvanted subunit vaccine composed of six recombinant Cb antigens was not reactogenic in sensitized guinea pigs, however this vaccine strategy showed moderate to severe reactions when combined with a combination of squalene and toll-like receptor

agonist adjuvants[71]. This suggests that reactivity to a Cb vaccine requires innate immune stimulation.

We previously investigated the immunopathogenesis of Cb WCV reactions by characterizing the infiltrating immune cells in a sensitized mouse model[158]. Immune cells extracted from vaccine site reactions showed an influx of CD4+ and CD8+ T cells. The CD4+ T cells were IFNγ+ and IL17a+, indicating a Th1-mediated hypersensitivity reaction. However, the roles of these infiltrating T cells and cytokines in producing these local reactive lesions is still uncertain. Here we evaluated the roles of CD4+ and CD8+ T cells as well as the roles of IFNγ and IL17a in mediating Cb WCV reactions. Additionally, we show that injection of whole cell vaccine material derived from Cb leads to chronic persistence of antigen within the injection site which is likely contributing to the granulomatous component of local vaccine reactions.

4.2. Materials and methods

4.2.1. Vaccine Materials

WCV was produced by growing cultures of Cb Nine Mile Phase I (NMI) RSA493 in ACCM-2 media as previously described, then inactivated in 2% formalin for 48 hours[71,102]. Culture of live Cb NMI RSA493 was performed in biosafety level 3 (BSL3) facilities at the Texas A&M Health Science Center.

4.2.2. Experimental animals

Female C57Bl/6JHsd mice at 6-8 weeks old were purchased from Envigo (Huntingdon, UK) and female SKH1-Elite mice at 6-8 weeks old were purchased from Charles River Laboratories (Wilmington, MA). Mice were housed in microisolator cages under

pathogen-free conditions with ad-lib food and water. Animals were housed in either biosafety level 1 or level 2 rooms and all experiments were performed with an approved animal use protocol as reviewed by the Institutional Animal Care and Use Committee at Texas A&M University.

4.2.3. Sensitization and Elicitation of Responses

For sensitization, mice were injected subcutaneously (SC) with 50 µg of WCV in 50 µL sterile PBS in the middle of the back, then rested for 6 weeks prior to elicitation. Mice were elicited with WCV as previously described[158]. Briefly, mice were anesthetized by IP injection of 100 mg/kg ketamine and 10 mg/kg xylazine. Hair was removed from elicitation sites using electric clippers followed by application of a depilatory cream. Mice were vaccinated SC with 10 µg WCV and elicitation sites were monitored for 14 days prior to collection for histopathology or flow cytometry.

4.2.4. Antibody-Mediated Depletion

For antibody-mediated depletion experiments, mice were injected IP with 200 µg anti-mouse antibodies 1 day prior to elicitation, followed by 150 µg at days 2, 5, 8, and 11 post-elicitation. Antibodies include anti-CD3ε (GK1.5), anti-CD8 (2.43), anti-IFNγ (XMG1.2), anti-IL17a (17F3), and isotype control (LTF-2) from BioXCell (Lebanon, NH, USA). Depletion of cells was evaluated by collecting cells from spleens and vaccine sites of depleted mice and staining with anti-CD3ε, anti-CD4, and anti-CD8a (Biolegend).

4.2.5. Adoptive and Passive Transfer

Donor mice were sensitized as previously described and rested for 6 weeks prior to collection. Spleens and axillary lymph nodes were collected from donor mice and formed

into a single cell suspension by pressing through a 70 µm cell strainer, twice in flow cytometry staining buffer (FACs buffer). Splenocytes were treated with ACK lysis buffer for 1 min to remove red blood cells. CD4 4+ T cells and total T cells were purified from cell suspensions using Mouse CD4+ T cell and total T cell Isolation Kits from Miltenyi Biotec (Auburn, CA, USA). Mice in each recipient group received a retro-orbital injection of $5x10^6$ cells in 50 µL sterile PBS or PBS alone one day prior to elicitation. Aliquots of purified cells were evaluated on flow cytometry to assess purity of transferred samples. Blood was collected from donor mice at euthanasia and used to provide serum for passive transfer. An aliquot of this serum measured anti-*C. burnetii* antibody titers of >3200 by ELISA performed as previously described[158].

4.2.6. Histopathology and Immunohistochemistry

At 14 days post-elicitation, vaccine sites (skin, subcutis, and underlying skeletal muscle) were collected entirely and placed in 10% neutral buffered formalin for a minimum of 24 hours. Tissues were serially trimmed (3-4 sections per tissue) and placed in cassettes before being sent for processing, embedding, and sectioning at 5 µm (AML Laboratories, Jacksonville, FL, USA). Slides were stained with hematoxylin and eosin (HE) for assessment by a board-certified pathologist. Slides were de-identified and scored for overall severity based on lesion size, immune cell infiltrate, and regions of suppurative necrosis (Table 4.1) or separately evaluated for major morphologic features: histiocytic inflammation, suppurative necrosis, and formation of ectopic lymphoid follicles (Table 2).

Overall Histopathologic Score	
0	No lesions
1	Minimal lymphohistiocytic inflammation
2	Mild, multifocal lymphohisitocytic inflammation
3	Moderate lymphohistiocytic inflammation
4	Severe lymphohistiocytic inflammation
5	Severe lymphohistiocytic inflammation with suppurative necrosis

Table 4.1 Semi-quantitative scoring system for evaluation of histopathology of vaccine site reactions on HE-stained slides.

Morphologic Evaluation	
Suppurative Necrosis	
0	None
1	One region of degenerate collagen/necrosis with few necrotic neutrophils
2	Multiple areas of degenerate collagen/necrosis with small numbers of necrotic neutrophils
3	Single central well-formed abscess
4	Multiple central well-formed abscesses
Inflammatory Cells	
0	None
1	Sparsely infiltrating immune cells
2	One region of diffuse immune cell infiltrate
3	Large, dispersed regions of immune cells
4	Large regions of densely packed immune cells
Number of ELFs	
	Absolute number

Table 4.2. Semi-quantitative and quantitative evaluation for evaluation of histopathology of vaccine site reactions on HE-stained slides.
Evaluation is divided into regions of suppurative necrosis, degree of histiocytic inflammation, and number of ectopic lymphoid follicles (ELFs).

For immunohistochemistry, 5 µm sections were cut from tissue blocks and placed on adhesive slides then processed as previously described[158]. Primary antibodies used for immunohistochemistry include rabbit anti-Cb polyclonal serum at 1:500.

4.2.7. Transmission Electron Microscopy

Regions within vaccination sites which were positive for anti-Cb antibodies were extracted from formalin-fixed paraffin blocks for transmission electron microscopy as previously described[159,160]. Briefly, tissues were cut from paraffin blocks, de-paraffinized and re-hydrated in xylene and decreasing concentrations of ethanol, then fixed in 2% glutaraldehyde and 1% osmium tetroxide. Tissues were then stained with saturated uranyl acetate and dehydrated in increasing concentrations of ethanol, followed by embedding with Eponate-12 Resin (Ted Pella, Redding, CA, USA) and cut into 100 nm sections.

4.2.8. Flow Cytometry

Vaccine sites were collected and processed into single cell suspensions as previously described[158]. Briefly, the skin, including the underlying skeletal muscle, at the site of elicitation was collected using a 10 mm punch biopsy and the epidermis was removed using a razor blade. The remaining tissue was placed in a gentleMACS C-tube and processed using the gentleMACS Mouse Adipose Tissue Dissociation Kit and the gentleMACS Octo Dissociator with heaters (Miltenyi Biotec). Cell suspensions were diluted to 10^7 cells/mL and kept on ice. Cells were stained with anti-mouse CD16/CD32 for 10 min, followed by 2 µL/mL Zombie Aqua live/dead dye (Biolegend) for 5 min, and lastly with fluorochrome-conjugated cell surface antibodies for 30 min. Cells were then fixed in 4% paraformaldehyde for 20 min and kept at 4°C until analysis.

Flow cytometric antibodies include CD45-APC, CD3ε-APC/Cy7, CD19-PE/Cy7, CD11b-PE, CD11c-BV711, Ly6G-FITC (Biolegend) and CD4-PerCP/Cy5.5 and CD8a-PAC Blue (BD Biosciences). Cells were evaluated using a BD LSRFortessa X-20 Flow Cytometer and analyzed using FlowJo v10.7.2 (FlowJo LLC.).

4.2.9. Statistics

Statistical analyses were calculated using Prism v7.0 (GraphPad Software Inc.). Results were compared using one-way ANOVA with Tukey's or Dunnett's correction for multiple comparisons. Differences were considered significant if p-value ≤ 0.05 (*), ≤ 0.01 (**), ≤ 0.001 (***), or ≤ 0.0001 (****).

4.3. Results

4.3.1. CD4+ T Cells are essential for Cb WCV hypersensitivity reactions

We previously determined that local vaccine reactions to Cb WCV in sensitized mice is characterized by an increase in in both CD4+ and CD8+ T cells[158]. However, the specific roles of these T cell populations in mediating these hypersensitivity reactions were unknown. To evaluate the roles of CD4+ and CD8+ T cells in facilitating reactions to Cb WCV in sensitized mice, we began by sensitizing mice with a SC vaccination of 50 µg of WCV in 50 µL sterile PBS in the middle of the back and rested mice for 6 weeks, then mice were elicited in the right flank with 10 µg WCV in 50 µL sterile PBS. One day prior to elicitation, mice received an IP injection of 200 µg anti-mouse CD4 (CD4-), CD8 (CD8-), both (CD4/CD8-), or an isotype control (Sensitized). Mice were re-dosed at days 2, 5, 8, and 11 post-elicitation with 150 µg of anti-mouse antibodies. Elicitation sites were monitored for 14 days prior to collection for histopathology.

HE-stained slides of vaccination sites showed a marked reduction in the severity of reactions in CD4- and CD4/CD8- groups compared to sensitized control mice based on semi-quantitative scoring of de-identified slides (Fig 4.1A-B). Vaccine site reactions in CD8- mice did not reveal any significant changes in lesion severity or histomorphology compared to sensitized mice. Histology of vaccine sites from sensitized and CD8- mice showed granulomatous and lymphocytic inflammation with areas of suppurative necrosis and degeneration as well as dense aggregates of lymphocytes consistent with ectopic lymphoid follicles. In contrast, vaccine sites from CD4- and CD4/8- mice showed mild, dispersed histiocytic inflammation with small aggregates of lymphocytes. There was no evidence of suppurative necrosis or collagen degeneration in any tissue sections from the CD4- and CD4/8- groups. This indicated the CD4 T cells, but not CD8 T cells, are necessary to produce vaccine site hypersensitivity reactions.

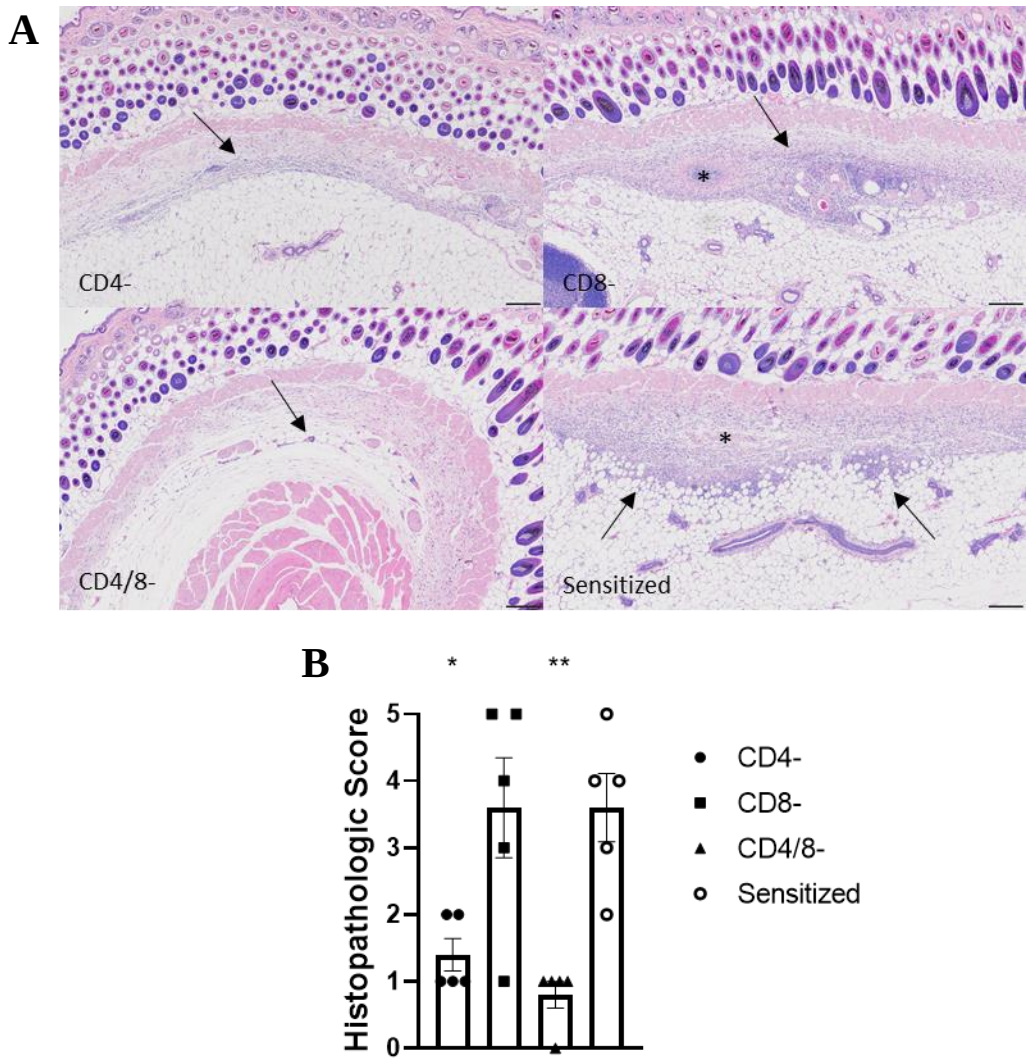

Figure 4.1 Depletion of CD4 T cells during elicitation abrogates reactogenicity of WCV.

A) Representative images of vaccine sites reactions from each experimental group. Sensitized control mice and CD8- mice show marked lymphohistiocytic inflammation (arrows) with regions of suppurative necrosis (*). CD4- and CD4/8- mice show only mild lymphohistiocytic inflammation. HE-stained slides, 4x. B) Semi-quantitative scoring of vaccine site reactions. CD4- and CD4/8- groups show a significant reduction in the severity of vaccine site reactions to Cb WCV. N=5 mice per group. Data were analyzed using one-way ANOVA with Dunnett's correction for multiple comparisons. Asterisks indicate significant differences compared to sensitized (*: $p<0.05$, **: $p<0.01$).

4.3.2. Adoptive transfer of serum enhances CD4+ T-mediated reactogenicity

We next evaluated whether local reactions to Cb WCV reactions are mediated by memory CD4 T cell responses. Donor mice were sensitized and rested as described in the previous experiment. Six weeks post-sensitization, donor mice were euthanized, blood was collected for serum, and spleens and axillary lymph nodes were collected and prepared as single cell suspensions. Aliquots of immune cells were purified for CD4+ T cells or total T cells. One day prior to elicitation, age-matched recipient mice received $5x10^6$ cells IV and/or 600 µL serum. Recipient mice were elicited with 10 µg WCV as described in the previous experiment and vaccine site reactions were compared to sensitized and unsensitized controls.

Mice receiving either CD4 T cells or a combination of CD4 T cells and serum showed significantly more severe vaccine site reactions compared to unsensitized mice based on semi-quantitative scoring (Fig. 4.2A-B). However, the CD4 T cell group also had significantly less severe inflammation compared to the sensitized group. Morphologically, both the CD4 T cell and CD4 T cell plus serum groups showed lymphohistiocytic inflammation and formation of ectopic lymphoid follicles, but CD4 T cell plus serum group showed consistently more severe inflammatory cell infiltrates compared to the CD4 T cell group. None of the reaction sites from these two groups contained areas of suppurative necrosis as observed in the sensitized control group. Total T cell and splenocyte groups also showed mild to moderate lymphohistiocytic inflammation, but these lesions were less severe than sensitized mice. The serum recipient group show no apparent increase in reactive lesions compared to unsensitized mice. These

results indicated that although anti-Cb antibodies alone do not produce hypersensitivity reactions to Cb WCV, they appear to enhance reactive lesions produced by CD4 T cells.

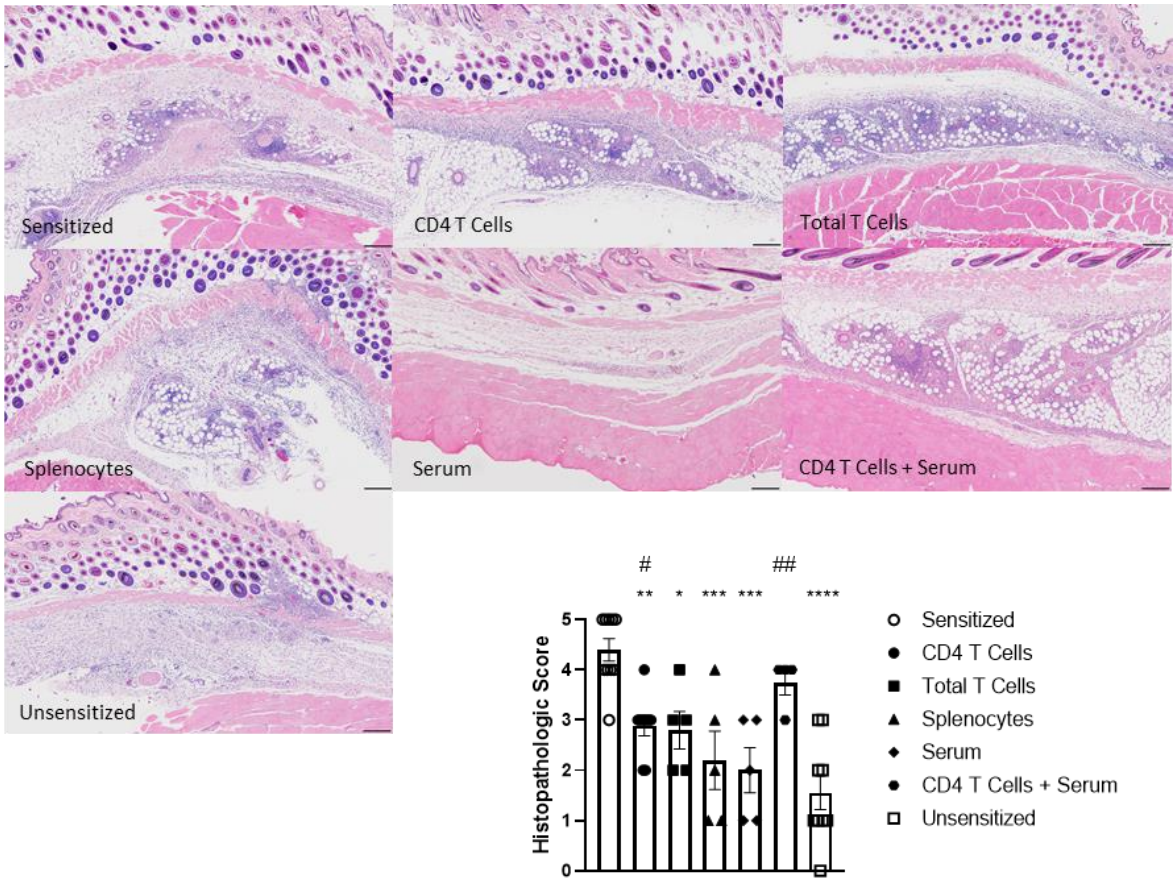

Figure 4.2 Adoptive transfer of CD4 T cells and immune serum conveys reactogenicity to WCV.
A) Representative images of vaccine site reactions from experimental groups. HE, 4x, bar = 200 µm. B) Semi-quantitative scoring of vaccine site reactions. CD4 T cell and CD4 T cell plus serum groups developed significantly more severe vaccine site reactions than unsensitized mice. Only CD4 T cell plus serum recipient mice show vaccine site reactions which do not significantly differ in severity from sensitized mice. N=5-10 mice per group. Data were analyzed using one-way ANOVA with Tukey's correction for multiple comparisons. Asterisks indicate significant differences compared to sensitized mice and pound signs indicate significant differences compared to unsensitized mice (*/#: $p<0.05$, **/##: $p<0.01$, ***: $p<0.001$, ****: $p<0.0001$).

4.3.3. Depletion of IFNγ alters local vaccine site reactions

Our previous work showed that infiltrating IFNγ+ and IL17a+ CD4 T cells extracted from elicitation sites are significantly increased in sensitized mice compared to unsensitized controls[158]. To investigate how CD4 T cells may mediate local vaccine site reactions, we assessed the role of IFNγ and IL17a in producing hypersensitivity responses. To do this, we used antibody-mediated depletion of IFNγ, IL17a, or both in sensitized mice during elicitation. Mice were sensitized as described above, then given IP injections of anti-mouse IFNγ and/or IL17a, or an isotype control using the same doses and schedule as the T cell depletion experiment. Mice were elicited in four sites on the right and left flanks. One site (right rear flank) was collected in formalin for histopathology and the remaining 3 sites were pooled and collected for flow cytometry.

Histology of the vaccine sites from sensitized and IL17a-depleted (IL17a-) mice were morphologically similar, showing severe lymphocytic and granulomatous inflammation with central areas of suppurative necrosis (Fig. 4.3A). Histology of vaccine sites in IFNγ- and IFNγ/IL17a- mice showed lymphohistiocytic inflammation as seen in sensitized controls, but lacked areas of suppurative necrosis. However, the overall severity of the vaccine sites reactions in depleted mice compared to sensitized mice did not significantly differ (Fig. 4.3B). To better assess these changes in morphology, semi-quantitative scoring of the inflammation was separated into three categories: suppurative necrosis, immune cell infiltration, and ectopic lymphoid follicles (Table 4.2, Fig. 4.3B). None of the vaccine site reactions in IFNγ- and IFNγ/IL17a- showed evidence of

suppurative necrosis, however, these groups showed a significant increase in the severity of immune cell infiltrate compared to sensitized mice. Additionally, IFNγ- and IFNγ-/IL17a- mice showed a significant increase in number of ectopic lymphoid follicles compared to unsensitized mice.

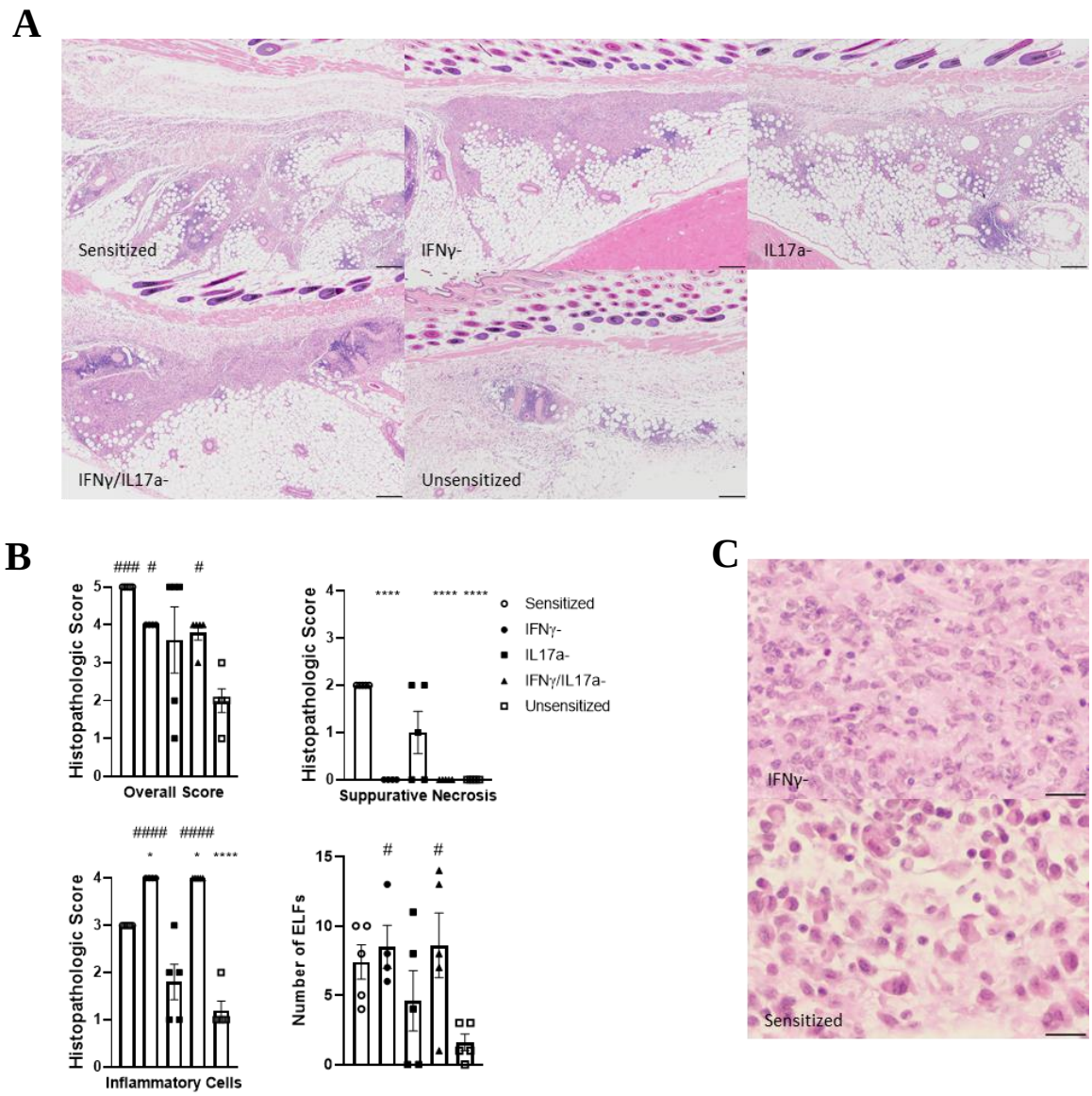

Figure 4.3 Depletion of IFNγ and IL17a alter the morphology of local reactions to WCV.

A) Representative images of vaccine site reactions from experimental groups. HE, 4x, bar = 200 µm. B) Semi-quantitative scoring of vaccine site reactions. Cytokine-depleted mice did not have significantly less severe reactions overall compared to sensitized controls. IFNγ-depleted mice showed a lack of suppurative necrosis, but an increase in immune cell infiltration compared to sensitized mice. C) Vaccine site reactions in IFNγ-depleted mice showed dense infiltration of innate immune cells compared to the dispersed immune cells with distinct cell borders seen in sensitized control mice HE, 40x, bar = 25 µm. N=5-10 mice per group. Data were analyzed using one-way ANOVA with Tukey's correction for multiple comparisons. Asterisks indicate significant differences compared to sensitized mice and pound signs indicate significant differences compared to unsensitized mice (*/#: $p<0.05$, ###: $p<0.001$, ****/####: $p<0.0001$).

Morphologically, in sensitized mice the infiltrating immune cells were more dispersed and have a moderate amount of eosinophilic cytoplasm with distinct cytoplasmic borders, consistent with activated macrophages. In contrast, the immune cell infiltrate from IFNγ- and IFNγ/IL17a- mice had abundant cytoplasm with indistinct cell borders (Fig. 4.3C). Flow cytometry of cells extracted from vaccine site reactions was performed to quantify infiltrating cell numbers. Although not statistically significant, CD45+CD11b+Ly6G- macrophages were decreased in IFNγ- and IFNγ/IL17a- mice compared to sensitized mice (Supplemental Figure 1). Similarly, numbers of CD45+CD11b+Ly6G+ neutrophils were mildly decreased in all three depletion groups compared to sensitized mice.

4.3.4. Antigens from the Cb WCV persist within injection sites

The granulomatous component to the vaccine site reactions with Cb WCV suggests an antigen which is difficult to degrade or remove from the injection site. To investigate how persistence of antigen may be contributing to vaccine site inflammation we evaluated areas of injection site reactions using immunohistochemistry (IHC). Elicitation sites (10 µg WCV) were evaluated at 14 days post-injection and sensitization sites (50 µg WCV) were evaluated at 8 weeks and 26 weeks post-injection. IHC with a polyclonal anti-NMI antibody showed positive staining, usually within central regions of suppurative necrosis and within the cytoplasm of adjacent macrophages, at all evaluated time points (Fig. 4.4A).

To further investigate the etiology of this persistent antigen, we collected regions of tissues from paraffin-embedded tissue blocks which were stained positively IHC with anti-Cb antibodies to evaluate using transmission electron microscopy. Transmission electron microscopy of the anti-Cb positive region from an elicitation site at 2 weeks post-injection revealed numerous, apparently intact, bacteria (Fig. 4.4B). These bacteria were rod-shaped, measuring 0.2 to 0.3 µm long and 0.1 to 0.2 µm wide, with a dense, central nucleoid. This indicates that the inability of the intact bacteria to be degraded by host cells *in vivo* is the cause of local antigen persistence.

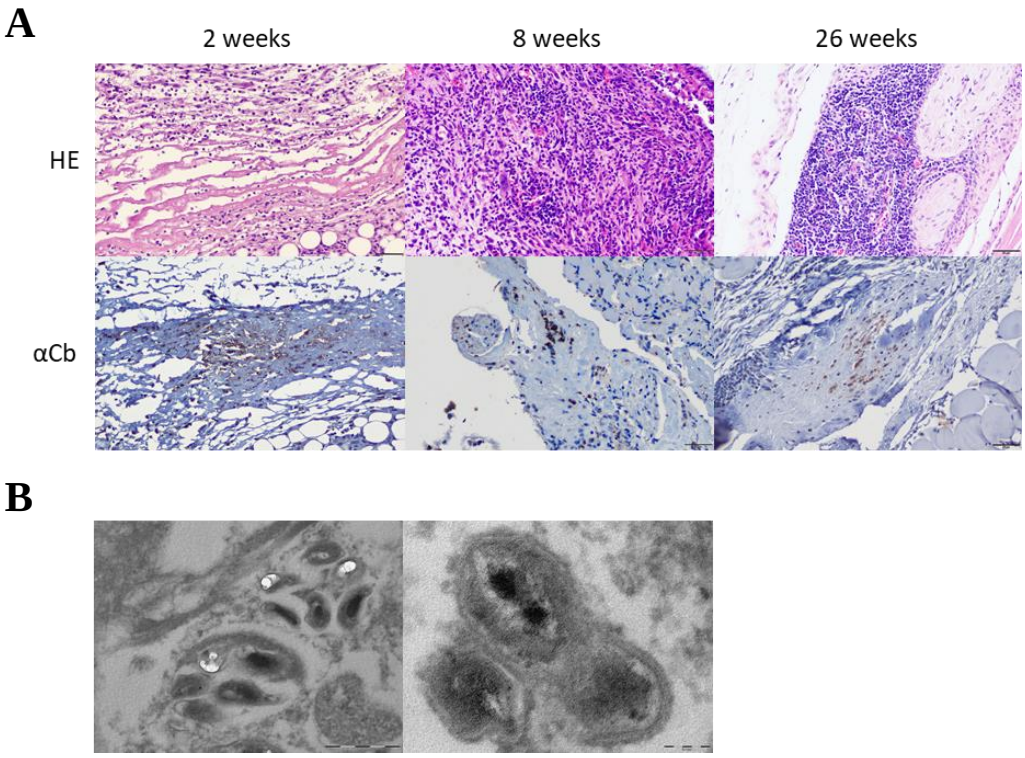

Figure 4.4 WCV persists as intact bacteria within injection sites.
A) Representative images of vaccine site reactions with WCV at 2 weeks (10 µg dose), 8 weeks and 26 weeks (50 µg dose). Anti-Cb IHC shows positive immunostaining at all time points. HE and DAB with hematoxylin counterstain, 20x, bar = 50 µm. B) TEM of a vaccine site at 2 weeks post-injection with WCV. Images show bacilli measuring up to 500 nm in length. Bars = 500 nm and 100 nm.

4.4. Discussion

While the severe reactogenic responses produced by vaccines against Cb have long stood as a major barrier to the widespread availability of a protective vaccine, the mechanisms and causes underlying these reactions are still poorly understood. It was previously shown that local Cb WCV reactions are characterized by an influx of CD4+ and CD8+ T cells in a sensitized mouse model[158]. To investigate the roles of these infiltrating T cells in mediating Cb WCV reactogenicity we performed antibody-mediated depletion and adoptive transfer experiments in a sensitized mouse model. Depletion of CD4, but not CD8 T cells in sensitized mice prior to elicitation with WCV markedly reduced the severity of local inflammation compared to control mice indicating that memory CD4 T cells play an essential role in producing Cb WCV reactogenicity. However, adoptive transfer of immune CD4 T cells alone did not fully re-create the severity of local vaccine reactions in sensitized mice. Interestingly, the addition of immune serum with adoptive transfer of memory CD4 T cells enhanced the severity of local reactions. This indicated that although local reactions are mediated by memory CD4 T cells, their activity is enhanced by a component of immune serum, presumably anti-Cb antibodies.

Prior studies in contact and delayed-type hypersensitivities have already indicated a role for antigen-specific antibodies. Antigen-specific IgM produced by immune B1 cells binds to antigens and activates complement, leading to T cell recruitment during elicitation[161]. Anti-Cb antibodies may similarly be enhancing CD4 T cell recruitment during elicitation with WCV. In previous work, antibodies targeting the phase I LPS of Cb have been shown to play an important role in the protective efficacy of the Cb

WCV[49,105]. Phase I LPS hides surface proteins from host immune cells during infection via steric hinderance[162]. Anti-LPS antibodies may similarly be enhancing immune responses to WCV during elicitation leading to more severe local reactions. However, further experiments are needed to elucidate the roles of anti-Cb antibodies in mediating Cb WCV reactogenicity.

Notable here is that both memory CD4 T cells and anti-Cb antibodies have been shown to be important for WCV-meditated protection during infection[49,105]. WCV elicits a Th1-dominant immune response which leads to formation of memory T cells and antibodies specific for phase I LPS which are essential for WCV-mediated protection[49]. Thus, the mechanisms of WCV-mediated protection appear to parallel the mechanisms of local reactogenicity. This, however, does not necessarily mean that severe reactogenicity is inevitable with an efficacious vaccine against Cb. Studies on immune responses during Cb infection indicate that although T cells are necessary for control of Cb during infection, CD8 T cells, which do not appear to contribute to reactogenicity, play an important role in clearance of bacteria during infection[49,85]. Additionally, mice depleted of CD4 T cells not only show decreased bacterial load, they display less lung pathology during pulmonary challenge with Cb, suggesting that reducing CD4 T cell responses will not preclude protection[85].

We next investigated the roles of IFNγ and IL17a in producing local Cb WCV reactions. Previously, these cytokines were shown to be increased during elicitation of hypersensitivity reactions to WCV[158]. Depletion of IFNγ and IL17a did not markedly reduce the overall severity of local hypersensitivity reactions as seen when mice were

depleted of CD4 T cells and mice depleted of IL17a showed no appreciable changes in the morphology of hypersensitivity reactions compared to sensitized mice. This was surprising considering that abscesses are commonly seen in Cb WCV reactions and IL17 is an important activator of neutrophils which has been implicated in abscess formation[163]. However, in this experiment we used antibodies specific for IL17a to deplete mice. Although IL17a is considered the main inducer of neutrophil responses in contact and delayed-type hypersensitivity, IL17f has also been shown to be an important mediator of neutrophil responses during bacterial infection[164]. Since Cb WCV reactogenicity is caused by responses to bacterial antigens, it is possible that IL17f or another IL17 subtype is involved in mediating neutrophil responses in Cb WCV reactogenicity.

In contrast to IL17a-depleted mice, IFNγ-depleted mice showed significant changes in the morphology of local reactions. Histologically, the local reactions in IFNγ-depleted mice lacked regions of suppurative necrosis and inflammation was composed of dense immune cell infiltrates with indistinct cytoplasmic borders while sensitized mice show dispersed immune cells with moderate cytoplasm and distinct cell borders. IFNγ is an important inducer of macrophage priming and activation. Classically activated macrophages, or M1 macrophages, are stimulated by a combination of IFNγ and TLR signaling leading to altered cellular metabolism which enhances pro-inflammatory cytokine production and phagocytic activity[134]. The lack of IFNγ in depleted mice may be inhibiting normal macrophage activation and phagocytosis of antigens, leading to the altered inflammatory infiltrate. For the absence of suppurative necrosis, CD4 T cells, especially Th1 cells, are known to be important in the formation of abscesses and IFNγ

production by CD4 and CD8 T cells enhances neutrophil activation[163,165,166]. Although IFNγ appears to play a significant role in mediating Cb WCV reactions, the presence of severe local reactions despite depletion of IFNγ indicates that CD4 T cells mediate these reactions by other mechanisms as well.

Lastly, we showed that the Cb WCV causes prolonged persistence of antigen at the injection site. Granulomatous delayed-type hypersensitivity reactions are associated with an antigen which is difficult to degrade or remove[81]. IHC for Cb on vaccine sites showed positive immunostaining at 2 weeks, 8 weeks, and 26 weeks post-injection. When we performed TEM on these positive tissue sites, we found intact bacteria present within the injection site. Several other researchers have shown that vaccines derived from individual proteins or extracts of Cb are able to reduce the severity of local reactogenicity[56,71,72]. A similar reduction in vaccine reactogenicity has also been described when comparing whole cell and acellular pertussis vaccines[167]. The use of intact bacteria in Cb vaccines may produce a depot effect, reducing the rate of clearance of antigen from the injection site, which can contribute to both protective efficacy and reactogenicity of these vaccines[168]. Cb in particular is known to form a small cell variant (SCV) which is highly resistant to degradation, however, other factors such as the use of formalin-fixation, which preserves proteins by cross-linking amines and other residues to prevent degradation, and the presence of phase I LPS, which shields Cb surface antigens from host cell recognition, may also be contributing to local persistence[162,169,170]. Although further work is necessary to determine which of these components may be contributing to Cb

WCV reactogenicity, all of these possibilities may be removed by avoiding the use of a whole cell vaccine.

Differentiation of protective and pathologic mechanisms of vaccine-induced immune memory is essential for development of safer vaccines. As discussed above, subunit or other non-whole cell vaccines will likely dramatically reduce the severity of local persistence of antigen. Indeed, the injection of unadjuvanted Cb antigens does not appear to induce significant reactogenicity[71]. However, this creates a significant reduction in protective efficacy, necessitating the use of adjuvants which can also cause marked reactogenicity when paired with Cb antigens[71]. Knowing that reactogenicity with WCV is mediated by CD4 T cells, adjuvant combinations in vaccines should be tailored towards producing CD8 rather than CD4 T cell memory responses. Fratzke et al. used a combination of several TLR agonists, especially TLR4 agonists, and Addavax, a squalene-based oil-in-water emulsion, as adjuvants. Only one of five tested formulations showed a significant reduction in reactogenicity compared to sensitized animals[71]. Addavax stimulates innate immune cells to create an immunocompetent environment which enhances CD4 T cell and B cell responses[171]. Similarly, TLR4 agonists are strong inducers of CD4 T cell memory[69]. Together the effects of these adjuvant combinations were likely producing strong CD4 T cell memory and antibody responses which could be the cause of the severe local reactions reported. In contrast, Gregory et al. used a TLR9 agonist, CpG ODN 1826, as an adjuvant in combination with a solubilized protein extract of Cb which resulted in a marked reduction in reactogenicity[72]. TLR9 is a strong inducer of CD8 T cell memory, which may partially explain the reduction in reactogenicity reported in those

experiments[67]. Overall, reduction in reactogenicity with novel Cb vaccines will likely require two main strategies. First, reducing local persistence of antigen to minimize granulomatous inflammation, and second, a focus on induction of strong memory CD8 T cell responses rather than CD4 T cell responses to reduce pathologic adaptive responses.

Here we investigated the roles of T cells, IFNγ, and IL17a in mediating Cb WCV reactogenicity as well as the long-term persistence of antigen with Cb WCV. Local vaccine site reactions in sensitized mice are mediated by CD4 T cells and enhanced by a component of immune serum, presumably anti-Cb antibodies. Additionally, IFNγ plays a significant role in producing local reactive lesions. Lastly, Cb WCV causes localized chronic persistence of antigen which is likely contributing to the chronicity and granulomatous component of local inflammation. Our work provides insights into the mechanisms of Cb WCV reactogenicity which may help guide the development of novel protective vaccines with enhanced safety profiles.

5. SUMMARY

Development of an effective and safe vaccine against *C. burnetii* requires an understanding of both the mechanisms of protective and pathologic responses to vaccination. Although there have been many studies published on understanding the mechanisms of protection from *C. burnetii* infection, prior to our work, little was known about the mechanisms of reactogenicity of the *C. burnetii* whole cell vaccine. Here, we began by testing the protective efficacy and reactogenicity of several novel subunit vaccine formulations using TLR agonist adjuvants before focusing on investigating the pathogenesis of reactogenicity using whole cell vaccine, a Q-VAX equivalent.

Earlier researchers suggested that the phase I LPS of *C. burnetii* was the likely cause of reactogenicity. In our initial work, we tested subunit vaccines composed of six immunodominant antigens from *C. burnetii* combined with different adjuvant formulations. Since these vaccines did not contain phase I LPS, we suspected that these would produce little reactogenicity. Although all of the adjuvanted formulations provided significant protection during pulmonary challenge, only one of these formulations resulted in a significant decrease in reactogenicity compared to WCV in a sensitized guinea pig model. The presence of severe reactions in many of the formulations and the lack of reactogenicity with an unadjuvanted formulation indicated that the mechanisms of WCV reactogenicity are more complex than a single antigen as the inciting cause.

To investigate the pathogenesis of this reactogenicity, we began by developing a novel sensitized mouse model of *C. burnetii* WCV reactogenicity. Prior to this work, the model of choice was a sensitized guinea pig model. Guinea pigs are much more susceptible

to *C. burnetii* than mice, produce pulmonary lesions similar to humans, and develop severe local reactions to WCV if previously sensitized as described in humans. However, reagents, such as species-specific antibodies, are severely lacking in guinea pigs which precludes in-depth investigation of immunologic mechanisms. In contrast, mice are available in a wide array of inbred and congenic strains, have well-characterized immune systems, and many reagents targeting components of the immune system are readily available. Our work shows that both C57Bl/6J and SKH1 mice produce hypersensitivity reactions to WCV similar to those described in humans and in the guinea pig model. Interestingly, BALBc mice did not produce hypersensitivity reactions to WCV despite developing the highest IgG titers post-sensitization.

We went on to characterize the local vaccine site reactions using histopathology, immunohistochemistry, and flow cytometry. Local vaccine reactions in sensitized C57Bl/6J mice show an influx of granulomatous inflammation with formation of areas of suppurative necrosis (abscesses) and ectopic lymphoid follicles. Immunohistochemistry showed a diffuse infiltration of T cells, while B cells were restricted to ectopic lymphoid follicles. Flow cytometry of cells extracted from vaccine sites showed an influx of CD4 and CD8 T cells with an increase in IFNγ+ and IL17a+ CD4 T cells, indicating a Th1-type hypersensitivity. This explained why BALBc mice, which have a Th2-skewed immunophenotype due to a decrease in IFNγ production, did not produce significant hypersensitivity reactions.

We then showed that while both CD4 and CD8 T cells infiltrate vaccine site reactions, only CD4 T cells appear to play a significant role in causing these reactions.

While depletion of CD8 T cells did not alter reactive lesions in sensitized mice, depletion of CD4 T cells almost completely prevented reactivity. Interestingly, adoptive transfer of CD4 T cells alone was not sufficient to induce hypersensitivity reactions in naïve mice, but the severity of these lesions was enhanced with the addition of passive transfer of immune serum. This indicates that anti-*C. burnetii* antibodies also play significant role in WCV reactogenicity, although passive transfer alone did not induce any significant reactions, indicating that this occurs through a memory CD4 T cell-dependent mechanism.

We also investigated the roles of IFNγ and IL17a in producing *C. burnetii* WCV reactogenicity. While depletion of IL17a did not alter reactive lesions, removal of IFNγ lead to an absence of suppurative necrosis and a change in the morphology of the immune cell infiltrate. Overall, this indicates that although IFNγ plays a significant role in the mediating WCV reactogenicity, CD4 T cells induce these reactions by other mechanisms as well. Further experiments are necessary to help elucidate the immunopathogenesis of these hypersensitivity reactions.

Lastly, we showed that injection of WCV leads to chronic persistence of antigen at the vaccine site. The granulomatous inflammation reported with *C. burnetii* WCV reactions suggested the presence of an antigen which is difficult to degrade or remove. Immunohistochemistry of injection sites showed regions of positive immunostaining with anti-*C. burnetii* antibody at 2 weeks, 8 weeks, and 26 weeks post-injection. In addition, transmission electron microscopy of positively staining areas showed the presence of intact bacteria. Thus, intact *C. burnetii* may be difficult for host to remove from the injection site, causing a persistent antigen which likely contributes to the chronicity and

severity of WCV reactogenicity. This resistance to degradation may be due to an innate aspect of the bacteria such as the formation of small cell variants or the presence of phase I LPS or it may be due to the use of formalin to kill the bacteria, which binds proteins and nucleic acids to prevent degradation. Further work is necessary to understand the causes of this persistence of intact bacteria with WCV.

Overall, the pathogenesis of *C. burnetii* WCV reactogenicity appears to involve both the cellular and humoral adaptive immune responses and is enhanced by persistent antigen stimulation. During elicitation with WCV, memory T cells home to the injection site, presumably under the influence of stimulated innate cells, and mature into effector memory cells. Although CD8 T cells do not appear to play a significant role in the induction of WCV reactogenicity, CD4 T cells are indispensable, partly through their production of IFNγ. Lack of IFNγ leads to an alteration in the morphology of the immune cell infiltrate and an absence of abscesses. However, significant vaccine site reactions still occur in the absence of IFNγ, indicating that CD4 T cells must induce WCV reactogenicity through other mechanisms as well. Finally, the intact bacteria in the WCV persist within the injection site for at least 6 months post-injection. The granulomatous component of WCV reactogenicity indicated that an antigen was persistent within the injection site, however, it appears that this is because the intact bacterium is difficult to degrade or remove, rather than persistence of a single antigen.

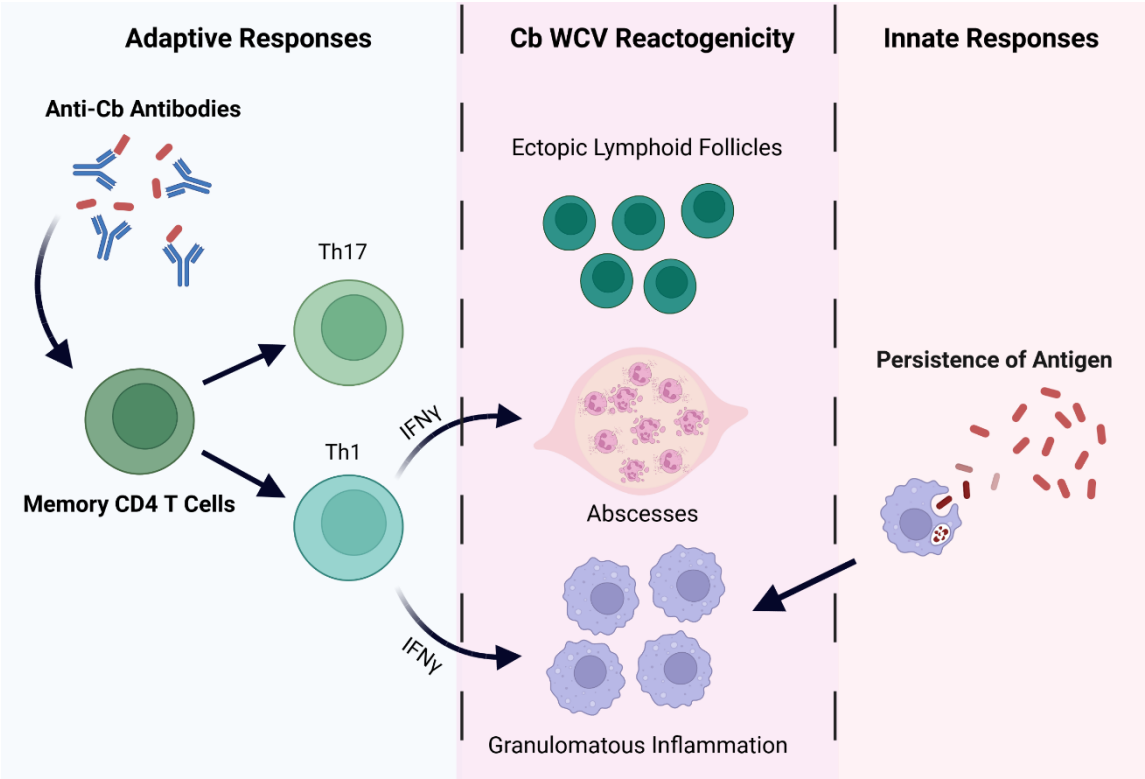

Figure 5.1 Schematic of the immunologic mechanisms of Cb WCV reactogenicity.

Our work begins to outline some of the mechanisms of *C. burnetii* WCV reactogenicity. The results of these experiments suggest that development novel *C. burnetii* vaccine that is less reactogenic will depend on reducing both local persistence of antigen and memory CD4 T cell responses, while maintaining or enhancing antibody and CD8 T cell responses. Future work can focus on understanding the mechanisms of CD4 T cell-mediated hypersensitivity responses which may lead to the discovery of early markers for predicting reactogenic responses to vaccines. Additionally, studies understanding how adjuvants and adjuvant combinations alter immune responses to antigens can dramatically enhance our ability to produce vaccines that are both effective and non-reactogenic.

REFERENCES

1. Hirschmann, J. V. The Discovery of Q Fever and Its Cause. *Am. J. Med. Sci.* **358**, 3–10 (2019).
2. Derrick, E. H. ‘Q’ fever, a new fever entity: clinical features, diagnosis and laboratory investigation. *Rev. Infect. Dis.* **5**, 790–800 (1983).
3. Derrick, E. H. The Epidemiology of Q Fever. *Epidemiol. Infect.* **43**, 357–361 (1944).
4. Burnet, F. M. & Freeman, M. Experimental studies on the virus of ‘Q’ fever. *Rev. Infect. Dis.* **5**, 800–808 (1983).
5. Davis, G. E. & Cox, H. R. A Filter-Passing Infectious Agent Isolated From Ticks. I. Isolation From Dermacentor Andersoni, Reactions in Animals, And Filtration Experiments. *Public Health Rep.* **53**, 2259–2267 (1938).
6. Cox, H. R. A FIlter-Passing Infectious Agent From Ticks. III. Description of Organism and Cultivation Experiments. *Public Health Rep.* **53**, 2270–2276 (1938).
7. Dyer, R. E. Similarity of Australian ‘Q’ Fever and a Disease Caused by an Infectious Agent Isolated from Ticks in Montana. *Public Heal. Reports* **54**, 1229 (1939).
8. Dyer, R. E. A Filter-Passing Infectious Agent From Ticks. IV. Human Infection. *Public Health Rep.* **53**, 2277–2282 (1938).
9. Derrick, E. H. Rickettsia Burneti: the Cause of “Q” Fever. *Med. J. Aust.* **1**, 14 (1939).

10. Philip, C. B. Comments on the Name of the Q Fever Organism. *Public Health Rep.* **63**, 58 (1948).

11. Burnet, F. M. & Freeman, M. Note on a Series of Laboratory Infections With the Rickettsia of "Q" Fever. *Med. J. Aust.* **1**, 11–12 (1939).

12. Huebner, R. J. Report of an outbreak of Q fever at the National Institute of Health. *Am. J. Public Health* **37**, 431–440 (1947).

13. Hornibrook, J. W., Nelson, K. R., Dyer, R. E., Topping, N. H. & Bengtson, I. A. An Institutional Outbreak of Pneumonitis. *Public Health Rep.* **55**, 1936–1954 (1940).

14. Smith, D. J. W., Brown, H. E. & Derrick, E. H. A Further Series of Laboratory Infections With the Rickettsia of "Q" Fever. *Med. J. Aust.* **1**, 13–14 (1939).

15. The Commission on Acute Respiratory Diseases Fort Bragg North Carolina. A Laboratory Outbreak of Q Fever Caused by the Balkan Grippe Strain of Rickettsia. *Am. J. Hygene* **44**, 123–157 (1946).

16. Young, F. W. Q Fever in Artesia, California. *Calif. Med.* **69**, 89–90 (1948).

17. Shepard, C. C. & Huebner, R. J. Q Fever in Los Angeles County. Description of Some of Its Epidemiological Features. *Am. J. Public Health* **38**, 781–788 (1948).

18. Luoto, L. & Huebner, R. J. Q Fever Studies in Southern California; IX. Isolation of Q Fever Organisms from Parturient Placenta of Naturally Infected Dairy Cows. *Public Health Rep.* **65**, 541–544 (1950).

19. Van Schaik, E. J., Chen, C., Mertens, K., Weber, M. M. & Samuel, J. E. Molecular pathogenesis of the obligate intracellular bacterium Coxiella burnetii.

Nat. Rev. Microbiol. **11**, 561–573 (2013).

20. Bewley, K. R. Animal models of Q fever (Coxiella burnetii). *Comp. Med.* **63**, 469–476 (2013).

21. Ruiz, S. & Wolfe, D. N. Vaccination against Q fever for biodefense and public health indications. *Front. Microbiol.* **5**, 1–7 (2014).

22. Angelakis, E. *et al.* Q fever and pregnancy: Disease, prevention, and strain specificity. *Eur. J. Clin. Microbiol. Infect. Dis.* **32**, 361–368 (2013).

23. Fournier, P., Etienne, J., Harle, J., Habib, G. & Raoult, D. Myocarditis, a Rare but Severe Manifestation of Q Fever: Report of 8 Cases and Review of the Literature. *Clin. Infect. Dis.* **32**, 1440–1447 (2001).

24. Jacobson, A. & Sutthiwan, P. Myocarditis: A rare manifestation of acute Q fever infection. *J. Cardiol. Cases* **20**, 45–48 (2019).

25. Munster, J. M. *et al.* Placental histopathology after Coxiella burnetii infection during pregnancy. *Placenta* **33**, 128–131 (2012).

26. Botelho-Nevers, E. *et al.* Coxiella burnetii infection of aortic aneurysms or vascular grafts: Report of 30 new cases and evaluation of outcome. *Eur. J. Clin. Microbiol. Infect. Dis.* **26**, 635–640 (2007).

27. Million, M., Thuny, F., Richet, H. & Raoult, D. Long-term outcome of Q fever endocarditis: A 26-year personal survey. *Lancet Infect. Dis.* **10**, 527–535 (2010).

28. Sukocheva, O. A. *et al.* Long-term persistence after acute Q fever of non-infective Coxiella burnetii cell components, including antigens. *Qjm* **103**, 847–863 (2010).

29. Arricau-Bouvery, N. & Rodolakis, A. Is Q Fever an emerging or re-emerging

zoonosis? *Vet. Res.* **36**, 327–349 (2005).

30. Straily, A., Dahlgren, F. S., Peterson, A. & Paddock, C. D. Surveillance for Q Fever Endocarditis in the United States, 1999-2015. *Clin. Infect. Dis.* **65**, 1872–1877 (2017).

31. Honarmand, H. Q fever: An old but still a poorly understood disease. *Interdiscip. Perspect. Infect. Dis.* **2012**, (2012).

32. Klemmer, J. *et al.* Q fever in Egypt: Epidemiological survey of Coxiella burnetii specific antibodies in cattle, buffaloes, sheep, goats and camels. *PLoS One* **13**, 1–12 (2018).

33. Esmaeili, S., Pourhossein, B., Gouya, M. M., Amiri, F. B. & Mostafavi, E. Seroepidemiological survey of Q fever and brucellosis in kurdistan Province, western Iran. *Vector-Borne Zoonotic Dis.* **14**, 41–45 (2014).

34. Mostafavi, E. *et al.* Seroprevalence of Q fever among high-risk occupations in the Ilam province, the west of Iran. *PLoS One* **14**, 1–10 (2019).

35. Eldin, C. *et al.* From Q Fever to Coxiella burnetii Infection: a Paradigm Change. *Clin. Microbiol. Rev.* **30**, 115–190 (2017).

36. Hilbink, F., Penrose, M., Ko Vacova, E. & Kazar, J. Q fever is absent from new zealand. *Int. J. Epidemiol.* **22**, 945–949 (1993).

37. Robbins, F. C., Gauld, R. L. & Warner, F. B. Q fever in the mediterranean area: Report of its occurrence in allied troops: II. Epidemiology. *Am. J. Epidemiol.* **44**, 23–50 (1946).

38. Robbins, F. C. & Ragan, C. A. Q fever in the mediterranean area: Report of its

occurrence in allied troops: III. Etiological agent. *Am. J. Epidemiol.* **44**, 51–63 (1946).

39. Smadel, J. E., Snyder, M. J. & Robbins, F. C. Vaccination against Q fever. *J. Bacteriol.* **54**, 77 (1947).

40. Robbins, F. C., Rustigian, R., Snyder, M. J. & Smadel, J. E. Q fever in the mediterranean area: Report of its occurrence in allied troops: III. Etiological agent. *Am. J. Epidemiol.* **44**, 51–63 (1946).

41. Marmion, B. P. *et al.* Vaccine Prophylaxis of Abattoir-Associated Q Fever. *Lancet* **324**, 1411–1414 (1984).

42. Marmion, B. P. *et al.* Vaccine prophylaxis of abattoir-associated Q fever: Eight years' experience in Australian abattoirs. *Epidemiol. Infect.* **104**, 275–287 (1990).

43. Woldeyohannes, S. M. *et al.* Q fever vaccine efficacy and occupational exposure risk in Queensland, Australia: A retrospective cohort study. *Vaccine* **38**, 6578–6584 (2020).

44. Gidding, H. F., Wallace, C., Lawrence, G. L. & McIntyre, P. B. Australia's national Q fever vaccination program. *Vaccine* **27**, 2037–2041 (2009).

45. de Cremoux, R. *et al.* Assessment of vaccination by a phase I Coxiella burnetii-inactivated vaccine in goat herds in clinical Q fever situation. *FEMS Immunol. Med. Microbiol.* **64**, 104–106 (2012).

46. Rousset, E. *et al.* Efficiency of a phase 1 vaccine for the reduction of vaginal Coxiella burnetii shedding in a clinically affected goat herd. *Clin. Microbiol. Infect.* **15**, 188–189 (2009).

47. Kazár, J., Brezina, R., Palanova, A., Tvrdá, B. & Schramek, S. Immunogenicity and reactogenicity of a Q fever chemovaccine in persons professionally exposed to Q fever in Czechoslovakia. *Bull. World Health Organ.* **60**, 389–394 (1982).

48. Robinson, D. M. & Hasty, S. E. Production of a Potent Vaccine from the Attenuated M-44 Strain of Coxiella burneti. *Appl. Microbiol.* **27**, 777–783 (1974).

49. Zhang, G. *et al.* Mechanisms of Vaccine-Induced Protective Immunity against Coxiella burnetii Infection in BALB/c Mice. *J. Immunol.* **179**, 8372–8380 (2007).

50. Williams, J. C. *et al.* Vaccines against Coxiellosis and Q Fever Development of a Chloroform:Methanol Residue Subunit of Phase I Coxiella burnetii for the Immunization of Animals. *Ann. N. Y. Acad. Sci.* **653**, 88–111 (1992).

51. Schramek, S., Brezina, R. & Visacka, E. Different antigenic properties of lipopolysaccharides isolated from Coxiella burnetii in phase I and pure phase II. *Zentralblatt fur Bakteriol. Mikrobiol. und Hyg. - Abt. 1 Orig. A* **255**, 356–360 (1983).

52. Stoker, M. G. P. & P. Fiset. Phase Variation of the Nine Mile and Other Strains of Rickettsia burneti. *Can. J. Microbiol.* **2**, 310–321 (1956).

53. Marmion, B. P. Development of Q-fever vaccines, 1937 to 1967. *Med. J. Aust.* **2**, 1074–1078 (1967).

54. Johnson, J. W., Mcleod, C. G., Stookey, J. L., Higbee, G. A. & Pedersen Jr., C. E. Lesions in Guinea Pigs Infected with Coxiella burnetii Strain M-44. *J. Infect. Dis.* **135**, 995–998 (1977).

55. Williams, J. C. & Cantrell, J. L. Biological and Immunological Properties of

Coxiella burnetii Vaccines in C57BL / 1OScN Endotoxin-Nonresponder Mice. *Infect. Immun.* **35**, 1091–1102 (1982).

56. Waag, D. M., England, M. J., Bolt, C. R. & Williams, J. C. Low-dose priming before vaccination with the phase I chloroform-methanol residue vaccine against Q fever enhances humoral and cellular immune responses to Coxiella burnetii. *Clin. Vaccine Immunol.* **15**, 1505–1512 (2008).

57. Isken, L. D. *et al.* Implementation of a Q fever vaccination program for high-risk patients in the Netherlands. *Vaccine* **31**, 2617–2622 (2013).

58. Royal, J. *et al.* Seroepidemiologic survey for Coxiella burnetii among US military personnel deployed to southwest and central Asia in 2005. *Am. J. Trop. Med. Hyg.* **89**, 991–995 (2013).

59. Gleeson, T. D., Decker, C. F., Johnson, M. D., Hartzell, J. D. & Mascola, J. R. Q Fever in US Military Returning from Iraq. *Am. J. Med.* **120**, 11–12 (2007).

60. Franz, D. R. *et al.* Clinical recognition and management of patients exposed to biological warfare agents. *J. Am. Med. Assoc.* **278**, 399–411 (1997).

61. Rauch, S., Jasny, E., Schmidt, K. E. & Petsch, B. New vaccine technologies to combat outbreak situations. *Front. Immunol.* **9**, 1–24 (2018).

62. Koup, R. A. & Douek, D. C. Vaccine design for CD8 T lymphocyte responses. *Cold Spring Harb. Perspect. Med.* **1**, 1–15 (2011).

63. Del Giudice, G., Rappuoli, R. & Didierlaurent, A. M. Correlates of adjuvanticity: A review on adjuvants in licensed vaccines. *Semin. Immunol.* **39**, 14–21 (2018).

64. Masopust, D. & Soerens, A. G. Tissue-Resident T Cells and Other Resident

Leukocytes. *Annu. Rev. Immunol.* **37**, 521–546 (2019).

65. Perdomo, C. *et al.* Mucosal BCG vaccination induces protective lung-resident memory T cell populations against tuberculosis. *MBio* **7**, 1–11 (2016).

66. Wang, H., Hoffman, C., Yang, X., Clapp, B. & Pascual, D. W. *Targeting resident memory T cell immunity culminates in pulmonary and systemic protection against Brucella infection*. *PLoS pathogens* **16**, (2020).

67. Dowling, J. K. & Mansell, A. Toll-like receptors: The swiss army knife of immunity and vaccine development. *Clin. Transl. Immunol.* **5**, e85 (2016).

68. Tom, J. K. *et al.* Applications of Immunomodulatory Immune Synergies to Adjuvant Discovery and Vaccine Development. *Trends Biotechnol.* **37**, 373–388 (2019).

69. Steinhagen, F., Kinjo, T., Bode, C. & Klinman, D. M. TLR-based immune adjuvants. *Vaccine* **29**, 3341–3355 (2011).

70. Gilkes, A. P. *et al.* Tuning Subunit Vaccines with Novel TLR Triagonist Adjuvants to Generate Protective Immune Responses against Coxiella burnetii . *J. Immunol.* **204**, 611–621 (2020).

71. Fratzke, A. P. *et al.* Subunit Vaccines Using TLR Triagonist Combination Adjuvants Provide Protection Against Coxiella burnetii While Minimizing Reactogenic Responses. *Front. Immunol.* **12**, 1–13 (2021).

72. Gregory, A. E. *et al.* Soluble antigens derived from Coxiella burnetii elicit protective immunity in three animal models without inducing hypersensitivity. *Cell Reports Med.* **2**, 100461 (2021).

73. Long, C. M. *et al.* Contributions of lipopolysaccharide and the type IVB secretion system to Coxiella burnetii vaccine efficacy and reactogenicity. *npj Vaccines* **6**, 1–14 (2021).

74. Bell, J. F., Lackman, D. B., Meis, A. & Hadlow, W. J. Recurrent Reaction at Site of Q Fever Vaccination In a Sensitized Person. *Mil. Med.* **129**, 591–595 (1964).

75. Biberstein, E. L. *et al.* Dermal reactions and antibody responses in dairy cows and laboratory animals vaccinated with Coxiella burnetii. *Cornell Vet.* **64**, 387-406. (1974).

76. Lackman, D. B., Bell, E. J., Bell, J. F. & Pickens, E. G. Intradermal sensitivity testing in man with a purified vaccine for Q fever. *Am. J. Public Health* **52**, 87–93 (1962).

77. Schoffelen, T. *et al.* Immunogenicity of the Q fever skin test. *J. Infect.* **69**, 161–164 (2014).

78. Schoffelen, T. *et al.* Adverse events and association with age, sex and immunological parameters of Q fever vaccination in patients at risk for chronic Q fever in the Netherlands 2011. *Vaccine* **32**, 6622–6630 (2014).

79. Sellens, E. *et al.* Frequency of adverse events following q fever immunisation in young adults. *Vaccines* **6**, 1–13 (2018).

80. Wilhelmsen, C. L. & Waag, D. M. Guinea pig abscess/hypersensitivity model for study of adverse vaccination reactions induced by use of Q fever vaccines. *Comp. Med.* **50**, 374–378 (2000).

81. Male, D., Brostoff, J. & Roth, D. B. Hypersensitivity (Type IV). in *Immunology*

(eds. Male, D., Jonathan, B., Roth, D. B. & Roitt, I. M.) 419–429 (Elsevier Ltd, 2012).

82. Christensen, A. D. & Haase, C. Immunological mechanisms of contact hypersensitivity in mice. *Apmis* **120**, 1–27 (2012).

83. McNeil, M. M. & DeStefano, F. Vaccine-associated hypersensitivity. *J. Allergy Clin. Immunol.* **141**, 463–472 (2018).

84. Hervé, C., Laupèze, B., Del Giudice, G., Didierlaurent, A. M. & Da Silva, F. T. The how's and what's of vaccine reactogenicity. *npj Vaccines* **4**, 1–11 (2019).

85. Read, A. J., Erickson, S. & Harmsen, A. G. Role of CD4+ and CD8+ T cells in clearance of primary pulmonary infection with Coxiella burnetii. *Infect. Immun.* **78**, 3019–3026 (2010).

86. Buttrum, L. *et al.* Both major histocompatibility complex class i (MHC-I) and MHC-II molecules are required, while MHC-I appears to play a critical role in host defense against primary coxiella burnetii infection. *Infect. Immun.* **86**, 1–13 (2018).

87. Chen, C. *et al.* Identification of CD4+ T cell epitopes in C. burnetii antigens targeted by antibody responses. *PLoS One* **6**, e17712 (2011).

88. Zhang, G. *et al.* Identification and Cloning of Immunodominant Antigens of Coxiella burnetii. *Infect. Immun.* **72**, 844–852 (2004).

89. Baeten, L. A. *et al.* Standardized Guinea pig model for Q fever vaccine reactogenicity. *PLoS One* **13**, 1–19 (2018).

90. Gregory, A. E., Van Schaik, E. J., Russell-Lodrigue, K. E., Fratzke, A. P. &

Samuel, J. E. Coxiella burnetii Intratracheal Aerosol Infection Model in Mice, Guinea Pigs, and Nonhuman Primates. *Infect. Immun.* **87**, e00178-19 (2019).

91. Shannon, J. G. & Heinzen, R. a. Adaptive Immunity to the Obligate Intracellular Pathogen Coxiella burnetii. *Immunol. Res* **43**, 138–148 (2009).

92. Sellens, E. *et al.* Coxiella burnetii seroprevalence in unvaccinated veterinary workers in Australia: Evidence to support Q fever vaccination. *Zoonoses Public Health* **67**, 79–88 (2020).

93. Echeverría, G. *et al.* Serological evidence of Coxiella burnetii infection in cattle and farm workers: is Q fever an underreported zoonotic disease in Ecuador? *Infect. Drug Resist.* **12**, 701–706 (2019).

94. Lee, S. & Nguyen, M. T. Recent Advances of Vaccine Adjuvants for Infectious Diseases. *Immune Netw.* **15**, 51–57 (2015).

95. Mogensen, T. H. Pathogen recognition and inflammatory signaling in innate immune defenses. *Clin. Microbiol. Rev.* **22**, 240–273 (2009).

96. Albin, T. J. *et al.* Linked Toll-Like Receptor Triagonists Stimulate Distinct, Combination-Dependent Innate Immune Responses. *ACS Cent. Sci.* **5**, 1137–1145 (2019).

97. Lynn, G. M. *et al.* In vivo characterization of the physicochemical properties of polymer-linked TLR agonists that enhance vaccine immunogenicity. *Nat. Biotechnol.* **33**, 1201–1210 (2015).

98. Madan-Lala, R., Pradhan, P. & Roy, K. Combinatorial Delivery of Dual and Triple TLR Agonists via Polymeric Pathogen-like Particles Synergistically

Enhances Innate and Adaptive Immune Responses. *Sci. Rep.* **7**, 14–16 (2017).

99. Heegaard, P. M. H., Boas, U. & Sorensen, N. S. Dendrimers for vaccine and immunostimulatory uses. A review. *Bioconjug. Chem.* **21**, 405–418 (2010).

100. Zeng, H., Little, H. C., Tiambeng, T. N., Williams, G. A. & Guan, Z. Multifunctional dendronized peptide polymer platform for safe and effective siRNA delivery. *J. Am. Chem. Soc.* **135**, 4962–4965 (2013).

101. Manna, S. *et al.* Immunomodulation of the NLRP3 Inflammasome through Structure-Based Activator Design and Functional Regulation via Lysosomal Rupture. *ACS Cent. Sci.* **4**, 985–995 (2018).

102. Omsland, A. *et al.* Isolation from Animal Tissue and Genetic Transformation of Coxiella burnetii Are Facilitated by an Improved Axenic Growth Medium. *Appl. Environ. Microbiol.* **77**, 3720–3725 (2011).

103. Zamboni, D. S. *et al.* Stimulation of Toll-like receptor 2 by Coxiella burnetii is required for macrophage production of pro-inflammatory cytokines and resistance to infection. *J. Biol. Chem.* **279**, 54405–54415 (2004).

104. Davies, D. H. *et al.* Profiling the humoral immune response to infection by using proteome microarrays: High-throughput vaccine and diagnostic antigen discovery. *Proc. Natl. Acad. Sci. U. S. A.* **102**, 547–552 (2005).

105. Zhang, G. *et al.* Formalin-inactivated coxiella burnetii phase i vaccine-induced protection depends on b cells to produce protective igm and igg. *Infect. Immun.* **81**, 2112–2122 (2013).

106. Vigil, A. *et al.* Profiling the Humoral Immune Response of Acute and Chronic Q

Fever by Protein Microarray. *Mol. Cell. Proteomics* **10**, M110.006304 (2011).

107. Vigil, A. *et al.* Genome-wide profiling of humoral immune response to Coxiella burnetii infection by protein microarray. *Proteomics* **10**, 2259–2269 (2010).

108. Russell-Lodrigue, K. E. *et al.* Coxiella burnetii isolates cause genogroup-specific virulence in mouse and guinea pig models of acute Q fever. *Infect. Immun.* **77**, 5640–5650 (2009).

109. Marrie, T. J. Q Fever Pneumonia. *Infect. Dis. Clin. North Am.* **24**, 27–41 (2010).

110. Nakamura, S., Hayashidani, H., Okabe, N. & Une, Y. Aberrant Forms of Yersinia pseudotuberculosis as Spheroplasts and Filaments in Yersiniosis in Squirrel Monkeys. *Vet. Pathol.* **52**, 393–396 (2015).

111. Andoh, M. *et al.* T cells are essential for bacterial clearance, and gamma interferon, tumor necrosis factor alpha, and B cells are crucial for disease development in Coxiella burnetii infection in mice. *Infect. Immun.* **75**, 3245–3255 (2007).

112. Chan, M. *et al.* Identification of Substituted Pyrimido[5,4-b]indoles as Selective Toll- Like Receptor 4 Ligands. *J. Med. Chem.* **56**, 4206–4223 (2013).

113. Mata-Haro, V. *et al.* The vaccine adjuvant monophosphoryl lipid A as a TRIF-biased agonist of TLR4. *Science* **316**, 1628–1632 (2007).

114. Goff, P. H. *et al.* Synthetic Toll-Like Receptor 4 (TLR4) and TLR7 Ligands Work Additively via MyD88 To Induce Protective Antiviral Immunity in Mice. *J. Virol.* **91**, 1–12 (2017).

115. Barton, G. M. & Medzhitov, R. Toll-Like Receptor Signaling Pathways. *Science*

300, 1525–1527 (2003).

116. Gaddis, D. E., Michalek, S. M. & Katz, J. TLR4 Signaling via MyD88 and TRIF Differentially Shape the CD4 + T Cell Response to Porphyromonas gingivalis Hemagglutinin B . *J. Immunol.* **186**, 5772–5783 (2011).

117. Cui, W. *et al.* TLR4 Ligands Lipopolysaccharide and Monophosphoryl Lipid A Differentially Regulate Effector and Memory CD8 + T Cell Differentiation . *J. Immunol.* **192**, 4221–4232 (2014).

118. Chen, L. *et al.* Mice Deficient in MyD88 Develop a Th2-Dominant Response and Severe Pathology in the Upper Genital Tract following Chlamydia muridarum Infection . *J. Immunol.* **184**, 2602–2610 (2010).

119. Bafica, A. *et al.* TLR9 regulates Th1 responses and cooperates with TLR2 in mediating optimal resistance to Mycobacterium tuberculosis. *J. Exp. Med.* **202**, 1715–1724 (2005).

120. Macedo, G. C. *et al.* Central Role of MyD88-Dependent Dendritic Cell Maturation and Proinflammatory Cytokine Production to Control Brucella abortus Infection . *J. Immunol.* **180**, 1080–1087 (2008).

121. Zhan, R., Han, Q., Zhang, C., Tian, Z. & Zhang, J. Toll-like receptor 2 (TLR2) and TLR9 play opposing roles in host innate immunity against Salmonella enterica serovar typhimurium infection. *Infect. Immun.* **83**, 1641–1649 (2015).

122. Sato-Kaneko, F. *et al.* A Novel Synthetic Dual Agonistic Liposomal TLR4/7 Adjuvant Promotes Broad Immune Responses in an Influenza Vaccine With Minimal Reactogenicity. *Front. Immunol.* **11**, 1–19 (2020).

123. Coler, R. N. *et al.* The TLR-4 agonist adjuvant, GLA-SE, improves magnitude and quality of immune responses elicited by the ID93 tuberculosis vaccine: first-in-human trial. *npj Vaccines* **3**, 1–9 (2018).

124. Martinsen, J. T., Gunst, J. D., Højen, J. F., Tolstrup, M. & Søgaard, O. S. The Use of Toll-Like Receptor Agonists in HIV-1 Cure Strategies. *Front. Immunol.* **11**, 1–13 (2020).

125. Evans, W. H., Desser, K. & Himmelhoch, S. R. Guinea Pig Heterophil and Eosinophil Peroxidase. *Arch Biochem Biophys* **148**, 452–465 (1972).

126. Mantovani, A., Cassatella, M. A., Costantini, C. & Jaillon, S. Neutrophils in the activation and regulation of innate and adaptive immunity. *Nat. Rev. Immunol.* **11**, 519–531 (2011).

127. Reynolds, J. M. *et al.* Toll-like receptor 2 signaling in CD4+ T lymphocytes promotes T helper 17 responses and regulates the pathogenesis of autoimmune disease. *Immunity* **32**, 692–702 (2010).

128. Ascher, M. S., Williams, J. C. & Berman, M. A. Dermal granulomatous hypersensitivity in Q fever: Comparative studies of the granulomatous potential of whole cells of Coxiella burnetti phase I and subfractions. *Infect. Immun.* **42**, 887–889 (1983).

129. Murata, A. & Hayashi, S. I. CD4+ Resident Memory T Cells Mediate Long-Term Local Skin Immune Memory of Contact Hypersensitivity in BALB/c Mice. *Front. Immunol.* **11**, 1–17 (2020).

130. Fyhrquist, N., Wolff, H., Lauerma, A. & Alenius, H. CD8+ T cell migration to the

skin requires CD4+ help in a murine model of contact hypersensitivity. *PLoS One* **7**, 4–12 (2012).

131. Samuel, J. E. & Hendrix, L. R. Laboratory maintenance of coxiella burnetii. *Curr. Protoc. Microbiol.* 1–16 (2009). doi:10.1002/9780471729259.mc06c01s15

132. Bankhead, P. *et al.* QuPath : Open source software for digital pathology image analysis. *Sci. Rep.* **7**, 16878 (2017).

133. Schaffer, B. S. *et al.* Immune Competency of a Hairless Mouse Strain for Improved Preclinical Studies in Genetically Engineered Mice. *Mol. Cancer Ther.* **9**, 2354–2364 (2010).

134. Mills, C. D., Kincaid, K., Alt, J. M., Heilman, M. J. & Hill, A. M. M-1/M-2 Macrophages and the Th1/Th2 Paradigm. *J. Immunol.* **164**, 6166–6173 (2000).

135. Baaten, B. J. G., Tinoco, R., Chen, A. T. & Bradley, L. M. Regulation of antigen-experienced T cells: Lessons from the quintessential memory marker CD44. *Front. Immunol.* **3**, 1–12 (2012).

136. Ho, A. W. & Kupper, T. S. T cells and the skin: from protective immunity to inflammatory skin disorders. *Nat. Rev. Immunol.* **19**, 490–502 (2019).

137. Jaigirdar, S. A. & MacLeod, M. K. L. Development and function of protective and pathologic memory CD4 T cells. *Front. Immunol.* **6**, 1–11 (2015).

138. Szabo, P. A., Miron, M. & Farber, D. L. Location, location, location: Tissue resident memory T cells in mice and humans. *Sci. Immunol.* **4**, 1–12 (2019).

139. Italiani, P. & Boraschi, D. From monocytes to M1/M2 macrophages: Phenotypical vs. functional differentiation. *Front. Immunol.* **5**, 1–22 (2014).

140. Honda, T., Egawa, G., Grabbe, S. & Kabashima, K. Update of immune events in the murine contact hypersensitivity model: Toward the understanding of allergic contact dermatitis. *J. Invest. Dermatol.* **133**, 303–315 (2013).

141. Kalish, R. S. & Askenase, P. W. Molecular mechanisms of CD8+T cell-mediated delayed hypersensitivity: Implications for allergies, asthma, and autoimmunity. *J. Allergy Clin. Immunol.* **103**, 192–199 (1999).

142. Honda, T., Egawa, G. & Kabashima, K. Antigen presentation and adaptive immune responses in skin. *Int. Immunol.* **31**, 423–429 (2019).

143. Yawalkar, N. *et al.* A Comparative Study of the Expression of Cytotoxic Proteins in Allergic Contact Dermatitis and Psoriasis. *Am. J. Pathol.* **158**, 803–808 (2001).

144. He, D. *et al.* IL-17 and IFN-y mediate the elicitation of contact hypersensitivity responses by different mechanisms and both are required for optimal responses. *J. Immunol.* **183**, 1463–1470 (2009).

145. Robinson, K. M., Manni, M. L., Biswas, P. S. & Alcorn, J. F. Clinical consequences of targeting IL-17 and TH17 in autoimmune and allergic disorders. *Curr. Allergy Asthma Rep.* **13**, 587–595 (2013).

146. Grogan, J. L. & Ouyang, W. A role for Th17 cells in the regulation of tertiary lymphoid follicles. *Eur. J. Immunol.* **42**, 2255–2262 (2012).

147. Gaffen, S. L. An overview of IL-17 function and signaling. *Cytokine* **43**, 402–407 (2008).

148. Lehtimäki, S. *et al.* The temporal and spatial dynamics of Foxp3+ Treg cell-mediated suppression during contact hypersensitivity responses in a murine

model. *J. Invest. Dermatol.* **132**, 2744–2751 (2012).

149. Honda, T., Miyachi, Y. & Kabashima, K. Regulatory T cells in cutaneous immune responses. *J. Dermatol. Sci.* **63**, 75–82 (2011).

150. Bian, R. *et al.* (E)-phenethyl 3-(3,5-dihydroxy-4-isopropylphenyl) acrylate gel improves DNFB-induced allergic contact hypersensitivity via regulating the balance of Th1/Th2/Th17/Treg cell subsets. *Int. Immunopharmacol.* **65**, 8–15 (2018).

151. Eisenstein, E. M. & Williams, C. B. The Treg/Th17 cell balance: A new paradigm for autoimmunity. *Pediatr. Res.* **65**, 26–31 (2009).

152. Gaide, O. *et al.* Common clonal origin of central and resident memory T cells following skin immunization. *Nat. Med.* **21**, 647–653 (2015).

153. Pipi, E. *et al.* Tertiary lymphoid structures: Autoimmunity goes local. *Front. Immunol.* **9**, 1–21 (2018).

154. Burny, W. *et al.* Inflammatory parameters associated with systemic reactogenicity following vaccination with adjuvanted hepatitis B vaccines in humans. *Vaccine* **37**, 2004–2015 (2019).

155. Rock, M. T., Yoder, S. M., Talbot, T. R., Edwards, K. M. & Crowe, J. E. Adverse events after smallpox immunizations are associated with alterations in systemic cytokine levels. *J. Infect. Dis.* **189**, 1401–1410 (2004).

156. Maurin, M. & Raoult, D. Q fever. *Clin. Microbiol. Rev.* **12**, 518–553 (1999).

157. Reeves, P. M., Paul, S. R., Sluder, A. E., Brauns, T. A. & Poznansky, M. C. Q-vaxcelerate: A distributed development approach for a new Coxiella burnetii

vaccine. *Hum. Vaccines Immunother.* **13**, 2977–2981 (2017).

158. Fratzke, A. P., Gregory, A. E., van Schaik, E. J. & Samuel, J. E. Coxiella burnetii Whole Cell Vaccine Produces a Th1 Delayed-Type Hypersensitivity Response in a Novel Sensitized Mouse Model. *Front. Immunol.* **12**, 1–15 (2021).

159. Graham, L. & Orenstein, J. M. Processing tissue and cells for transmission electron microscopy in diagnostic pathology and research. *Nat. Protoc.* **2**, 2439–2450 (2007).

160. Kimble, K. M. *et al.* Systemic Toxoplasmosis in a Horse. *J. Comp. Pathol.* **182**, 27–31 (2021).

161. Szczepanik, M. *et al.* B-1 B Cells Mediate Required Early T Cell Recruitment to Elicit Protein-Induced Delayed-Type Hypersensitivity. *J. Immunol.* **171**, 6225–6235 (2003).

162. Hackstadt, T. Steric hindrance of antibody binding to surface proteins of Coxiella burnetii by phase I lipopolysaccharide. *Infect. Immun.* **56**, 802–807 (1988).

163. Chung, D. R. *et al.* CD4 + T Cells Mediate Abscess Formation in Intra-abdominal Sepsis by an IL-17-Dependent Mechanism . *J. Immunol.* **170**, 1958–1963 (2003).

164. Ishigame, H. *et al.* Differential Roles of Interleukin-17A and -17F in Host Defense against Mucoepithelial Bacterial Infection and Allergic Responses. *Immunity* **30**, 108–119 (2009).

165. Tzianabos, A. O. *et al.* Bacterial pathogens induce abscess formation by CD4+ T-cell activation via the CD28-B7-2 costimulatory pathway. *Infect. Immun.* **68**,

6650–6655 (2000).

166. Pelletier, M., Micheletti, A. & Cassatella, M. A. Modulation of human neutrophil survival and antigen expression by activated CD4 + and CD8 + T cells . *J. Leukoc. Biol.* **88**, 1163–1170 (2010).

167. Patterson, J., Kagina, B. M., Gold, M., Hussey, G. D. & Muloiwa, R. Comparison of adverse events following immunisation with acellular and whole-cell pertussis vaccines: A systematic review. *Vaccine* **36**, 6007–6016 (2018).

168. Bachmann, M. F. & Jennings, G. T. Vaccine delivery: A matter of size, geometry, kinetics and molecular patterns. *Nat. Rev. Immunol.* **10**, 787–796 (2010).

169. Thavarajah, R., Mudimbaimannar, V. K., Elizabeth, J., Rao, U. K. & Ranganathan, K. Chemical and physical basics of routine formaldehyde fixation. *J. Oral Maxillofac. Pathol.* **16**, 400–405 (2012).

170. McCaul, T. F. & Williams, J. C. Developmental cycle of Coxiella burnetii: Structure and morphogenesis of vegetative and sporogenic differentiations. *J. Bacteriol.* **147**, 1063–1076 (1981).

171. O'Hagan, D. T., Ott, G. S., De Gregorio, E. & Seubert, A. The mechanism of action of MF59 - An innately attractive adjuvant formulation. *Vaccine* **30**, 4341–4348 (2012).

APPENDIX A - CHAPTER 3 SUPPLEMENTAL FIGURES*

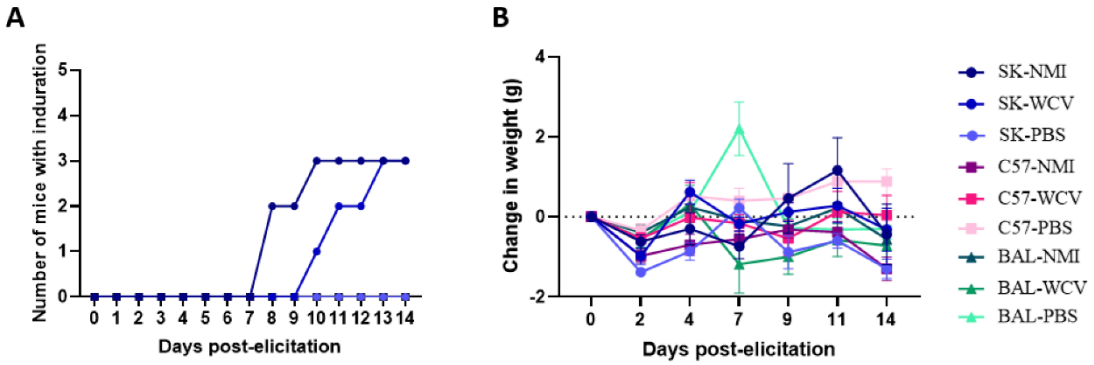

Supplemental Figure 1. Post-elicitation monitoring for weight change and vaccine site induration.
(A) Presence of local induration in each experimental group. Only infection- and vaccine-sensitized SK mice showed grossly visible induration at the elicitation site. Focal induration measured 2 mm thick compared to 1 mm for normal skin. **(B)** Change in weight during 14 days post-elicitation. There is no significant weight loss in any experimental group during elicitation. Weight data shows the means of each group (n=5) with error bars showing the standard error of the mean.

* Reprinted with permission from: Fratzke AP, Gregory AE, Van Schaik EJ, Samuel JE. 2021 *Coxiella burneti*i Whole Cell Vaccine Produces a Th1 Delayed-type Hypersensitivity Response in a Mouse Model. *Frontiers in Immunology*. Sep;12:1-15. doi: 10.3389/fimmu.2021.754712

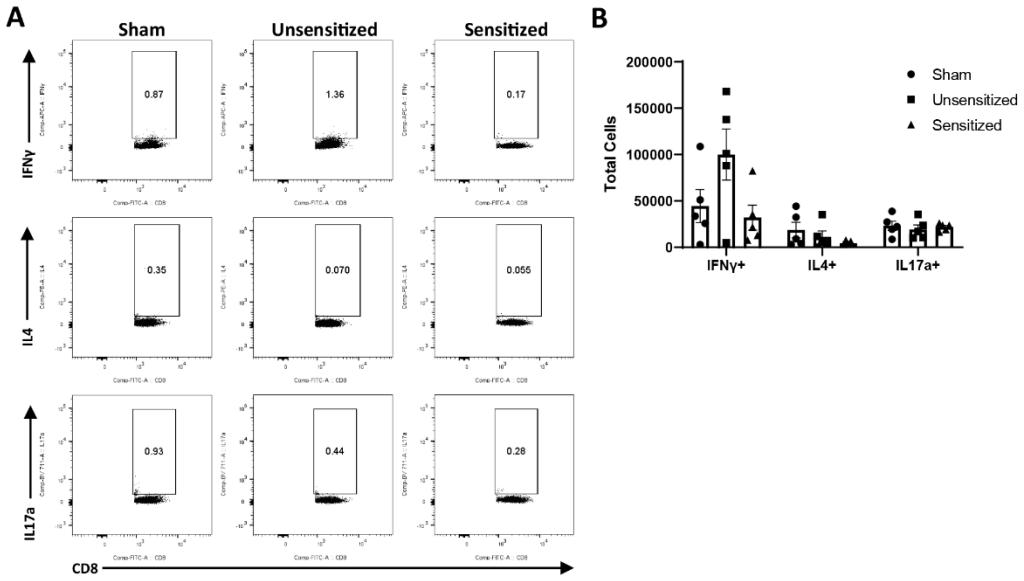

Supplemental Figure 2. CD8 T cells from vaccine sites do not show increased production of IFNγ, IL4, or IL17a.

(A) Representative gates for IFNγ, IL4, and IL17a production by CD8+ T cells from vaccination sites. **(B)** Summary of total IFNγ+, IL4+, and IL17a+ CD8+ T cells. There were no significant differences in cytokine production by CD8+ T cells across experimental groups. Graphs show the means of each group with error bars that represent the standard error of the mean. Cell counts are the sum of four vaccination sites from each mouse, n=5 mice per group. Data were analyzed using one-way ANOVA with Dunnett's correction for multiple comparisons.

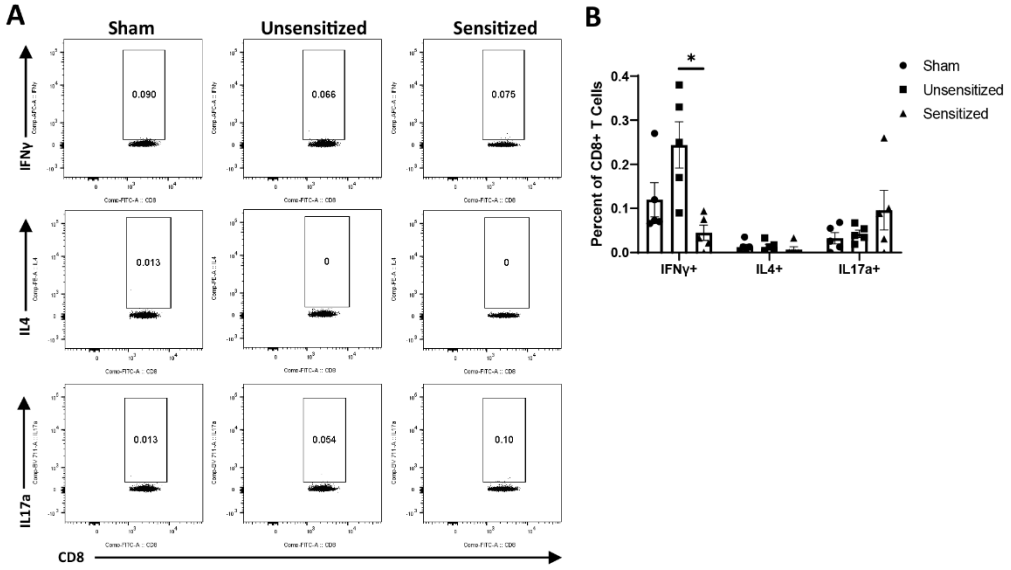

Supplemental Figure 3. Flow cytometric evaluation of cytokine production by CD8+ T cells extracted from spleens.

(A) Representative flow cytometry gates for IFNγ, IL4, and IL17a production by CD8+ T cells from spleens. **(B)** Summary of total IFNγ+, IL4+, and IL17a+ CD8+ T cells. IFNγ+ CD8+ T cells are mildly increased compared to sensitized mice but not sham mice. There are no significant changes in IL4+ and IL17a+ CD8+ T cells across groups. Graphs show the means of each group with error bars that represent the standard error of the mean. Cell counts are the sum of four vaccination sites from each mouse, n=5 mice per group. Data were analyzed using one-way ANOVA with Dunnett's correction for multiple comparisons. Asterisks indicate significant differences between groups (*: $p<0.05$).

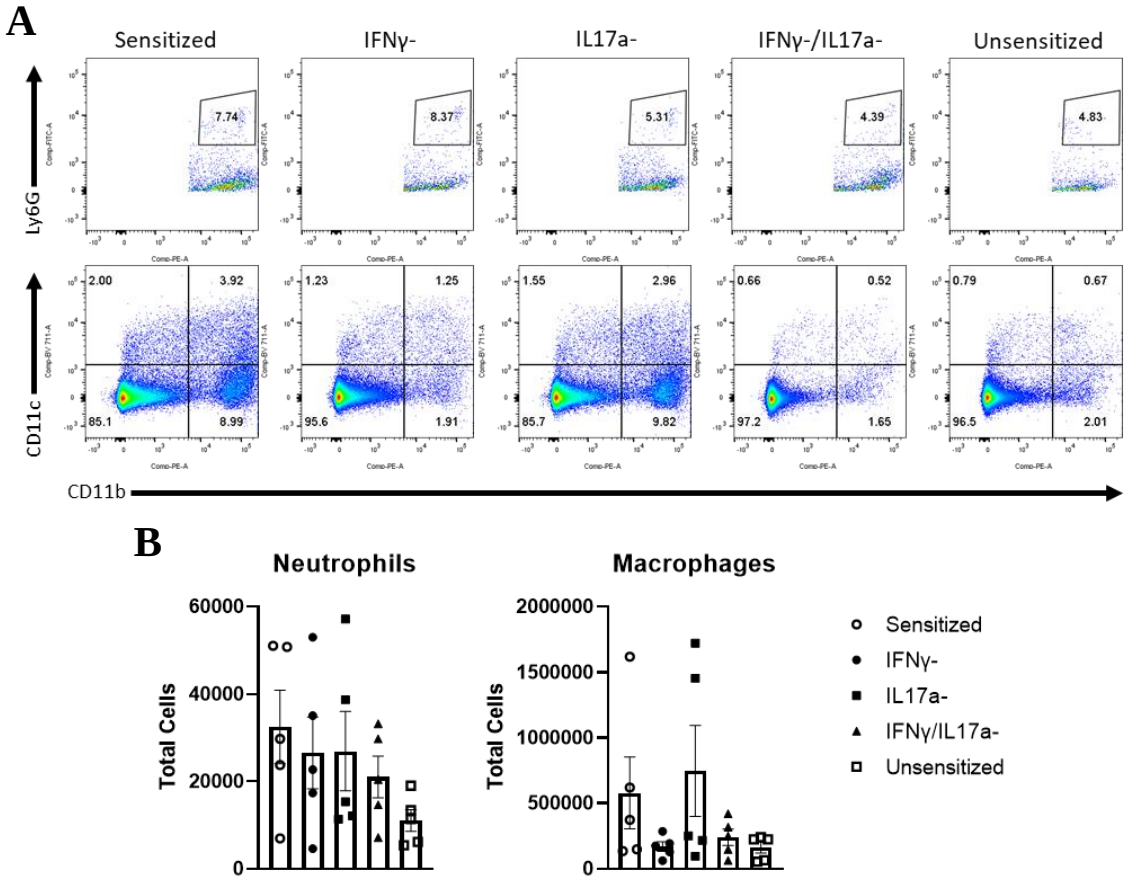

Supplemental Figure 1. Flow cytometry of cells extracted from vaccine site reactions. A) Representative gates for each experimental group. B) Summary graphs of total CD11b+CD11c-Ly6G+ neutrophils and CD11b+CD11c-Ly6G- macrophages. All depletion groups and unsensitized mice show a mild decrease in neutrophils compared to sensitized mice. IFNγ- and IFNγ-/IL17a- mice show a decrease in macrophages compared to sensitized mice. N=5 mice per group.